EXPLORING TUNGSTEN IN THE ENVIRONMENT: GEOCHEMICAL STUDY OF AN EMERGING CONTAMINANT

by

CHAD HOBSON

B.S., Georgia College and State University, 2010

A THESIS

submitted in partial fulfillment of the requirements for the degree

MASTER OF SCIENCE

Department of Geology
College of Arts and Sciences

KANSAS STATE UNIVERSITY
Manhattan, Kansas

2014

Approved by:

Major Professor
Saugata Datta

Abstract

Tungsten (W) has become an element of greater concern in recent years. Investigations by the Centers for Disease Control implicated W as a possible link to several cases of childhood acute lymphatic leukemia (ALL) clusters in the western United States. In Fallon NV, 17 cases of ALL were reported from 1997-2001. Previously, it was difficult to attain knowledge about the geochemical behavior of W due to low concentrations and difficulties in detection in natural environments. Modern analytical techniques allow for a greater range of sensitivity, allowing for in depth W analysis. Elucidating information on the factors contributing to the fate and transport of W in low temperature environments will provide insight into how W moves through the environment and provide information to help mitigate W contamination in the future.

Three sites were chosen for comparison of W concentration and how that may be linked to local geochemical factors. Fallon NV, Sierra Vista AZ, and Cheyenne Bottoms Refuge KS were chosen based on published literature and personal communications. The objectives for this study were to characterize W concentrations in these three climatologically distinct areas followed by using methods to speciate and semi-quantitatively characterize W phase association within the surficial sediments and using synchrotron X-Ray methods to define W valencies and elemental associations within the sediments.

Tungsten occurs in varying concentrations in the study areas, from 17.8 mg/kg to ~25,907 mg/kg. Fallon has the highest average W concentration of the three sites as well as the highest amount of W associated with phases other than the organic matter or residual phase. Speciation of soluble W revealed no polytungstates, however tungstates are present in the samples as well as undefined W species, suggesting there are other forms of W that are readily soluble in water, hence bioavailable. Tungsten has a very heterogeneous distribution in sediments, creating dispersed but highly concentrated clumps of W hotspots. Spot analyses under X-Ray mapping reveal W may co-localize with other metals such as Ti, Co, and Zn.

Table of Contents

List of Figures

List of Tables

Acknowledgements

The author would sincerely like to thank all those who helped during the 2+ years it took to complete this work. First special thanks goes to those who helped with field work and the collection of the water samples. Thank you to Dr. Mark Witten and Dr. Paul Sheppard from the University of Arizona for their correspondence and personal assistance with sampling in Fallon, NV and Sierra Vista, AZ as well as insight into sampling into Kansas. This work would not have been possible without their help and guidance. A thank you also goes out to those who helped with the students of the Geology department who helped with the sampling process: Robinson Barker, MS Sankar, and Guilherme Sonntag Hoerlle. Their help is very appreciated for helping with the work load of driving to field sites and collecting, transporting and storing samples.

A very HUGE and special thanks goes out to all the people who took time to help me in the lab procedures. This research could not have been completed without the help of many individuals guidance and advice. A special thanks to Anthony Bednar of the US Army Engineer Research and Development, Environmental Chemistry Laboratory for the guidance in the procedures necessary to analyze tungsten and for allowing the author to us his laboratory space and instruments for total digestions, sequential extractions, and water extractions. A very special thanks to Dr. Ganga Hettiarachchi of the Kansas State University Agronomy and her students for help during digestions. Thank you to Dr. Hettiarachchi for allowing me to use her laboratory space and Philip Defoe for help and guidance during the procedure, and use of the ICP-OES. The author would like to also thank Dr. Dan Boyle of the Kansas State University Biology Department for use of the scanning electron microscope/energy dispersive x-ray spectrometer.

Another HUGE thank you to Ryan Bednar from microprobe beam line X27A from the National Light Source, Brookhaven National Lab. The synchrotron work conducted, analysis of samples, numerous questions, problem troubleshooting would have been an insurmountable task without his consistent help, guidance and advice.

The author would like to thank the Geology Department of Kansas State University for its help throughout the 2+ years. Dr. George Clark for his support, Lori Page-Willyard for administrative assistance, and the rest of the faculty for helpful conversations and advice along the way with this project and presentations.

Sincere thanks goes to the author's graduate committee for first of all serving on the committee: Dr. Sambhudas Chaudhuri for research related guidance, Dr. Matt Brueseke for guidance in optical mineralogy and great instruction and field trips, and Dr. Ganga Hettiarachchi for the invaluable help in the use of her lab and guidance in the procedures used.

Last but not least, the author would like to extent his greatest thank you to his advisor Dr. Saugata Datta. For help and guidance through the whole process, numerous opportunities to travel, grow, and learn. For funding this project, his encouragement, patience, and valuable time devoted to helping this project and more import the author himself succeed. Thank you.

Chapter 1 - Introduction

Tungsten (W) has become an element of greater interest in the past decade. This is due to recent health and environmental problems, which prompted the EPA to classify W as an emerging contaminant and nominate it for carcinogenic studies (EPA 2008). Tungsten is a naturally occurring element that exists in nature in mineral form, as oxyanions, and a comprehensive and incomplete list of compounds but never as W metal (Seiler et al., 2005). In nature, W primarily exist as tungstate (WO_4^{2-}), its most stable form, can polymerize with itself to form polytungstates (Gbaruko and Igwe 2007). Tungsten was once thought to be benign and stable in the environment, it has been shown that W can be mobile in sediments and ground water, and has a complex geochemistry and polymerization process (Bednar et al., 2006; Koutsospyros et al., 2006; Seiler et al., 2005). There is a lack of robust knowledge of W toxicity and its potentially harmful environmental effects, and this becomes even more difficult since the variety of forms W can exist in alter its toxicity, mobility, and bioavailability (Koutsospyros et al., 2006). Currently there are no environmental regulations for W in any setting (sediment, recreational water, drinking water, etc.) in the US with the exception of industrial air quality standards for workers (Koutsospyros et al., 2006). The challenge of W research lies in the unknowns of its persistence, transport, and fate in environmental settings. It is important to find information detailing how W exists in natural sediments, while also determining what concomitant trace elements and/or anionic complexes play a role in its biogeochemistry (Bednar et al., 2006, Ogundipe et al., 2009; Ringelberg et al., 2009).

Tungsten Geochemistry

Tungsten is a group VI element that is similar to Molybdenum (Mo) and Chromium (Cr) but with very unique properties that makes it incredibly versatile and useful in many applications. I has a variety of oxidation states (0, 2+, 3+, 4+, 5+, 6+) but the most stable and common in water and oxidative environments is 6+ (Seiler et al., 2005). It has the highest melting point of all metals (3410-3422ºC) and is only second to Carbon (Gbaruko and Igwe 2007). Tungsten is used in a variety of industrial, military, and domestic applications as W, tungsten carbide (WC), or various alloys. Tungsten has a high tensile strength, low expansion

coefficient, high density (more than lead at 19.3 g/cm^3 at 20ºC) and a low vapor pressure. It resists corrosion very well and is listed as having limited chemical activity, even as non-reactive with water and mineral acids (Koutsospyros et al., 2006; Gbaruko and Igwe 2007). Many of these factors have made it desirable, and alloying with other elements such as C extends its uses by slightly altering its properties. It is Ws physical and chemical properties that also make it a challenge to model geochemically. As mentioned, W in nature is most stable in its 6+ oxidation state as WO_4^{2-}. Anthropogenic use of W utilizes W metal or WC, which are thermodynamically unstable and when introduced into environmental systems begins to alter to a more stable form (WO_4^{2-}) (Andersson and Bergstrom 2000). Fig. 1.1 below shows an experimentally determined Eh-pH diagram for W (Ryzhenko 2010).

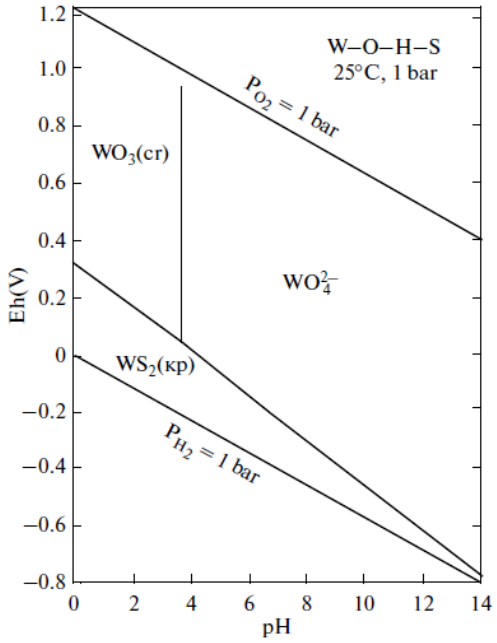

Figure 1.1 Eh-pH diagram for the W-O-H-S system at 25ºC, concentrations of W 10^{-8} *m* and S 10^{-3} *m*

The largest use of W is in WC and W metal alloys (Koutsospyros et al., 2006). When emitted in air, W will almost always remain in the particulate phase because of its low vapor pressure (4.27 Pa) (Gbaruko and Igwe 2007, Koutsospyros et al., 2006), and it will eventually fall and mix with soil. Volatilization from soil is unlikely because of its low vapor pressure and in soils W tends to have moderate to low mobility with sorption coefficients ranging from 10-50,000 at pH 5-6.5. In water W tends to adsorb to suspended particles and sediment (Gbaruko and Igwe 2007). In sediment and water, W and WC are resilient to water and fairly immobile.

What does happen is that W/WC are easily oxidized to tungsten oxide (WO_3) is more soluble in water and this begins a very complicated process that is environmentally dependent (Koutsospyros et al., 2006; Venkataramana and Krishnan 1982).

In the presence of oxygen, W forms WO_3 which easily dissolves in the presence of water to form WO_4^{2-}. Since W has many coordination numbers and oxidation states, numerous possibilities exist for the formation of complexes with many inorganic and organic ligands (aqua-, oxo-, halide-, organo-, and mixed) with different implications for mobility in either surface or subsurface environments (Koutsospyros et al., 2006).Varying pH also begins to play a role in the geochemistry of W. With decreasing pH, WO_4^{2-} starts to polymerize with itself (forming a wide range of polytungstates) or compounds in the environment, this process is not well studied or documented and the full extent of W pathways have barely been recognized, much less explored and defined. At neutral to basic pH, WO_4^{2-} remains monomeric but is more mobile than it is at lower pHs (Andersson and Bergstrom 2000; Warren et al., 2009; Seiler et al., 2005; Koustsospyros et al., 2006). With decreasing pH, WO_4^{2-} would be become less mobile but it polymerizes more readily with decreasing pH, and changes species and these other W compounds have varying degrees of mobility.

When looking at metallic W and soil column experiments, it can be seen that more soluble W is available over time (aging of soil). This is most likely due to metallic W having more time to oxidize and release WO_4^{2-} into the system. Polytungstates also have a lower K_d than monomeric WO_4^{2-} (Bednar et al., 2008). The anionic nature tends to cause monomeric WO_4^{2-} to have increased sorption as soil oxides protonate (Bednar et al., 2009). In a column test, Bednar et al., (2009) found polytungstates to be more prevalent than monomeric WO_4^{2-}in solution with deionized (DI) water extractions. This could be because of the cumulative effects described where the dissolution and oxidation of metallic W acidifies soils while creating WO_4^{2-}. This decreased pH also adds to the polymerization processes described by Bednar et al., (2008; 2009). This process has only recently begun to be described and effort should be made to fully explore this as it is necessary to understand the fate and transport of W as well as its toxicity and bioavailability, which is species dependent and thus for W ill-defined and highly variable (Bednar et al., 2008; Tuna et al., 2012). Since the distribution coefficient K_d is based on assuming a single chemical species as well as established equilibrium conditions, care needs to go into these studies since W can exist as many chemical species and is known to take time to

reach equilibrium between the solid and aqueous phases (Griggs et al., 2009). To better understand W and analyze it in the environment many factors about its complex pH dependent chemistry still need to be addressed and experiments describing its many chemical species need to be performed.

Natural Tungsten and Tungsten Minerals

The majority of Earth's W is located in the core (>90%). Tungsten is moderately siderophilic and when the metallic core separated from the silicate portion of the Earth, approximately 10 to 70 million years after the formation of the solar system, it was largely sequestered in the core. Geochemically, W is largely incompatible during crust formation and mantle melting which has left the core strongly enriched in W as well as the continental crust and the modern mantle depleted (Arevalo and McDonough 2008). In high temperature geochemistry, W has given insights into many factors in understanding the Earth's interior in both core-mantle segregation and differentiation of silicate Earth, because of these properties. Being so incompatible has left W to be most significantly associated with hydrothermal processes in natural settings (Ivanova 1986). Tungsten deposits can be found in igneous and metamorphic rocks, and especially in hydrothermal altered substrate such as skarns and quartz veins (Neiva 2008; Nokleberg 1981).

The average crustal abundance of W is approximately 1.3 mg/kg (Koutsospyros et al., 2006). While W deposits are largely derived from hydrothermal fluids, granitoid plutons are also a source of W, where W is derived from fluid that has equilibrated with granitic magma and deposited in the country rock. Typically, mineralization of W is most often hosted by skarn assemblages (Nokleberg 1981, Wood and Samson 2000). It is in these fluid altered areas that most W mineralization occurs. There are over 20 recognized W minerals, two oxotungstates predominate. Indeed, most of the W minerals are oxotungstates, with one sulphide and one silicate which rarely occur (Pavlu 1986).

The two most common W minerals are solid series groups. The first and most dominant W mineral on Earth is the scheelite group, with scheelite ($CaWO_4$) and powellite ($CaMoO_4$) as its end members. Here because of the similarities between Mo and W, MoO_4^{2-} and WO_4^{2-} substitute for each other. The other major W mineral is the solid solution series wolframite ($FeMnWO_4$). The end members of this group are ferberite ($FeWO_4$) and heubnerite ($MnWO_4$),

where wolframite is classified as a mix containing less than 80% of either end member (Seiler et al., 2005). Scheelite is usually found in granitic pegmatites, high temperature hydrothermal veins, contact metamorphic deposits, subvolcanic vein deposits and stratiform deposits. It is usually mineralogical associated with fluorite, apatite, molybdenite, quartz, wolframite, sphalerite, garnets, and amphiboles. Wolframite on the other hand is relatively rarer and is usually found in pegmatites and plutonic-hydrothermal veins, and commonly is associated with pyrite and arsenopyrite and sometimes molybdenite (Pavlu 1986; Seiler et al., 2005).

Chapter 2 - Background

With the increased use of W in military and industrial applications, increased concern over W geochemistry and biochemistry have also grown. Until recently, W chemistry knowledge has been mostly limited to the industrial field. With a lack of knowledge about environmental repercussions stemming from gaps in geochemical knowledge about W, many W products and projects were implemented with the false sense that W is safe and immobile in the environment. One such project was the use of W as a replacement for Pb and U in ammunition for hunting and recreational shooting, for fishing weights, and for military ammunition (i.e., high kinetic energy penetrators and small arms ammunition; Strigul et al., 2005; Koutsospyros et al., 2006; Bednar et al., 2007, 2008). The use of W as a replacement for Pb was originally conceived as a way to limit the addition of toxic Pb to the environment by what was thought to be a non-toxic, inert metal of low environmental mobility (Koustsospyros et al., 2006; Bednar et al., 2007). Nevertheless, despite the initial beliefs that W was a non-toxic, chemically inert heavy metal, laboratory studies clearly reveal that W can be carcinogenic (e.g. Kalinich et al., 2005), and field-based investigations indicate that it is mobile in the environment (e.g., Johannesson et al., 2000; Dermatas et al., 2004, 2006; Petrunic and Al, 2005; Seiler et al., 2005; Arnórsson and Óskarsson, 2007; Clausen et al., 2007; Clausen and Korte, 2009; Johannesson and Tang, 2009). Many of these studies stem from a recent disaster that has befallen many in the western United States, in which W has been implicated as a culprit in several clusters of leukemia (Koutsospyros et al 2006; Seiler et al., 2005).Earlier studies on wildlife suggested that elevated levels of W had no significant biological repercussions (e.g. Mitchell et al., 2001; Peuster et al., 2003), which supported the belief that W was non-toxic. In 2002, the Center for Disease Control (CDC) investigated several clusters of acute lymphatic leukemia (ALL) in both Nevada and in Arizona. These areas have natural W mineral deposits as well as former W mining and smelting operations in the area and nearby military bases. The first area surveyed by the CDC and the United States Geological Survey (USGS) was Fallon, NV. It was discovered that this area constituted a statistical "cluster." Between the years of 1997 to 2002 15 cases of ALL and one case of myelocytic leukemia were diagnosed in children and teenagers living in the area. The number of cases for a town the size of Fallon was described as having a very small likelihood of

being a random event, with what would be considered an average occurrence of 3 cases/100,000 children/5 years (Koutsospyros et al., 2006; Seiler et al., 2005; Sheppard et al., 2007c).

The investigation by the CDC highlighted that the residents had urinary W levels above the 95th percentile for the United States (Seiler et al., 2005; Koutsospyros et al., 2006). This prompted the CDC to nominate W for more intensive carcinogenic studies (EPA 2010). Investigations by Sheppard et al., (2006, 2007a, b, c) have investigated the W present in surface and air dust in Fallon and have found it is indeed extremely high (up to 934 ppm; Sheppard et al., 2007b) and highly variable with a coefficient of variability of 732%. With the exception of As (71%) and Co (77%) all the other metals sampled had coefficients of variability >50%. Sheppard et al., (2006) also noted that the most notable metal in Fallon dust was W with Co as a secondary interest. Also noted was the spatial covariance of W with Co. They also established that outside of Fallon, the concentration of W was <10 ppm, suggesting levels close to normal background levels found in nature (Sheppard et al., 2007b). The W found in airborne particles and surface dust is implicated as anthropogenic and not natural, however, further research should be done to resolve this issue (Sheppard et al., 2007a). An earlier study by Seiler et al., (2005) stated that W in Fallon, especially its ground waters is of natural, not anthropogenic origin. Seiler et al., (2005), stated four separate mechanisms that could be responsible for the W in ground water, and incidentally drinking water of Fallon residents. These include: (1) evaporative concentration of W in local river waters followed by recharge of underlying aquifers; (2) dissolution of primary W-bearing minerals within the aquifer sediments; (3) mixing with high W geothermal waters, which are common in the Carson Desert; and (4) reductive dissolution of Fe/Mn oxides/oxyhydroxides within the aquifer sediment and subsequent release of adsorbed or co-precipitated W to the groundwaters (Seiler et al., 2005). Others have suggested that the W is natural as well (Pardus and Sueker 2009), however, the study of W geochemistry is complicated and it is more likely that sources, given the high concentrations recorded in various media, could be of mixed origins both natural and anthropogenic. While it is critical that W geochemistry become more precisely defined, it is also of great importance to more accurately define the extent to which W may be toxic to humans.

The study of W biochemistry has only recently begun. After the Fallon cluster, the CDC nominated W for carcinogenic research since previous studies on the toxicology of W are non-existent. It has been known for some time that sodium tungstate is a good anti-diabetic agent, but

the toxicology of W, WO_4^{2-}, polytungstates, W metals, or the various undescribed W compounds is only just starting to be researched (Altirriba et al., 2009; Seiler et al., 2007). Witten et al., have contributed a lot of the current research on the subject of the link between W and leukemia. Current Research indicates that W could be carcinogenic especially if exposure occurs along with other factors (Fastje et al., 2012, Sun et al., 2003, Witten et al., 2012). Kalinich et al., (2005) also showed tumor formation in rats that had been embedded with weapons grade W alloys. There are many factors to consider when evaluating an elements environmental toxicity to humans, and this is often difficult to accurately identify, since there are many factors that could play a role. One issue of concern however, is the relationship of W to Mo. Molybdenum is an essential element and is a part of many important enzymes, this is of great concern since W can replace Mo, and thus inhibit the enzyme from performing its functions (Ivanova 1986; Koutsospyros et al., 2006). This isn't the only way in which W has been shown to disrupt biological pathways. Johnson et al., (2010), showed that WO_4^{2-} can disrupt intracellular functions by polymerizing extensively with phosphate (PO_4^{3-}). As this happens cellular phosphorylation and dephosphorylation reactions are disrupted. Kumar et al., (2011) studied the effects of WO_3 with human DNA. They found that in PCR test, WO_3 would inhibit Taq polymerase (a bacteria polymerase) and suppress the amplification of DNA. These studies show that even though W is not essential to eukaryotic cells (it is essential in enzymes for Archaea and some bacteria, while Mo is essential for Eukarya and Bacteria; Bevers et al., 2009) it can still interact with and disrupt vital processes. Although some believe W is not of toxicological concerns to humans without occupational exposure (Pardus et al., 2009).

Pardus et al. (2009) and Thomas et al., (2009) state that W is of little toxicological concern in the envir,onment and that use of W, especially in ammunitions, does not constitute a concern for human health. Thomas et al., (2009) argues that W from ammunitions does not effectively add W in enough concentration to be of an environmental concern, but rather it is the Ni or Co that is often associated with W alloys that is more of a concern since they are more established carcinogens. Pardus et al., (2009) on the other hand rules out W as being harmful all together stating "…that tungsten simply does not cause harm to humans under ordinary conditions of use, or from known environmental exposure." Schell and Pardus (2009) further argue that the gap in W toxicological information is more due to the lack of human toxicological effects. They state that W has low potency when compared to other compounds related to

industry. They used published data and calculated preliminary risk based concentrations for W in soil and water (7821 mg/ks and 3650 µg/L respectively).

Leukemia is not well understood, so some work needs to be done to better fill in the gap in that information (Fastje et al., 2012; Wiemels 2012). However, Witten et al., 2012 and Strigul et al., 2010, have inconclusive but strong evidence that starts to point toward the fact that W interacts with the human acute lymphoblastic leukemia cell line. Other researchers have also linked various tungstates and polytungstates as bioavailable and toxic to fish (Strigul et al., 2010). Tungsten compounds have also been shown to be bioavailable to various plants and animals including sunflowers and earthworms (Johnson et al., 2009; Inouye et al., 2006).

Chapter 3 - Objectives and Hypothesis

Objectives

The main goal of this project was to elucidate information about the geochemistry of W in sediments, to help better establish the factors controlling its fate and transport through sediments and ground water. This work focused on three areas of varying levels of W concentration and sources of W, in Fallon, NV, Sierra Vista AZ, and Cheyenne Bottoms Refuge, KS. To establish basic parameters about the geochemical behavior of tungsten in natural sediments, a multi-faceted approach was used to identify mineralogical and elemental associations. This can be broken down into several sub-objectives:

1) Establish the extent of W occurrence in sediments of sampling sites of Fallon, Cheyenne Bottoms, and Sierra Vista (three climatologically and geologically distinct areas). Sierra Vista has little geochemical work conducted on W. Cheyenne Bottoms has never had geochemical work conducted there before so it is important to establish baseline data for W. Fallon has had the most research done with W of any site, however the bulk of the work has consisted of mainly groundwater and surface/air dust studies. It is critical as the first part of this work to develop data on the W concentrations in these sites as a starting point to understand the geochemical behavior of W in sediments.
2) To better understand the occurrence of W in sediments, it is necessary to characterize it further beyond just the concentration. To do this, sequential extractions, water extraction and speciation studies needed to be performed which describe the phase association of W in the sediment as well as the W species that exists in the dissolved phases of these sediments. This is important because W can exist in a variety of forms, all of which have varying degrees of mobility in the subsurface, and bioavailability.
3) To characterize spatial association of W in sediments with x-ray adsorption spectroscopy and scanning electron microscopy. This helped identify spatial distribution of W in sediments and the elemental associations. Information was obtained about speciation and oxidation states of W present in the dry sediments with x-ray absorption near edge structure (XANES) studies.

Chapter 4 - Methods

To accomplish the goals of this work a multi-faceted approach was taken to establish the geochemical parameters of the sediment of our sample sites. This was done to assess environmental conditions that control the fate and transport of W. Sediments samples were collected from three different localities based on prior knowledge of higher than normal W concentrations. Surface water samples were collected from one of the sites (Cheyenne Bottoms), but no other water samples were able to be collected for analysis.

Study Area

The sampling locations picked for this study are Fallon, NV, Sierra Vista, AZ, and Cheyenne Bottoms Refuge, KS. Details of the sampling sites are located in Appendix A.1. These sites were selected because previous work by others have identified them as having higher than average concentrations of W present and it was important for this study to have higher W levels to ensure that measurable W was available for analysis. Having relatively larger quantities of W allows for the ability to analyze the W interactions more easily.

Fallon, NV

Fallon was selected as a sampling site in this study because it was the beginning of W research as a contaminant. It has been recorded as having higher than average W levels in sediment, ground water, air particulate and surface dust (Cutler 2011; Seiler et al., 2005; Sheppard et al., 2006). Many researchers have done research on the distribution of W in Fallon in surface and air dust as it may pertain to the leukemia clusters (Francis et al 2012; Schell et al 2009; Sheppard et al., 2006; Sheppard et al., 2007; Sheppard et al., 2007; Sheppard et al., 2007; Seiler et al., 2005; Seiler 2012; Pardus and Sueker 2009). Extensive work has been conducted on the ground water quality as well, as this could be a pathway for W to humans (USGS 2001; Seiler et al., 2007). Using these works as a starting place helps to establish conditions in Fallon as this work begins to examine the sediment and the status of W in the upper most layers of sediment in Fallon.

Fallon lies in the Carson sink at the terminus of the Carson River in the Lahontan valley (Seiler 2012). Fallon is in the rain shadow of the Sierra Nevada Mountains and receives little rain

each year (~12.7cm a year). The primary land use is agricultural and this area is supplied with ground water from three unconsolidated basin-fill aquifers and a consolidated basalt aquifer. The basin-fill aquifers are composed of unconsolidated Quaternary sediments from the ancient Lake Lahontan, as well as unconsolidated and semi-consolidated Tertiary sediments (Seiler et al., 2005). Varying lake levels and conditions have led to the sediments to have a complex sequence of interbedded and interfingering deposits of gravel, sands, silts, and clays (Cutler 2011; Seiler 2012). The sediments were deposited by the lake and the Carson River from granitic rocks in the Sierra Nevada and volcanics upstream of the Lahontan Valley, which have been deposited since the Pleistocene (Seiler 2012; Seiler et al., 2007). The basalt aquifer, known as Rattlesnake Hill, is a mushroom shaped consolidated rock body. It consist of vastly ranging permeability with fractured lava flows, basalt rubble and cinders. The basalt body was formed from Quaternary volcanicanism (Seiler et al., 2007).

Tungsten in sediments and ground water has been speculated to be derived from weathering of scheelite deposits nearby and/or from geothermal fluids upwelling and mixing with the groundwater (Cutler 2011, Seiler et al., 2005).

Sampling in Fallon was guided by personal correspondence with Paul Sheppard who has previously conducted many published works on W in the area. The samples were taken from inside the town itself in publicly available areas, except samples FNAS002, FNSG001, FNPS001 which were collected with permission from private property.

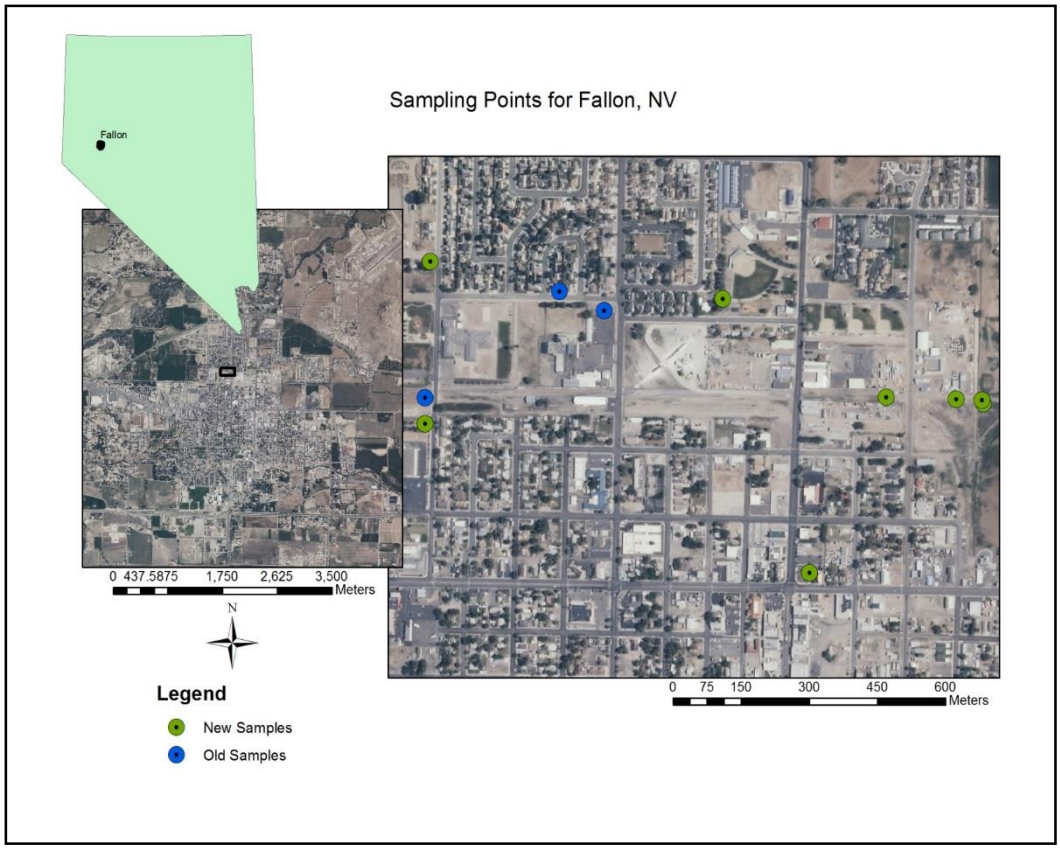

Figure 4.1 Sampling locations for Fallon, NV. The inset map shows location of Fallon within the state of Nevada. Samples were collected twice, the blue sites represent samples collected by Paul Sheppard and Mark Witten. The Green Samples represent samples collected fall 2012, under this current study. All these samples are sediment samples and are a combination of surface grab, auger, and soil probe collected samples.

Sierra Vista, AZ

Sierra Vista, while not frequently mentioned in the literature has been recorded as having similar problems as Fallon with W (Koutsospyros et al., 2006). This knowledge, along with personal correspondence with Mark Witten and Paul Sheppard led to the inclusion of Sierra Vista into this study, as it was confirmed that at least in the air particulate and surface dust, higher than average W levels were present (Sheppard and Witten, per comms).

Sierra Vista, AZ lies in between the Dragoon and Huachuca mountain ranges. It is in these ranges that W has been previously mined and it is believed that veins run in between the ranges. Sierra Vista lies closer to the Huachuca range, in its eastern piedmont. The range is composed of Precambrian granite, Paleozoic sedimentary rocks, and Mesozoic volcanic and sedimentary rocks. Sierra Vista itself is in the southern Basin and Range province of the Mexican

highland subprovince. The basin is filled with alluvium which is being deposited off of the Huachuca range. The primary post-tectonic sediments in the area are basin-fill from the Pliocence-early Pleistocene St. David Formation (Demsey and Pearthree 1994).

Sampling in Sierra Vista was guided by personal correspondence with Mark Witten. Having previously investigated the area, sampling locations were selected based on areas previously shown to have higher W concentrations in areas where sampling was accessible.

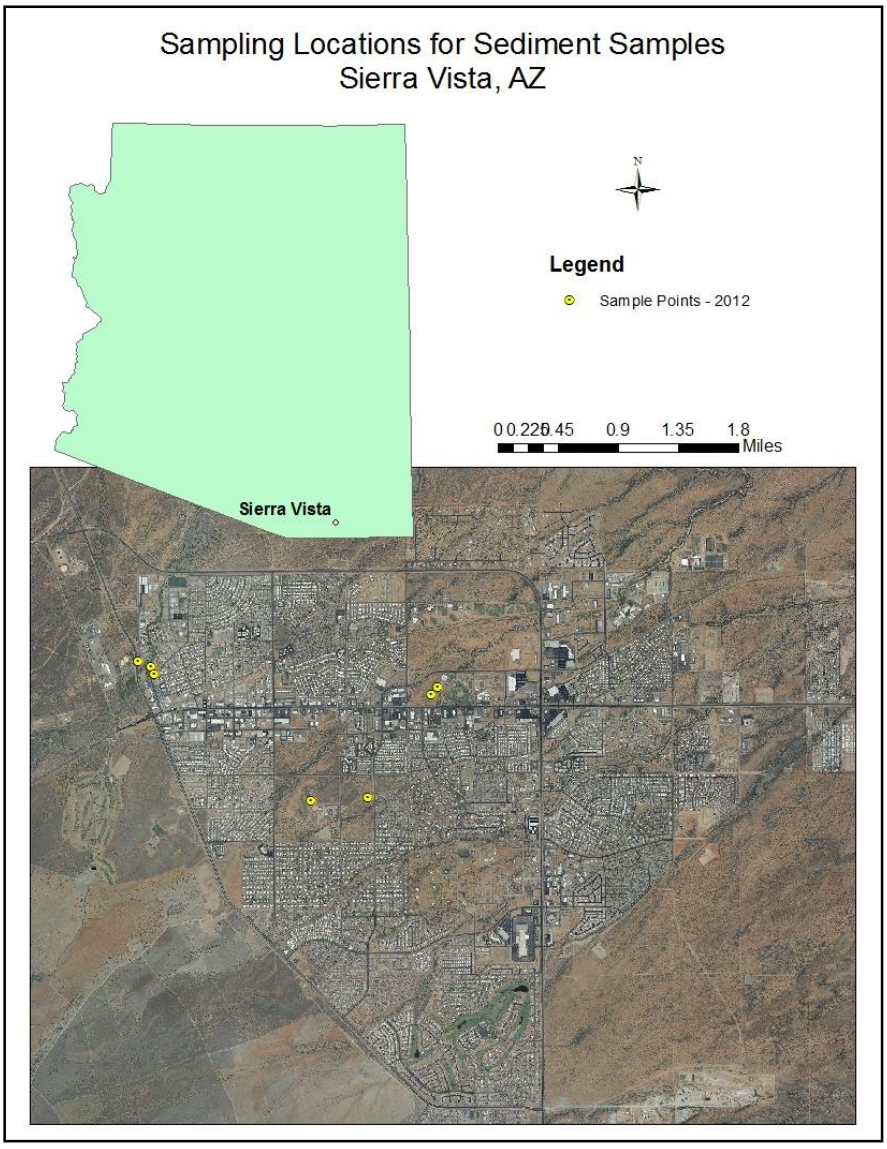

Figure 4.2 Sampling locations for Sierra Vista, AZ. The inset map shows location of Sierra Vista within the state of Arizona. Samples were collected in Spring 2012, represented by the yellow dots. All these samples are sediment samples and are a combination of surface grab, auger, and soil probe collected samples.

.

Cheyenne Bottoms Refuge

Cheyenne Bottoms Refuge is a wetland and migratory bird habitat in central Kansas. This wetland has had no geochemical research performed here in the past, however thanks to personal correspondence with Mark Witten, it came to be known that work done in the area was found to have very high W concentrations in tree rings, some of the highest found in the U.S.A. by Sheppard and Witten. Through conversation with a local, they found out that during WWII the wetland was used as a practice bombing range by the US Air Force base in Salina, to simulate short bombing runs. The W in this site supposedly originated from the bomb casings which contained a tungsten-steel alloy. This site is managed by the State of Kansas as a bird habitat as well as for bird hunting.

Cheyenne Bottoms is a natural land sink, the entire basin is approximately 41,000 acres and is located in Barton County, KS (Cheyenne Bottoms Wildlife Area Management Plan). It is part of the Smokey Hills physiogeographic area of KS and is part of the mixed-grass region. The site is characterized by Tabler-Drummond and Drummond silt loams. The area and the loams possess high sodium and soluble salts which originate from the Hutchinson salts of the Wellington formation. This formation is Permian in age and occurs primarily 10-45m below the surface but add salt to the soil as well as accumulate on the surface (Kindscher et al., 2004).

Sampling here was conducted on two separate trips. The soil itself is very dense, sticky clay and doesn't allow for depth profiles to be collected by hand. The area is quite large so a small transect was chosen for having features representative of the entire basin, including submerged areas, wet barren areas, wet vegetated areas, dry vegetated areas, dry barren areas, deep and shallow surface water. Water samples were collected in the deeper areas by berms and from the main pool.

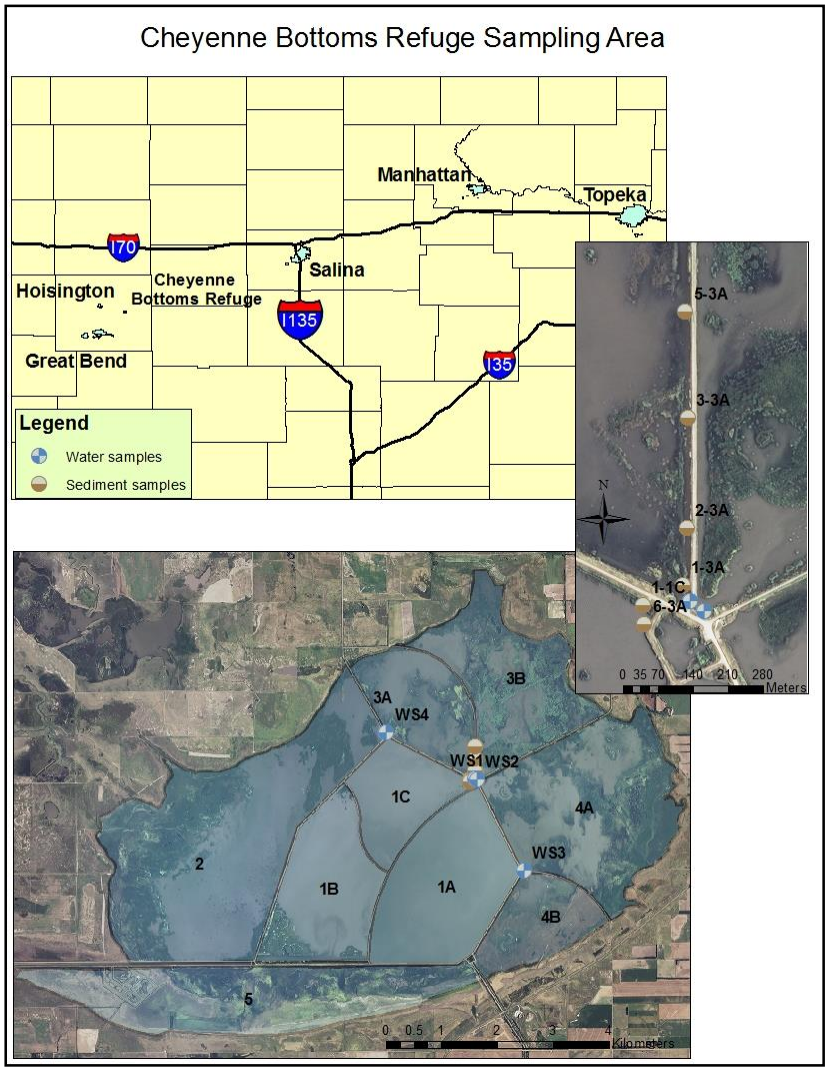

Figure 4.3 Sampling locations for Cheyenne Bottoms Refuge near Hoisington, KS. The inset map shows location of Cheyenne Bottoms within the state of Kansas. Samples were collected twice, first in Spring 2012, and then in Summer 2012. Brown samples represent sediment samples, while blue dots represent water samples. All the sediment samples are a combination of surface grab, auger, and soil probe collected samples.

Sample Collection

Sediment Sampling

Sediment samples were collected by hand auguring, collected at approximately 6" increments for the top 2' of sediment. This was done to understand the distribution of W with depth. The topmost surficial sediment was collected with hand trowels, stored in remel bags, and

placed in a cooler with dry ice. The augured sediments were preserved in the coring sleeves with anaeropouches®, filled with nitrogen gas and capped immediately after collection and placed in a cooler with dry ice for transportation back to Kansas State University where they were placed in the freezer until analysis.

Water Samples

The water samples collected from Cheyenne Bottoms were collected following standard EPA protocol. During collection, each bottle was submerged, filled and rinsed with sample water then the water was discarded, three times. The bottles were acid washed, and for each sample numerous bottle sizes were used for different types of analysis back at Kansas State University. For collection the bottles were fully submerged and capped under water so that no air was present in the sample. The samples were chilled in a cooler, transported back to Kansas State where they were refrigerated until needed. At each collection site, a Hach® Hydrolab was used to measure temperature, pH, resistivity, salinity, LDO, ORP, TDS, and specific conductance.

Laboratory Analysis

Total Extraction of Sediment

When investigating an elements presence in sediment it is first necessary to identify how much is present in the sediment as well as what other elements are there. This is the first step when investigating what relationships may be present in the samples.

Sediments were digested following a modified procedure outlined by Bednar et al., (2010a, b). The sediment samples were crushed and sieved with a 45 µm sieve to remove larger mineral fragments. For the extraction, 0.5 g of the prepared sampled was weighed out and placed in teflon tubes. To the sample was added 1mL concentrated phosphoric acid and 5mL 1:1 nitric acid:deionized water, the sample was heated to 95°C for 30 min. Four more additions of 2.5 mL conc. nitric acid were added every 30 min., after the final aliquot the mixture was heated for 2 hours. After cooling, 3 mL of 30% hydrogen peroxide was added and the mixture was heated again for 15 min. After cooling, 2mL 30% hydrogen peroxide was added and the mixture was heated for an additional 2 hours. Then, the digestate was cooled to room temperature and filtered with Whatman #40 paper and diluted to 50 mL with 1% nitric acid. The samples were then

diluted to lower the amount of P going through the instrument with a 1:4 dilution. Tungsten concentrations were determined by Inductively Coupled Plasma Mass Spectrometry (ICP-MS following modifications of EPA Method 6020A), using a Perkin Elmer Elan DRC-II equipped with a MiraMist nebulizer and cyclonic spray chamber. The ICP-MS plasma was operated at 1250W and nebulizer gas flow of 0.85 mL/min. Tungsten was quantified at m/z 182 with confirmation using m/z 184 after correction for 184Os. The ICP-MS was calibrated using NIST-traceable standards containing 0, 0.001, 0.01, and 0.1 mg/L tungsten, and used holmium and terbium as internal standards to correct for instrumental drift. All calibration responses were linear and had correlation coefficients of at least 0.9999. A second source calibration verification standard was analyzed immediately after calibration; analyte recoveries were within ±10 % of the nominal value. Continuing calibration verification standards and blanks were analyzed periodically throughout the analytical batch, with recoveries within ±10 % of the nominal and subsequent blanks below the instrument reporting limits.

Sequential Extractions of Sediment

To help ascertain the W fractionation in various sediment fractions a six-phase sequential extraction procedure was used to characterize the W present in the exchangeable, carbonate, manganese oxide, iron oxide, organic matter, and the sulfide/residual phases. This procedure was not performed on all samples, but rather a smaller representative number of samples. The method was adapted from Cutler (2011) and Tessier (1979). The first step in this procedure was an exchangeable phase extraction using 10mL 1M ammonium chloride, shaken for 2 hours at 20°C. Then the carbonate phase was extracted using 25mL 1M ammonium acetate at pH 5, shaken for 24 hours at 20°C. For the manganese oxide phase 25mL 0.1M hydroxylamine hydrochloride at pH 2 was used, shaken for 30 minutes at 20°C. The iron oxide phase was extracted with 20mL 0.04M hydroxylamine hydrochloride with 25% (v/v) acetic acid for 6 hours at 95°C. For the organic matter phase, 25mL 0.1M sodium hydroxide was used for 24 hours at 20°C. Finally, the residual/sulfide phase was extracted with 1mL concentrated nitric acid and 3mL hydrochloric acid mixture for 1 hour at 100°C. Before heating 4mL 30% hydrogen peroxide was added, and heated until consumed. This was repeated twice more with the addition of 1mL concentrated nitric acid and 4mL 30% hydrogen peroxide. The phase extractions are summarized in Table 4.1.

After digestion, each phase was diluted with 1% nitric acid and analyzed by ICP-MS and ICP-AES.

Table 4.1 Steps for Sequential Extractions used, modified from Tessier (1979) and Cutler (2011)

Step	Reagent	Phase	Time/Temp.
1	1M NH_4Cl	Exchangeable	2 h, 20°C
2	pH 5, 1M NH_4OAc	Carbonate	24 h, 20°C
3	pH 2, 0.1M NH_2OH*HCl	Mn Oxides	0.5 h, 20°C
4	0.04M NH_2OH*HCl in 25% (v/v) HOAc	Fe Oxides	6 h, 96±3°C
5	0.1M NaOH	OM	24 h, 20°C
6	Conc. HNO_3 + conc. HCl + 30% H_2O_2	Sulfides/Residual	1 h, 100°C x3

Water Extractions

Water extractions were performed by shaking 0.5g of sediment with 5 mL deionized water overnight. The extract was centrifuged for 10 minutes then decanted, filtered with a 0.45 µm syringe filter, then diluted 1:2 with DI water and analyzed by HPLC-ICP-MS to determine the W species present (Bednar et al., 2009).

Water Analysis

Water collected from Cheyenne Bottoms Refuge was analyzed on site with a Hach® hydrolab probe. Samples collected where then sent to ACT labs for multielement and anion analysis by ICP-MS and IC.

Spectroscopic Analysis

To ascertain more information about the elemental associations of W as well as provide information about the speciation of the W present in the samples, solid state analyses were conducted at the National Synchrotron Light Source I at Brookhaven National Laboratory and at Kansas State University.

Scanning Electron Microscope/Energy Dispersive X-ray Spectroscopy

At Kansas State University in the Department of Biology Scanning Electron Microscopy-Energy Dispersive x-ray spectroscopy was performed. The SEM provides imaging of the samples which can help with the composition of the samples. With EDX, elemental scans and overlays were produced that identify were W was in the sample as well as what it is associated with. While this isn't conclusive, it gives an idea about where the W is and what it may be interacting with.

X-Ray Absorption Spectroscopy

To assist in the chemical characterization of the soils, synchrotron studies were conducted at the microprobe beam line X27A at the National Synchrotron Light Source, Brookhaven National Laboratory. For each site, several samples were selected that were thought to contain the highest W for that site. The sampling procedure was to first lightly grind the sediment to achieve a homogenous grain size. The samples were then lightly scattered onto Kapton tape and placed in front of the beam for analysis. This was done right before the sample was to be analyzed to help prevent oxidative change in the sample. The samples were first analyzed using micro X-ray fluorescence (µXRF) imaging to determine W distribution in the sample and to evaluate if any co-localization with other chemical elements occured. Typical XRF scans were conducted on a 1 x 1 mm area with the incident beam energy set at 11 keV. Full XRF spectra were recorded for each pixel and it was common practice to compare images of W Lb and W La to verify that spectral overlaps with Ka and Kb emissions of other elements did not interfere with the W signal. Once W "hotspots" were found, µXRD (at 17479 eV) was used to determine the mineralogy. After this, µXANES were run on the same spot over the W L3 edge to produce spectra which were compared with known standards to determine W speciation. Standards were run to establish data for the W oxidation states 0, IV, and VI. The standards used were W metal powder, WS_2, and WO_3.

Chapter 5 - Results

Total Digestions

All samples had measurable levels of W by ICP-MS. In the Fallon samples, the highest concentrations are seen with Fallon 3 having the most at 25907 mg/kg (Fig. 5.1). There is a wide range in W concentration for the Fallon samples, with the low at 37.4 mg/kg for sample FNPS001. These values vary over space and depth. The samples typically decrease in W concentration with depth, and vary over space with the highest concentrations near the center of the sample area.

In Sierra Vista the W concentrations are lower with a range of 20.2 mg/kg (TF020) to 1515.9 mg/kg (MS002). The samples show a similar trend of decreasing W concentration with depth, except for the MS samples which increase drastically with depth. The samples that had 3 different depths sampled (LA001, LA010, LA011; PK001, PK010, PK012; TF010, TF020, TF021) show a decrease with the initial depth (~0-15cm) and then an increase in concentration to the next depth (~15-30cm).

The Cheyenne bottoms samples show the narrowest range in values ranging from 16.5 mg/kg (CBR2_3a) to 246.8 mg/kg (CBR1_1c). Unlike the other two sites, the Cheyenne Bottoms samples do not have samples with depth increments. Since these samples were hand augured the limits of sampling were determined by the substrate and the clay in Cheyenne Bottoms would not allow for collection by hand at further depths. With these samples, the only relationship that can be relayed is one of horizontal relationship. CBR 1_1c was the sample with the highest concentration, and it was also the only sample from one of the main central pools of the wetland. The other samples from the smaller ponds to the north north-east had very similar concentrations an order of magnitude lower than that of CBR1_1c.

Table 5.1 Bulk W concentration in sediment samples in mg/kg, from all sample sites analyzed by ICP-MS. CBR stands for Cheyenne Bottoms Refuge, FN is for Fallon samples, samples Joyce through TF are from Sierra Vista where LA stands for open land, MS for middle school, PK is for park, and TF is for the University of Arizona trust fund land.

Sample	W (mg/kg)	Sample	W (mg/kg)
CBR1_1a	16.1	FNSG004	80.5
CBR1_1c	246.8	FNSG005	104.1
CBR2_3a	16.5	FNSG006	80.9
CBR4_3a	27.0	FNSG007	378.1
Fallon1	7069.6	Joyce	21.8
Fallon2	333.5	LA001	33.1
Fallon3	25907.4	LA010	22.8
FNAS001	296.7	LA011	40.8
FNAS002	124.7	MS001	460.5
FNAS003	737.0	MS002	1515.9
FNAS004	92.6	PK001	25.2
FNAS005	59.4	PK010	19.8
FNAS006	76.3	PK012	31.2
FNAS007	61.5	PK020	41.2
FNPS001	37.3	PK030	37.3
FNPS002	37.6	Pool3B	28.0
FNPS003	107.3	TF001	26.6
FNSG001	179.7	TF010	20.0
FNSG002	1286.6	TF020	20.1
FNSG003	674.6	TF021	17.8

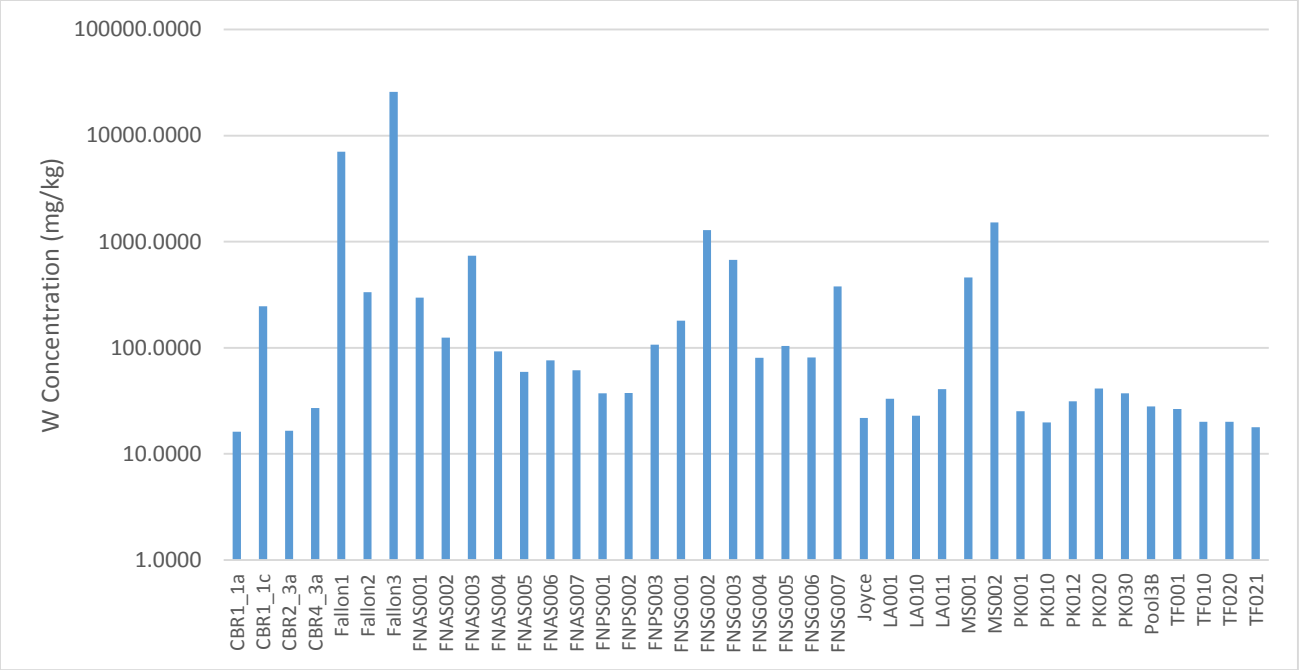

Figure 5.1 Bar graph depicting bulk W concentration in sediments in mg/kg from three sites; Fallon, NV, Sierra Vista, AZ, and Cheyenne Bottoms, KS.

Tungsten also shows a correlation with Co in the Fallon samples ($r^2 = 0.95$). It does not seem that other good correlations exist with W in these sediments. These relationships change somewhat with the removal of two outliers (Fallon 1, Fallon2). For Co the r^2 value changes to 0.62. The r^2 for Cheyenne Bottoms for W/Co is 0.73. Sierra Vista however has a r^2 value of 0.06, this could have implications on the origin of the W in the sediment, as Co is often used in alloys to delay oxidation (Ogundipe et al., 2009).

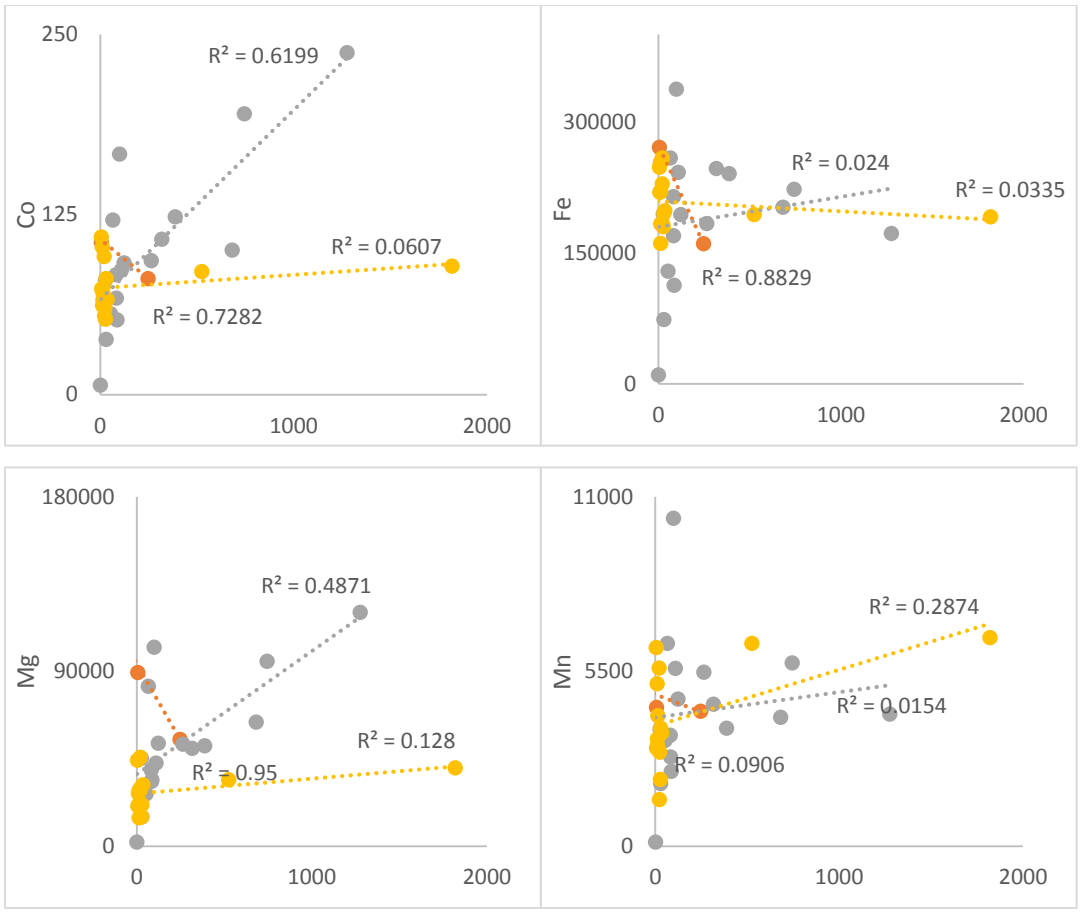

Figure 5.2a Correlation plots of total concentration for select elements with W in mg/kg for each sampling site (Grey -Fallon, Yellow - Sierra Vista, Red - Cheyenne) with respective r^2 values. Outliers (Fallon 1, Fallon 2) have been removed to better show correlation.

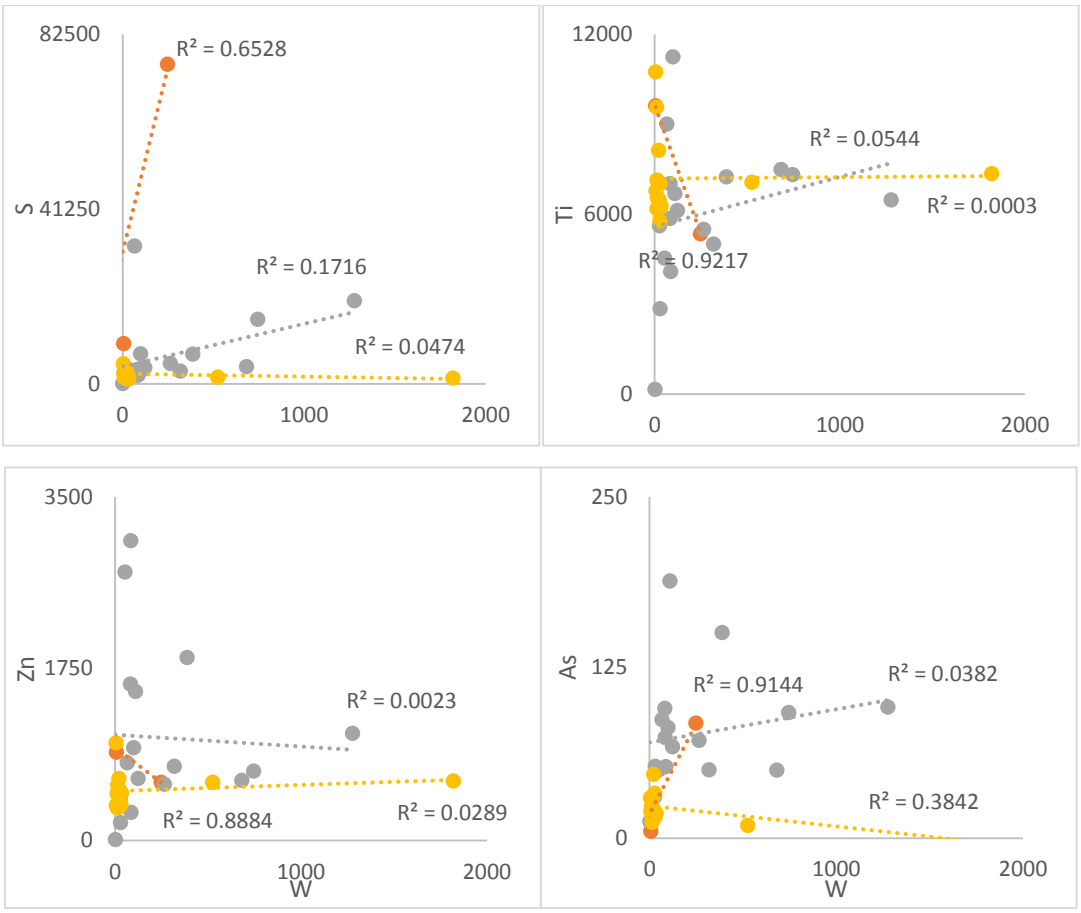

Figure 5.2b Correlation plots of total concentration for select elements with W in mg/kg for each sampling site (Grey -Fallon, Yellow - Sierra Vista, Red - Cheyenne) with respective r^2 values.

Sequential Extraction

The sequential extractions were performed on a smaller number of samples than the total extraction, focusing on samples that were related to each other and having relevant W concentrations. In all 3 sites, the largest fractions are the OM and sulfide/residual phases. These vary from sample to sample with no pattern in regards to depth or spatial relation. The third largest fraction is the exchangeable phase, where some patterns do emerge.

In Fallon, the exchangeable phase shows a trend of decreasing in W concentration with depth, except for samples FNSG001/FNAS002. The Sierra Vista samples show the same trend from depth 1 to depth 2. However, the change to the final depth shows an increase in W concentration in the exchangeable phase. Also, it seems that the W concentration in the exchangeable phase does not correlate directly with total W concentration. So, the percent of W in the first phase is not directly linked to an increase in total concentration.

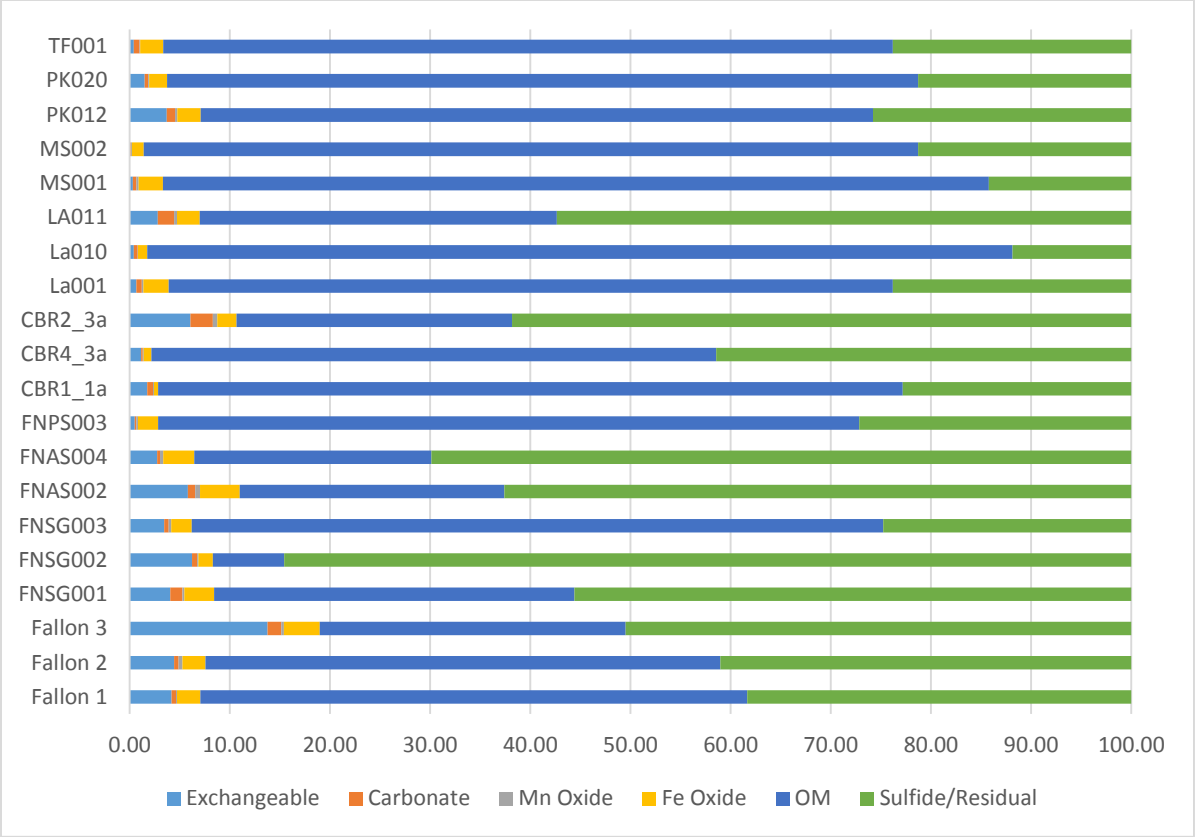

Figure 5.3 Bar diagram to represent percent composition of W in the six phases of the sequential extraction as analyzed by ICP-MS. Here FN samples are from Fallon, CBR samples are from Cheyenne Bottoms, and samples LA-TF are from Sierra Vista.

Depth Comparison

Several sampling locations in Fallon and Sierra Vista represent shallow depth profiles. In Fallon and Sierra Vista all samples show a decrease in bulk W concentration from the surface to a depth of approximately ~1ft, with the exception os sample MS001/MS002. The Sierra Vista samples have another depth increment which indicates a depth of ~6 in. to 2ft. Samples LA001/LA010/LA011 and PK001/PK010/PK012 show an increase in bulk W concentration from ~1ft to 2ft, while sample TF010/TF020/TF021 show a slight decrease in bulk W concentration at this depth. Samples at depths below ~6 in to 1ft were not able to be collected from Cheyenne Bottoms.

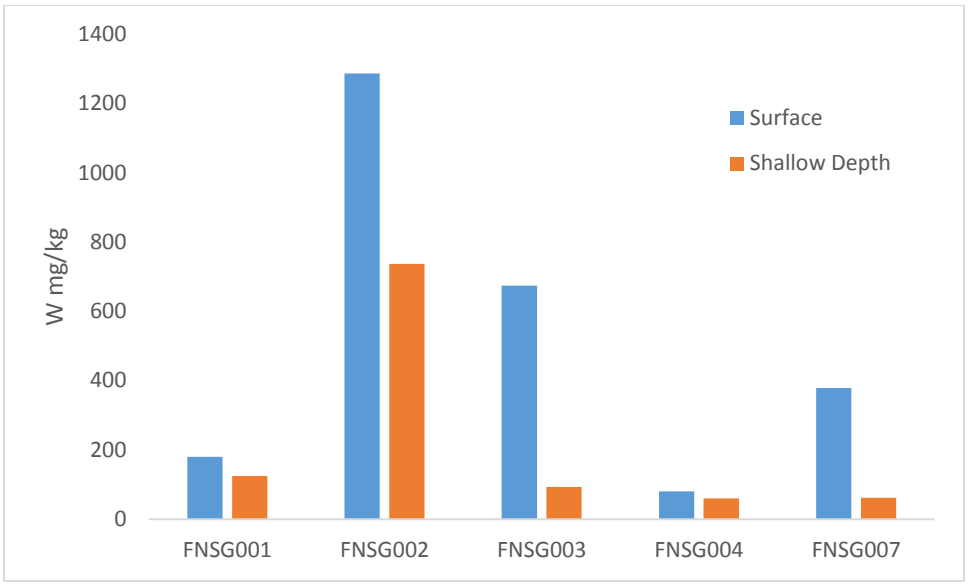

Figure 5.4 Comparison of samples representing a shallow depth profile for Fallon, NV. Labels indicate the surface sample at the specific sampling location.

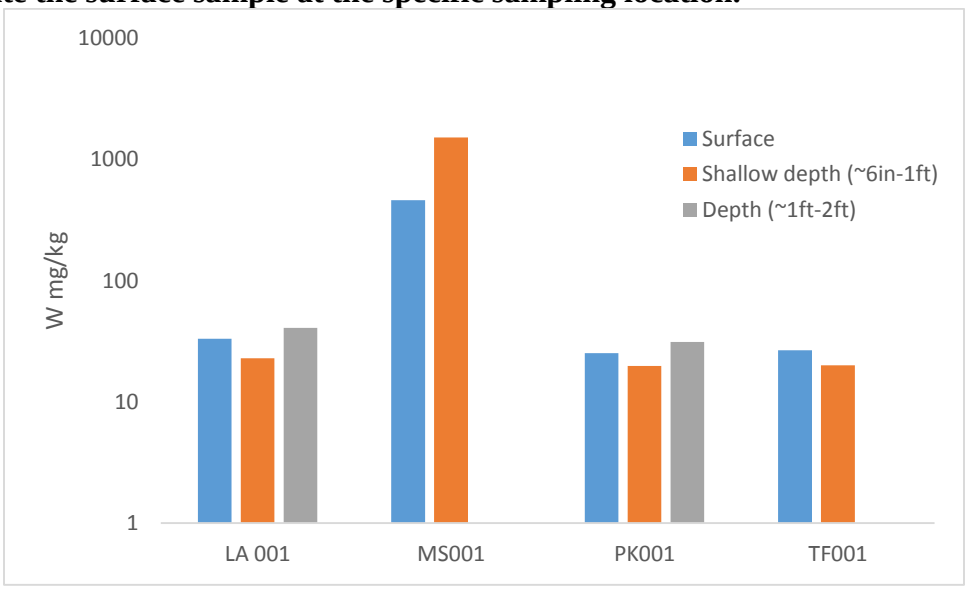

Figure 5.5 Samples from Sierra Vista, showing change in bulk W concentration within depth profiles.

Water Extractions

The extractions were performed on samples that had enough W in the exchangeable phase of the sequential extraction to be accurately detected by the HPLC-ICP-MS. Due to observed W concentrations in the exchangeable phases, all of the samples analyzed for W speciation were from Fallon. The samples used were Fallon 1 (3429 µg/L), Fallon 2 (90 µg/L), Fallon 3 (6931 µg/L), FNSG002 (270 µg/L), FNSG003 (280 µg/L), FNSG005 (46 µg/L), and

FNSG006 (110 µg/L).The concentrations listed above are lower than what was seen by Bednar et al., (2009) in their extractions (125 mg/L) but are still measurable and not loaded with metallic W as where the soils in their experiments. These extractions suggest that W does occur in exchangeable form in the Fallon samples. In Fig. 5.6, we see several W species present in these samples. In general, there appears to be two major forms of W present, tungstate, and an unidentified tungsten species. Due to the mechanism of retention in size exclusion chromatography, large polymeric species elute first, followed by tungstate, as shown by the standards in Fig. 5.6. However, any species that elutes after tungstate must be smaller than tungstate (which is not practical) or is retained on the column by a secondary mechanism (e.g. ion exchange or hydrophobicity). Therefore, it is postulated that the late eluting tungsten species observed in Fig. 5.6 are likely polymeric species that may have organic moieties associated that provide hydrophobic retention mechanisms. Currently this is only hypothesized, as more structurally informative Mass Spectrometric analysis is needed to confirm (Bednar et al., 2009).

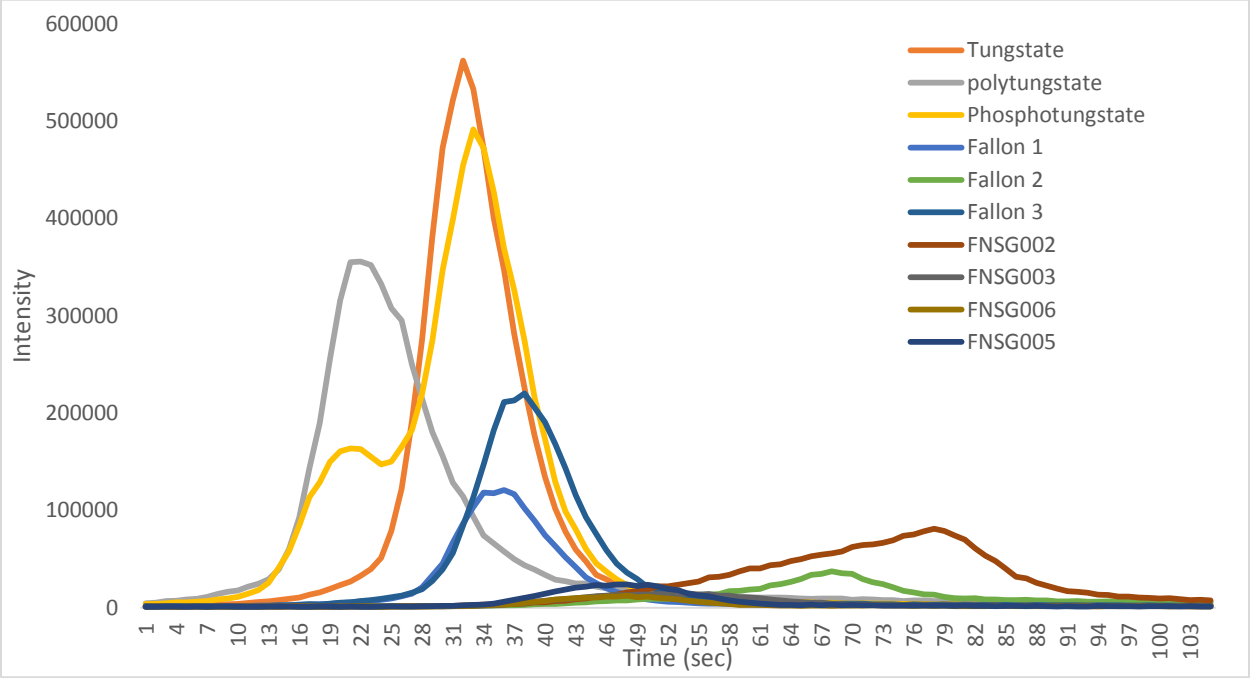

Figure 5.6 Speciation of water extractable W by HPLC-ICP-MS for only selected samples (with known high bulk concentrations of W). The standards here are tungstate, polytungstate, and phosphotungstate. The only samples shown here are from Fallon. Fallon 1, 2, and 3 are old samples and the FN samples are from this study.

μXRF

Fig. 5.7 shows the discretely dispersed, but highly concentrated "spotty" nature of the W that is present in sediments in the Fallon, Sierra Vista, and Cheyenne Bottoms samples. These patterns show W tends to be highly localized rather than uniformly dispersed. For comparison, Fig. 5.8 demonstrates how other elements tend to be more heterogeneous in samples. Since W is more dispersed with very localized concentrations the microprobe beam line set up was more applicable than a bulk beam line, where the W would be less noticed since the bulk concentration is low. Here the hotspots can be individually analyzed on the μm scale, where the area measured is the width of the beam. All 3 sites displayed the same trend of scattered, concentrated hotspots with some minor differences.

Fallon contained more hotspots per area than the other two sites. Fallon also contained a wider range of intensity (qualitative measure of concentration) for the hot spots. Sierra Vista and Cheyenne Bottoms both had significantly fewer hot spots per area, but contained higher overall intensities. In Fig. 5.7 it can be seen by the scale that the hot spots for all samples are an order of magnitude higher than the background. However, the hot spots for Sierra Vista are an order of magnitude higher than in Fallon, and in Cheyenne Bottoms they are two orders of magnitude higher than Fallon.

μXANES

It can be seen from the comparison of the spectra and the LCF analysis that the majority of the samples contain similar forms of W. The sample spectra appear simple, without pre-edge features, and similar post edge features and mostly overlapping white lines. The predominate form is a mix of W (0) and W (VI), except for a sample from Sierra Vista where some W (IV) appears to be present over W (VI) and another from Sierra Vista that contains all 3 W oxidation states, with W (IV) being significantly less than W (0) and W (VI). It can be inferred that the W particles in the sediment could be W metal particles undergoing oxidation/dissolution. While our analysis were not comprehensive (more runs with a larger variety of standards need to be done) to obtain exact speciation, it allowed for qualitative oxidative-state speciation fo W. In general they showed small variation of the oxidative species present in the dry sediment.

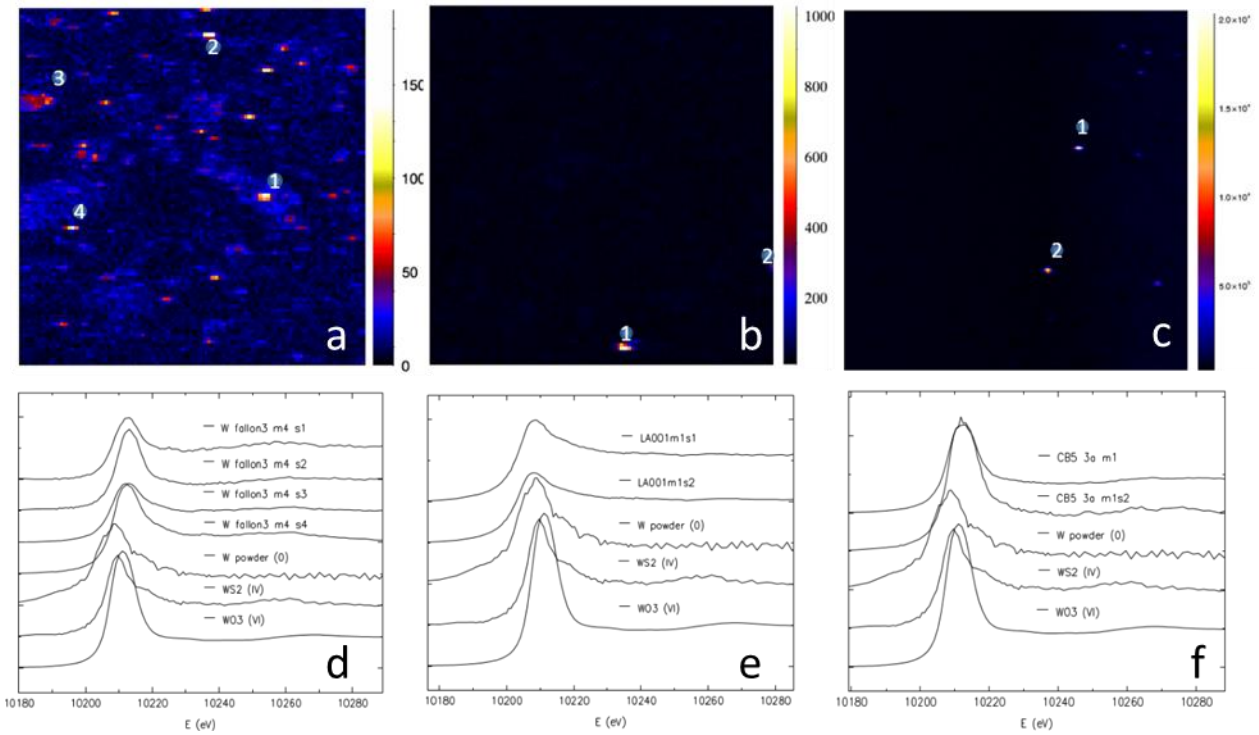

Figure 5.7 µXRF maps of Fallon, Sierra Vista, and Cheyenne Bottoms samples and µXANES of selected hotspots. Figure 9a, b, c respectively are from Fallon, Sierra Vista and Cheyenne Bottoms. Figure 9d, e, f represents the W XANES spectra from the selected points along with standard spectra. Spectrum number correspond to labeled points on XRF maps.

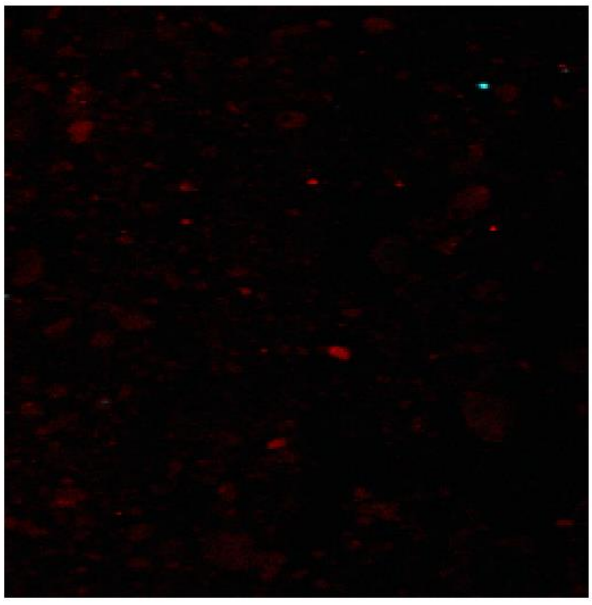

Figure 5.8 Multi-element XRF plot from sample Fallon 3, to show the combined presence of Fe (red) and W (blue). Here, Fe shows a more homogenous presence throughout the sample, while W is much more spotty in occurrence, as shown in the dispersion pattern map above.

Linear Combination Fitting

In Athena, spectra are compared using linear combination fitting, which estimates the composition of the sample using the given standards. Given the standards used the results are summarized below in Fig. 5.9. Fallon and Cheyenne Bottoms samples show a mix of W metal and W oxide. Sierra Vista show two spectra with components of WS_4, while one spectra is a mix of W metal and W oxide like in Fallon and Cheyenne Bottoms.

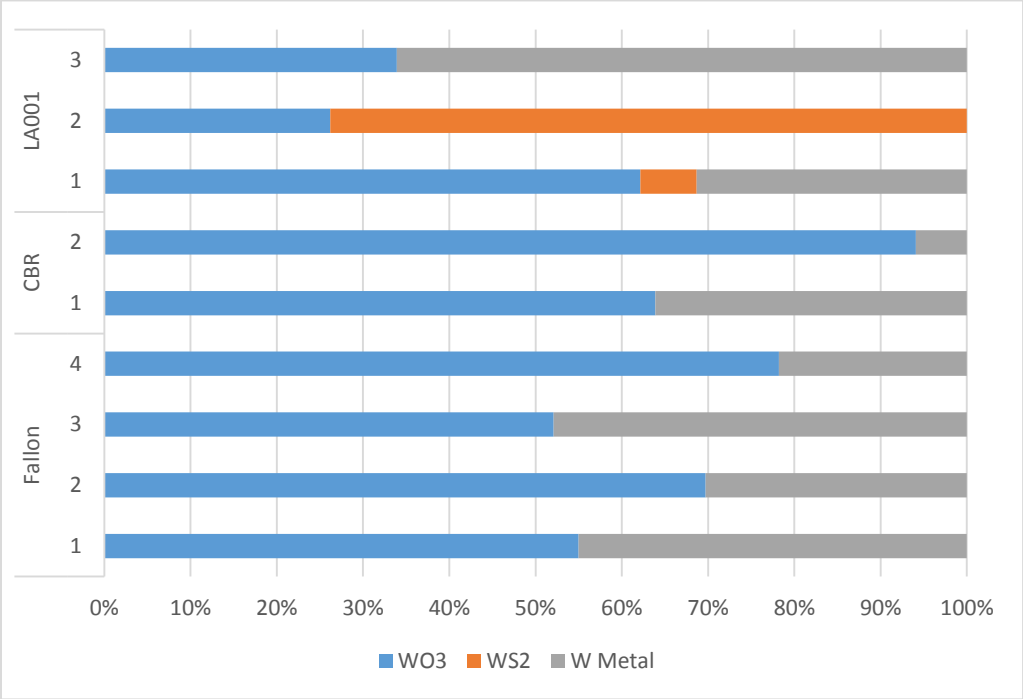

Figure 5.9 Results of several XANES spectra analyzed in Athena for samples from Fallon, Cheyenne Bottoms and Sierra Vista as percent of each standard.

Table 5.2 Statistical results for the Linear Combination Fitting performed on samples in Athena.

Sample	Spot	R-factor	chi-squared	reduced chi-sq.	WO_3%	WS_2%	W Metal%
Fallon	1	0.31	21.97	0.36	55	0	45
	2	0.20	17.35	0.36	69.7	0	30.3
	3	0.27	18.65	0.35	52.1	0	47.9
	4	0.08	10.32	0.21	78.2	0	21.8
CBR	1	0.14	11.94	0.17	63.9	0	36.1
	2	0.028	5.12	0.07	94.1	0	5.9
LA001	1	0.04	4.36	0.10	62.1	6.5	31.3
	2	0.10	7.17	0.16	26.2	73.8	0
	3	0.15	12.06	0.22	33.9	0	66.1

SEM-EDX

The SEM analysis reveals a similar dispersion pattern as the µXRF. The SEM does not include as many instances of W hotspots, however, the scale of the area imaged is much finer (150 µm x 100 µm) than the area imaged by the micro probe (1 x 1mm). Fallon and Cheyenne Bottoms were the only samples analyzed because of the scale. The frequency of hot spots in Sierra Vista led to it not being able to be included in analysis since no W hot spots were located. The EDX analysis reinforces the W dispersion pattern and shows that it tends to co-localize with several other metals as well as common mineral forming elements. Since, SEM-EDX measures a depth, while displaying a 2D surface, direct mineral correlations are not necessarily accurate since the W can be related to, a part of, or just near the particle imaged. One thing both sites have in common is that the EDX analysis of W for the total image is low, while spot scans reveal much higher W weight percent's. This reinforces the notion that when analyzing W it is important to have fine scale methods so that the W can be detected and analyzed. The Fallon data and the Cheyenne Bottoms data do show some different relationships.

In Fallon, W shows co-localization with Co, Cu, Ti, and Zn (appendix c). In the Cheyenne Bottoms samples though, the W does not appear to co-localize with any elements. Interestingly, each sample from Cheyenne Bottoms does illustrate Mo, W's close relative element, with several associations (Ba, S appendix c). This is interesting since W and Mo tend behave very similarly and replace each other in various scenarios.

Chapter 6 - Discussion

The aim of this study was to gather information on the occurrence of W in the environment and make inferences to be extrapolated towards modes of occurrence of W in sediments. Chemical analyses by state of the art geochemical techniques were used to understand the behavior of this element in the three areas studied. By studying the three different sites a comparison of the results can infer more about W's behavior in sediments.

Fallon

The highest bulk concentrations of W are seen in Fallon as compared from the other two areas of study. The average total W for Fallon (1886. 3 mg/kg) is two orders of magnitude higher than in Cheyenne Bottoms (66.9 mg/kg) and one order of magnitude higher than in Sierra Vista (155.6 mg/kg). There is also a broad range of values obtained from Fallon spanning three orders of magnitude (37.4-25,907 mg/kg). This heterogeneous nature of W distribution in Fallon was previously shown by Sheppard et al., (2007b). Spatial variability of W concentration in Fallon shows that in the 1.2km x 650 km area sampled, higher concentrations tend to occur to the northeast corner of the area sampled (Fig. 4.1). Fallon samples collected near a facility within the study area (samples Fallon 1 and Fallon 3) are significantly higher than all the other samples analyzed. The highest of the samples used to frame the study area (NE, NW, SW, SE corners of the extent of study area) was FNSG003 (1286 mg/kg) in the northeast corner. A transect was delineated during the second Fallon trip, which is a west to east trending transect. The transect shows decreasing W concentration going west to east, or away from the center of the area sampled (378 mg/kg at FNSG007; to 104 mg/kg; 80 mg/kg; 76 mg/kg in FNSG006, FNSG004, FNAS006 respectively).

The only element to show a correlation with W in Fallon is Co (Fig. 5.2b). Bulk Co concentrations are lower than the bulk W bulk concentrations in the sediments in Fallon, but bulk Co concentrations also vary spatially the same way as W. The only samples that break this pattern are Fallon 1 and Fallon 2. Of these two samples, Fallon 1 has the higher W bulk concentration but the lower Co bulk concentration, while Fallon 2 has higher bulk Co and less bulk W concentrations. Wind direction and speed are important factors in the distribution of W

(and possibly Co) in Fallon, but distance from the center of the study area (approximately near Fallon3) is the most important factor (Sheppard et al., 2006).

Generally, the trend indicates that W bulk concentrations tend to decrease with increasing distance from the center of the study area. All Fallon samples also show a decrease in bulk W with depth (0-0.6m). The shallow depths analyzed in this study differ from other sediment work executed in Fallon. Cutler (2011) sampled sediments at depths ranging from 6 to 36m, mostly around the city of Fallon, whereas the current study analyzed sediments from within the city. Samples analyzed by Cutler (2011) also demonstrate a trend of decreasing W concentration with depth (with the exception of sample CDP-39 which had a slight increase of ~2 mg/kg over 11m). These two studies show vastly different depth profiles, but the same trend exist. However, further comparison warrants careful consideration since the W present at depth is of a different origin, or has undergone significant geochemical alteration, since the hypothesized method for W deposition in Fallon is from air. Sheppard et al., (2006, 2007b) analyzed air and surface dust, finding significant quantities of W (up to 935 mg/L). Fallon, NV is in an area with natural W deposits, and subsurface concentrations may be of natural origin (Cutler 2011; Seiler et al., 2005) as suggested by several researchers, this does not explain the high concentrations found in air particulate and near surface samples by Sheppard et al., (2006) and this study. A more likely scenario is one of mixing, where there is anthropogenic input at the surface and some component of mixing in the subsurface. Support for this is also in Sheppard et al., (2007a), where morphological and chemical characterization techniques were used on W particles found in Fallon and they found them to be of anthropogenic origin.

By SEM-EDX, it is demonstrated that W in Fallon tends to co-localize with Mn and occasionally other elements (Co, Ti, Zn; with Co being a common alloying metal with W, see appendix C). Interestingly, Mo which is closely related to W, is not found associated with W (as may be expected in natural settings), but rather with S, possibly in mineral associations like molybdenite (MoS_2). It is common for W and Mo to replace each other in a variety of compounds, in all the samples analyzed by SEM-EDX Mo is found co-localized with S while W is not found associated with neither S nor Mo. Given the difficult nature of analyzing W in these sediments at such a fine resolution (µm scale), the only samples used for SEM from Fallon were surface samples, where the bulk W concentrations were higher. This could explain why there are not many elemental associations found. Since it is postulated that the W in the near surface

samples in Fallon are of metallic origin, it would not be expected to be associated W with anything besides alloying metals since the W metal is only beginning to be oxidized and dissolved and hasn't yet begun to polymerize or engage in geochemical reactions with the surrounding sediment.

In both SEM and μXRF mapping, W distribution in sediments is relatively sparse, when compared with other elements (Fig. 5.8). The W "hot spots" are typically highly concentrated, suggesting a high W content and are typically only a few microns wide. The LCF interpretations also reveal an affinity for the W (0) and W (VI) forms, which are a combination of the W metal and oxide forms. XANES analyses of these W hotspots reveal most of them to be of similar composition with minor variation. It seems that the W is of the W (VI) form which supports the idea that WO_4^{2-} is prevalent in the Fallon samples. Some limitations do exist in further interpretation with the lack of available standards and reference materials. However, based on the available reference materials it is evident that the tungsten is mostly in the VI form with some W being seen as a mix of W metal (O) and W (VI). Bostick and Sun, (2013) showed in their samples that the W present in firing range soil (e.g. of a W metal source) had rapid oxidation and prevalence of WO_4^{2-} and polytungstates with a lack of mineral phases. These were poorly retained in the soil, suggesting that W species were highly soluble. As was shown in the XRF images, the W is highly localized onto concentrated hotspots. The lack of homogeneity in these samples could also lead to disproportionate extracts in analyzing the sample, in terms of recovering W. This is an important factor to keep in mind in association with bulk concentrations. Since the majority of W is related to a few, highly concentrated, dispersed particles.

Since the W in this study is of a metallic origin it is important to consider the fate of metallic W in the environment. As the metallic W or WC is oxidized and dissolved, following a process that has been well documented, WO_4^{2-} is released as the product in the presence of water (Warren et al., 1996; Andersson and Bergstrom 2000). As the W migrates, polymerization can occur and the monomeric or poly- W species can be adsorpted onto the surface of Mn/Fe oxides in the sediment, this is an important process (Cutler 2011; Bednar et al., 2008). Bednar et al., (2008) compared solubilities of WO_4^{2-} and polytungstates and found that all the W species found had lower K_d values than monomeric WO_4^{2-}. This study (Bednar et al., 2008) also noted that while some of the polytungstate species were stable, other poly- species were not stable and

usually changed speciation over time, altering partition coefficients. In the current study, no polytungstate species were detected, although one may have been detected that was retained in the column (unknown W species found Fig. 5.6). In the water extraction performed for this study, all of the WO_4^{2-} was from surface samples. Tungstate is the first stable species W metal will form under oxidizing conditions (Warren et al., 1996). Both Bednar et al., (2009) and Xu et al., (2009) showed W and WO_4^{2-} can easily be sequestered by sorption reactions. In Bednar et al., (2009), it was pointed out that the leaching sediment containing W over clean sediment, the W was retarded in the sediment. Xu et al., (2009), demonstrated the strong affinity of WO_4^{2-} to sorption onto the surface of goethite. These studies illustrate the variable nature of sequestration where W species is an important factor. It is likely that the metallic W found in surficial sediments was oxidized, and then mobilized as WO_4^{2-} which was found in the water extraction results. Since W can be sequestered more easily as monomeric WO_4^{2-} than as polytungstates, it is important to consider phase association of W since that will give insights into W mobility.

Sequential extraction results from Fallon show a larger amount of W to be present in all phases (by percent) relative to the other sampling sites. The sequential extractions results from this study are considerably different from Cutler (2011) study. W was shown to be mostly in Mn/Fe oxides phases and the OM (Cutler 2011). In the current study, W is seen to be mostly associated within the less bioavailable phases (sulfide/residual and organic matter (OM). Fallon samples show W also associated with exchangeable phase and not so much to the carbonate and Fe/Mn oxide phases. W in the exchangeable phases is also present in higher quantities in the Fallon samples than the other two sites, with Fallon averaging ~5%, with ~3% in Cheyenne Bottoms, and ~1.2% in Sierra Vista. In the sequential extractions performed by Cutler (2011), marginal quantities of W were recovered in the exchangeable phase (>0.3 mg/kg). The dominant phases of Cutler's (2011) extraction were the crystalline Fe oxides (36%), non-crystalline Fe oxides (29%), and the OM phases (28%). Since the samples in Cutler's study represent greater depths, this can corroborate what was found in this study, where there is a decrease in the exchangeable phase and an increase in the oxide phases (starting at the near surface, extending to a shallow depth). While the phase associations of W shown by Cutler (2011) differ from what is stated in this study, it is important to keep in mind the differences of sampling depth. These studies do not necessarily contradict each other, rather, together fill out more information about

W since Cutler (2011) did not collect surface or near surface samples which was the target of this study.

Sierra Vista

In Sierra Vista, W analyzed shows some different trends geochemically. From bulk concentrations, it is shown that there are no correlations with other elements like what we see in Fallon (highest $r^2 = 0.38$ in correlation for W and As). Tungsten concentration in Sierra Vista shows a range of two orders of magnitude (17.81-1515.96 mg/kg). However, all of the sample points besides MS001/MS002 (460.51 mg/kg and 1515.96 mg/kg respectively) are in the range of ~20-40 mg/kg of bulk W. Thus, no spatial pattern can be established in Sierra Vista. However, samples LA001/LA011/LA010 and PK001/PK010/PK012 show that W concentration increases (45% and 39% respectively)at the depth of 6"-1' (Fig. 5.4).Sample series TF010/TF020/TF021 show a slight decrease (11% decrease) in W concentration from ~6"-1'. The phase associations of W in Sierra Vista also indicate W mostly present in the organic matter and sulfide/residual phases. Depth analyses for Sierra Vista samples do reveal that W concentration decrease with depth for all samples up to 6". While Fallon showed variable change based on phase association(Only exchangeable and Mn oxide phases showed a pattern), Sierra Vista samples show an initial decrease (~0"-6") in phase associated W followed by an increase (~6"-1') in W phase association for the exchangeable, carbonate, and Fe/Mn oxide phases. For samples LA001/LA010/LA010 the organic matter phase shows an increase in phase associated W from 0' to 6" and a decrease from 6"-1'.

In Sierra Vista, W concentration decreases with depth but so does its association with oxide phases. Here, W is less present or less available at a depth of ~6" compared to the near surface. However, there is more W present in exchangeable, carbonate, and oxide phases. While Fallon showed a decrease in bulk concentration but higher phase associated W with depth, Sierra Vista shows an initial decrease followed by an increase in bulk W concentration and phase association at the max depth measured. Since there is less data available in Sierra Vista (due to sampling constraints) more work needs to be done to further characterize the geochemical reactions taking place, since they seem to differ from Fallon. This is could be because of a different reaction pathway than in Fallon, originating from a different source of W. While there

are sources of natural W nearby, there has not been work done to classify the nature of the W like has been done in Fallon (Sheppard et al., 2007a).

Cheyenne Bottoms

Cheyenne Bottoms is the most difficult of the three sites to characterize given the absence of background information available for the site. Of the three sites, Cheyenne Bottoms was the only site sampled without guidance from researchers who have previously conducted work in the area. Cheyenne Bottoms has the smallest variation in W concentration (16.2-246.83 mg/kg) and the lowest average W concentration (66.92 mg/kg) within the sediments. With the exception of CBR1_1c all the samples are in the range of ~15-30 mg/kg. This is significant since all the samples beside CBR1_1c and CBR1_1a are northwest of the main pools (1a, 1b, 1c) (Fig. 4.3). The highest bulk W concentrations are located in the northern main pool (1c), which was almost entirely under water during sampling. The other samples represent a variety of different sampling conditions (described earlier) but all fall in a lower range of W concentration, although all samples are above established background levels (1.55 mg/kg for crustal abundance, 3.25 mg/kg for surface soils; Koutsospyros et al., 2006). In Cheyenne Bottoms, the W phase association is dominated by the organic matter and sulfide/residual phases, with the other phases constituting >10%. Cheyenne Bottoms is a wetland that goes through regular drying cycles, where the ponds are completely devoid of water. Given this is a major migratory bird habitat containing fish and a variety of marsh plants, the dominance of the organic matter phase is not surprising. Tungsten has been shown to have an affinity for organic matter and humic substances in sediment, similar to other oxyanions, and Tuna et al., (2012) found in their study that W had the highest adsorption in the soils with the highest organic content. It was also discovered in cattail samples from Cheyenne Bottoms that W is bioavailable, as it was seen in the cattail through μXRF imaging (appendix C). Depth increments were not obtained from Cheyenne Bottoms due to limitations in sampling. In Cheyenne Bottoms, the proposed source of the W is from WWII practice bomb raids from the Salina Air Force Base. Tungsten is used in the bomb casings and W in the sediment is hypothesized to be fragments from the bombing (personal conversation with Witten et al.). Work by Sheppard et al., (per comms) found that nearby trees contained the highest concentration of W measured in the US. While W was found in surface waters, it was in very

minute concentrations (>0.5 µg/L), suggesting W in Cheyenne Bottoms is not available in the exchangeable phase.

Conceptualized Mobilization Model

A conceptual mobilization model was constructed from this work, portraying the release of W from metallic W into sediments. From Sheppard et al., (2007) we know that there is a significant contribution of anthropogenic W into the surrounding environment. Anthropogenic W consist of W metal or WC. Since we also see W associated with Co and only Co in the surficial sediments it is safe to say that the W seen in this study is mostly of an anthropogenic origin. This W metal is oxidized and deposited from the air to the sediment where it mixes with the surface dust.

In the near surface the WO_3 coating the W metal is slowly released as it comes into contact with water, follow the reaction:

$$\mathbf{WO_3 + H_2O \rightarrow WO_4^{2-} + H^+}$$

This release monomeric WO_4^{2-} into the sediment which was found in the water extraction of this work. The transformation also release H^+ which decreases the pH of the soil, which has been noted in other works, possibly altering the WO_4^{2-} further.

With depth we see a smaller fraction of W associated in the exchangeable phase and a greater association of W with the Mn oxide phase. We know that WO_4^{2-} competitively sorbs to oxide phases, but poly-tungsten species all have a lower sorption coefficient than monomeric WO_4^{2-}. This could lead to 2 separate pathways for W in this scenario.

The first is that monomeric WO_4^{2-} migrates downward and is sequestered by oxide phases through a surface sorption reaction, especially since the release of H^+ will increase the strength of this reaction.

The second possibility is that some poly-tungsten species (also seen in the DI water extraction) or alteration of the WO_4^{2-} to a poly- species, with its lower K_d will continue to migrate until some other factor further changes it speciation or it is sequestered.

A third possibility is that both of these reactions are occurring simultaneously and the stronger affinity of monomeric WO_4^{2-} to oxides leads it to be sorbed, and the less competitive sorption of the poly- species leads it to be left mobile in the sediment, in this example.

Chapter 7 - Conclusion

This study set out to investigate the geochemistry of W in sediments in areas of relatively high W concentration. By following proven methods (Bednar et al., 2006, 2010; Bostick 2013; Cutler 2011) sediment samples were characterized geochemically to describe W sediment fate and transport processes. In Fallon, available W decreases with depth (`0-1') as W metal is oxidized and then dissolved releasing WO_4^{2-} which is polymerized and adsorbed onto Fe/Mn oxides. Tungsten in surficial sediments is primarily in the form of exchangeable WO_4^{2-} as well as an undescribed polytungstate species. From SEM data, it is seen that W tends to co-localize with other metals (Co, Zn, Ti) and is sometimes found associated with Mn in near surface soils. In Sierra Vista, W is available near surface but decreases in concentration at a depth of ~6". Tungsten phase association shifts after 6" and becomes more associated with the exchangeable, carbonate, and Fe/Mn oxide phases. Cheyenne Bottoms however, due to its higher amount of organic matter input retards W migration through sorption reactions with organic matter for which W has a high affinity.

A simple model was shown to conceptualize W mobilization from an anthropogenic source. In this model, metallic W is deposited from the air and as oxidation takes place (creating WO_3), WO_4^{2-} is created as H_2O interacts with the WO_3. This dissolved WO_4^{2-} is released in surficial sediments but then undergoes two pathways: the first is WO_4^{2-} is polymerized and this remains mobile; and WO_4^{2-} is sequestered by Mn oxides with increasing depth.

This study details some of the processes through which W migrates through sediments and polymerizes and illustrates the need for more rigorous experiments on the subject to further detail the complex polymerization process and describe the many poly- species WO_4^{2-} can form.

References

Bednar, A.J., Jones, W.T., Chappell, M.A., Johnson, D.R., Ringelberg, D.B., 2010. A modified acid digestion procedure for extraction of tungsten from soil. Talanta, 80, 1257-1263.

Bednar, A.J., Mirecki, J.E., Inouye, L.S., Winfield, L.E., Larson, L.S., Ringelberg, D.B., 2006. Specition and geochemistry of tungsten in soil. U.S. Army Engineer Research and Development Center, Environmental Labrotory, Vicksburg, MS.

Bethke, C. M., 2008. Geochemical and Biogeochemical Reaction Modeling. 2nd ed. Cambridge University Press (Cambridge, UK), 543 p.

Bethke, C. M., Ding, D., Jin, Q., Sanford, R. A., 2008. Origin of microbiological zoning in groundwater flows. Geology 36, 739-742.

Bostick, B.C., Sun, J., Landis, J.D., Clausen, J.L, 2010. Quantitative tungsten speciation and solubility in munitions-impacted soils. Unpublished

Bostcik, Band Jing Sun, 2013. Polyoxometalates and Their Effect on Tungsten Speciation and Transport. Goldschmidt 2013.

Dave, H., 2008. Geochemical investigation of tungsten in two groundwater flow systems: The Carrizo Sand Aquifer, Texas, USA, and the Aquia aquifer, Maryland, USA. Thesis.

EPA. 2008. Emerging Contaminant-Tungsten. http://www.epa.gov/fedfac/documents/emerging_contaminant_tungsten.pdf. Updated, 2010, Accessed Oct, 2011.

Fastje, C., Harper, K., Terry, C., Sheppard, P., Witten, M. 2012. Exposure to sodium tungstate and Respiratory Syncytial Virus results in hematological/immunological disease in C57BL/6J mice. Chemico-Biological Interactions, 196: 89-95.

Grafe, M., Landers, M., Tappero, R., Austin, P., Gan, B., Grabsch, A., Klauber, C. 2011. Combined Application of QEM-SEM and hard x-ray microscopy to determine mineralogical associations and chemical speciation of trace metals. Journal of Environmental Quality 40, 767-783.

Gustafsson, J. P., 2003. Modelling molybdate and tungstate adsorption to ferrihydrite. Chem. Geol. 200, 105-115.

Haque, S., Johannesson, K., 2006. Arsenic concentrations and speciation along a groundwater flow path: The carrizo Sand aquifer, Texas, USA. Chemical Geology, 288, 57-71.

Hsu, L. C., 1977. Effects of oxygen and sulfur fugacities on the scheelite – tungstenite and powellite – molybdenite stability relations. Econ. Geol. 72, 664-760.

Hoffman, M., Darab, J., Heald, S., Yonker, C., Fulton, J., 2000. New experimental developments for in situ XAFS studies of chemical reactions under hydrothermal conditions. Chemical Geology, 167, 89-103.

Johannesson, K. H., Tang, J., 2009. Conservative behavior of arsenic and other oxyanion-forming

trace elements in an oxic groundwater flow system. J. Hydrol. 378, 13-28.

Johannesson, K. H., Zhou, X., 1999. Origin of middle rare earth element enrichments in acid waters of a Canadian High Arctic lake. Geochim. Cosmochim. Acta 63, 153-165.

Johnson, D.R., Inouye, L.S., Bednar, A.J., Clarke, J.U., Winfield, L.E., Boyd, R.E., Ang, C.Y., Goss, J., 2009. Tungsten bioavailability and toxicity in sunflowers (*Helianthus* annuus L.). Land Contamination and Reclamation, 17(1), 141-151.

Kalinich, J. F., Emond, C. A., Dalton, T. K., Mog, S. R., Coleman, G. D., Kordell, J. E., Miller, A. C., McClain, D. E., 2005. Embedded weapons-grade tungsten alloy shrapnel rapidly

induces metastatic high-grade rhabdomyosarcomas in F344 rats. Environ. Health Perspect. 113, 729-734.

Keon, N. E., Swartz, C. H., Brabander, D. J., Harvey, C., Hemond, H. F., 2001. Validation of an arsenic sequential extraction method. Environ. Sci. Technol. 35, 2778-2784

Kletzin, A., Adams, M. W. W., 1996. Tungsten in biological systems. FEMS Microbiol. Rev. 18, 5-63.

Koutsospyros, A., Braida, W., Christodoulatos, C., Dermatas, D., Strigul, N., 2006. A review of tungsten: From environmental obscurity to scrutiny. Journal of Hazardous Materials, 136, 1-19.

Kusmin, A., Purans, J., 2001. Local atomic and electronic structure of tungsten ions in AWO_4 crystals of scheelite and wolframite types. Radiation Measurements, 33, 583-586

Lassner, E., Schubert, W. D., 1999. Tungsten – Properties, Chemistry, Technology of the Element, Alloys, and Chemical Compounds. Kluwer Academic Publishers, New York.

McNear, D., Tappero, R., Sparks, D., 2005. Shining light on metals in the environment. Elements, 1 (4), 211-216.

Mitchell, R., Fitzgerald, S., Aulerich, R., Balander, R., Powell, D., Tempelman, R., 2001. Hematological effects and metal residue concentrations following chronic dosing with tungsten-iron and tungsten-polymer shot in adult game-farm mallards. Journal of Wildlife Diseases, 37(3), 459-467.

Ogundipe, A., Pavlov, J., Braida, W., Koutsospyros, A., Sen, G., Christodoulatos, C., O'Connor, G., 2009. Evaluation of analytical methods to address tungsten speciation. Global Nest, 11(3), 308-317.

Peuster, M., Fink, C., Wohlsein, P., Bruegmann, M., Gunther, A., Kaese, V., 2003. Degradation of tungsten coils implanted into the subclavian artery of New Zealand white rabbits is not associated with local or systemic toxicity. Biomaterials, 24(3), 393-399.

Ringelberg, D.B., Reynolds, C.M., Winfield, L.E., Inouye, L.S., Johnson, D.R., Bednar, A.J., 2009. Tungsten effects on microbial community structure and activity in a soil. Journal of Environmental Quality, 38, 103-110.

Ryzhenko, B.N. 2010. Technology of Groundwater Quality Prediction: 1. Eh-pH diagram and Detention Coefficient of Molybdenum and Tungsten in Aqueous Solutions. Geochemistry International, 48 (4), 407-414.

Seiler, R., Stollenwerk, K., Garbarino, J., 2005. Factors controlling tungsten concentrations in ground water, Carson Desert, Nevada. Applied Geochemistry, 20, 423-441.

Sheppard, P., Ridenour, G., Speakman, R., Witten, M., 2006. Elevated tungsten and cobalt in airborne particulates in Fallon, Nevada: Possible implications for the childhood leukemia cluster. Applied Geochemistry, 21,. 152-165.

Sheppard, P., Speakman, R., Ridenour, G., Witten, M., 2007. Temporal variability of tungsten and cobalt in Fallon, Nevada. Environmental Health Perspectives, 115 (5), 715-719.

Sholkovitz, E. R., 1990. Rare-earth elements in marine sediments and geochemical standards. Chem. Geol. 88, 333-347.

Strigul, N. 2010. Does speciation matter for tungsten ecotoxicology? Ecotoxicology and Environmental Safety 73,1099-1113.

Strigul, N., Koutsospyros, A., Christodoulatos, C., 2009. Tungsten in the former Soviet Union: review of environmental regulations and related research. Land Contamination and Reclamation, 17(1), 189-215.

Strigul, N., Koutsospyros, A., Arienti, P., Christodoulatos, C., Dermatas, D., Braida, W., 2005. Effects of tungsten on environmental systems. Chemosphere, 61, 248-258.

Sun, N., Fastje, C., Wong, S., Sheppard, P., Macdonald, S., Ridenour, G., Hyde, J., Witten, M. 2003. Dose-Dependent transcriptome changes by metal ores on a human acute lymphoblastic leukemia cell line. Toxicology and Industrial Health, 19: 157-163.

Tang, J., 2004. Rare earth element geochemical behavior in natural terrestrial waters. PhD dissertation. Old Dominion University, Norfolk, Virginia.

Tang, J. Johannesson, K., 2006. Controls on the geochemistry of rare earth elements along a groundwater flow path in the Carrizo Sand aquifer, Texas, USA . Chemical Geology, 225, 156-171.

Tessier, A., Campbell, P. G. C., Bisson, M., 1979. Sequential extraction procedure for the speciation of particulate trace metals. Anal. Chem. 51, 844-851.

Wenzel, W. W., Kirchbaumer, N., Prohaska, T., Stingeder, G., Lombi, E., Adriano, D. C., 2001. Arsenic fractionation in soils using an improved sequential extraction procedure. Anal. Chim. Acta 436, 309-323.

Willis, S., Haque, S., Johannesson, K., 2011. Arsenic and Antimony in groundwater flow systems: A comparative study. Aquatic Geochemistry, 17, no.6, 775-807

Witten, M., Sheppard, S., Witten, B. 2011. Tungsten toxicity. Chemico-Biological Interactions, 196: 87-88.

Yamazoe, S., Hitomi, Y., Shishido, T., Tanaka, T., 2008. XAFS study of tungsten L- and L-edges: Structural Analysis of WO species loaded on TiO as a catalyst for photo-oxidation of NH. Journal of Physical Chemistry, 112 (17), 6869-6879.

Appendix A - Sediment Chemistry

This section contains the sediment chemistry data from the lab work conducted both on Kansas State University and performed in other labs.

A.1 Sediment Samples

This table is a list of all sediment samples collected organized by field site. The X, Y coordinates are in Universal Transverse Mercator (UTM)

Table A.1 Sediment Sample list of samples collected from all three sampling locations.

Location	Sample #	Type	Depth	X	Y
Cheyenne Bottoms	CBR 1_3a	core	0-12'	531627	4259006
	CBR 2_3a	core	0-12'	531635	4259120
	CBR 4_3a	core	0-6'	531632	4259551
	CBR 1_1c	core	0-6'	531547	4258967
	CBRS 1_1a	SG	surface	531651	4258991
	CBRS 3b	SG	surface	531669	4258954
Fallon	Fallon 1	SG	surface	346395	4371359
	Fallon 2	SG	surface	346669	4371628
	Fallon 3	SG	surface	346764	4371560
	FN-AS-001	Auger	0-12'	347195	4371017
	FN-AS-002	Auger	0-12'	346359	4371681
	FN-AS-003	Auger	0-12'	347004	4371601
	FN-AS-004	Auger	0-12'	346348	4371335
	FN-AS-005	Auger	0-12'	347575	4371385
	FN-AS-006	Auger	0-12'	347578	4371378
	FN-AS-007	Auger	0-12'	347364	4371392
	FN-PS-001	Probe	0-6'	347195	4371017
	FN-PS-002	Probe	0-24'	346359	4371681
	FN-PS-003	Probe	0-24'	347004	4371601
	FN-PS-004	Probe	0-3'	346348	4371335
	FN-SG-001	Surface Grab	Surface	346359	4371681
	FN-SG-002	Surface Grab	Surface	347004	4371601
	FN-SG-003	Surface Grab	Surface	346348	4371335
	FN-SG-004	Surface Grab	Surface	347575	4371385
	FN-SG-005	Surface Grab	Surface	347518	4371387
	FN-SG-006	Surface Grab	Surface	347518	4371387
	FN-SG-007	Surface Grab	Surface	347364	4371392
Sierra Vista	LA 001	SG	surface	569153	3491457
	PK 010	SG	surface	569153	3491457

PK 007	SG	surface	565789	3491753
PK 020	SG	surface	565809	3491753
PK 030	SG	surface	565643	3491853
TF 001	SG	surface	568338	3490160
PK 012	core	1"-14'	569153	3491457
MS 001	core	0-6'	568338	3490160
PK 001	core	0-6'	569153	3491457
TF 010	core	0-6'	568338	3490160
PK 011	core	0-6'	569153	3491457
MS 002	core	6-14'	568338	3490160
TF 020	core	1-8'	567677	3490161
LA 010	core	0-6'	569153	3491457
LA 011	core	6-12'	569153	3491457
TF 021	core	8-14'	568338	3490160
PK 021	core	0-6'	565809	3491753

A.2 Total Extraction

This section contains the data for the total extractions which were analyzed both by ICP-MS and ICP-AES.

ICP-AES

The ICP-AES provides a multi-element analysis approach but lacks the sensitivity of other instruments like the ICP-MS. Negative values indicate that the analyte measured was below detection limits.

Table A.2 Data for Total Extraction performed at US Army Engineers Research and Development Center, Environmental Chemistry lab in Vicksburg, MS. This data set provides multiple elements, analyzed by ICP-AES, mg/kg.

Analyte	Carrizo	CBR1_1a	CBR1_1c	CBR2_3a	CBR4_3a	Fallon 1
Ag	-2.71	-1.50	-0.63	-4.26	-5.52	-1.26
Al	148952.50	429303.76	226155.01	504993.68	446952.70	69450.24
As	28.19	19.42	84.25	24.99	5.17	46.08
B	54.14	434.59	361.46	457.37	395.90	146.04
Ba	292.81	3287.42	1770.97	2261.43	2671.54	635.99
Be	1.04	10.66	6.05	12.78	11.47	0.23
Ca	3795.05	355788.75	241738.47	164401.18	89523.58	31772.70
Cd	2.33	10.92	14.34	11.32	8.78	0.94
Co	10.83	99.19	80.53	119.55	105.69	290.16
Cr	69.98	338.28	216.05	400.70	356.77	80.85
Cu	12.88	176.60	296.97	197.03	168.44	78.78
Fe	54701.14	253452.77	160304.63	304209.86	270666.79	121183.83
K	10916.33	115529.91	64795.16	131523.20	113341.15	20519.94
Li	46.09	273.31	146.80	313.73	278.27	91.52
Mg	5189.45	92607.14	55121.22	101670.74	89422.13	26746.84
Mn	175.47	3977.57	4254.57	5978.59	4372.92	2253.60
Mo	-0.05	-6.17	0.29	-14.59	-16.48	-9.61
Na	1547.18	30749.45	21565.82	29968.51	33370.29	4397.78
Ni	33.11	239.99	262.78	276.61	243.95	68.37
Pb	-8.28	74.87	87.93	88.53	78.18	-11.95
S	1478.90	43776.71	75476.61	36167.33	9509.44	2552.17
Sb	-4.10	-68.62	-37.53	-76.46	-71.43	-45.44
Se	65.54	302.40	240.53	323.16	349.17	132.80
Si	2445.46	2101.92	1521.46	2699.28	2577.63	1413.90
Sn	9.43	78.65	45.56	89.08	91.16	33.83
Sr	72.89	1519.46	1413.92	1092.00	779.61	319.73

Analyte	Carrizo	CBR1_1a	CBR1_1c	CBR2_3a	CBR4_3a	Fallon 1
Ti	1947.69	9037.38	5348.26	10566.22	9620.83	4828.04
Tl	9.89	15.05	8.20	6.31	5.01	7.44
V	147.09	820.20	597.15	930.76	834.87	336.32
W	5.82	-10.48	247.33	-8.55	6.05	6954.95
Zn	114.95	908.59	593.74	1047.91	898.67	531.37
Analyte	**Fallon 2**	**FNAS001**	**FNAS002**	**FNAS003**	**FNAS004**	**FNAS005**
Ag	1.68	-1.70	-0.42	4.79	-0.52	0.58
Al	213550.45	138772.54	130070.72	179319.34	90166.48	67994.40
As	94.79	50.22	66.91	92.09	52.57	50.40
B	721.33	147.08	186.44	992.77	163.29	94.90
Ba	2304.99	2567.91	1204.78	1720.32	668.29	1180.02
Be	1.49	2.73	1.69	2.51	1.09	0.80
Ca	185232.78	64970.46	89067.53	161003.38	35156.85	26204.04
Cd	3.80	2.31	2.28	3.42	1.62	13.36
Co	3193.17	107.89	91.33	194.88	51.77	56.04
Cr	524.70	150.90	130.93	141.67	72.28	75.97
Cu	306.42	234.40	165.57	235.89	88.29	198.84
Fe	313547.43	246618.08	193748.74	222785.24	112814.54	128944.69
K	60569.07	12513.96	35299.56	59484.37	17572.08	18111.56
Li	287.36	309.61	175.00	257.85	118.68	94.15
Mg	91349.91	50482.74	53148.78	95262.69	34256.10	27113.14
Mn	5605.12	4469.68	4637.90	5773.23	2355.52	3337.84
Mo	-10.12	-12.76	-8.94	-6.85	-2.73	-4.94
Na	28014.80	12613.32	5628.03	29667.77	5880.52	3121.61
Ni	296.52	204.80	111.92	128.99	62.72	80.76
Pb	292.98	29.84	20.95	64.05	-9.50	1395.70
S	16945.93	3000.97	3870.19	15236.38	2067.67	2337.47
Sb	-127.12	-65.13	-47.64	-59.06	-26.93	-24.81
Se	325.85	297.55	243.14	281.11	146.38	158.08

Analyte	Fallon 2	FNAS001	FNAS002	FNAS003	FNAS004	FNAS005
Si	2314.65	1182.20	916.30	1172.43	1103.03	1026.85
Sn	100.59	55.12	51.44	74.50	38.40	38.13
Sr	1461.29	379.85	754.89	1446.19	379.47	289.02
Ti	11306.53	5007.16	6122.13	7321.80	4084.82	4530.11
Tl	30.39	0.40	-2.18	0.16	2.66	0.10
V	884.51	811.53	531.24	592.52	290.16	309.87
W	24152.63	317.49	123.02	744.42	86.09	53.14
Zn	1309.94	753.97	632.79	705.66	287.55	2733.32
Analyte	**FNAS006**	**FNAS007**	**FNPS001**	**FNPS002**	**FNPS003**	**FNSG001**
Ag	11.22	-3.48	-3.74	-1.20	-4.03	-1.56
Al	234536.32	67537.60	81864.47	38017.57	321364.51	127094.03
As	86.90	12.53	30.46	52.82	80.97	71.75
B	514.98	30.55	119.71	36.11	356.19	205.31
Ba	1657.68	182.93	707.84	418.31	2145.78	1309.75
Be	3.04	0.22	0.30	-0.07	4.69	1.39
Ca	97777.77	4402.34	92863.96	13802.46	52944.22	79080.70
Cd	4.80	0.21	0.81	0.87	5.08	2.54
Co	121.23	6.52	79.30	38.40	166.95	93.03
Cr	147.97	8.19	137.39	55.72	202.72	115.58
Cu	367.54	9.45	148.22	33.36	340.18	139.90
Fe	258554.59	10505.44	194557.62	73545.05	337399.90	183451.17
K	45753.78	1199.96	16012.98	8739.69	41467.08	35916.93
Li	280.11	8.34	136.65	49.89	366.95	166.99
Mg	82432.78	2253.15	45411.58	15116.04	102516.16	52625.98
Mn	6386.66	134.04	3692.76	1972.13	10325.62	5480.64
Mo	-1.45	-0.32	0.79	-1.88	-0.84	-8.14
Na	42334.96	486.57	6512.20	1941.65	48253.72	5416.33
Ni	140.67	3.45	112.04	78.20	201.11	98.97
Pb	141.60	1.37	-31.50	-38.93	56.11	38.95

Analyte	FNAS006	FNAS007	FNPS001	FNPS002	FNPS003	FNSG001
S	32532.95	76.81	1611.62	1084.87	7147.30	4860.90
Sb	-65.78	-1.53	-54.05	-8.90	-88.28	-47.60
Se	277.75	6.02	241.15	95.33	338.73	224.04
Si	1426.30	11.94	1325.16	956.04	2182.03	1731.82
Sn	78.10	1.42	44.85	19.17	132.23	51.94
Sr	1003.62	14.13	463.98	149.81	853.89	757.25
Ti	9010.08	153.22	5609.42	2852.85	11244.12	5493.63
Tl	-3.81	0.03	0.22	-0.05	-9.48	-2.99
V	680.39	11.43	583.25	205.63	921.34	479.81
W	65.76	0.90	26.76	29.80	99.17	264.32
Zn	789.59	10.32	430.93	181.73	943.35	574.03
Analyte	**FNSG002**	**FNSG003**	**FNSG004**	**FNSG005**	**FNSG006**	**FNSG007**
Ag	6.39	-3.81	-0.49	-0.81	-0.67	2.49
Al	130222.76	160727.23	84072.63	96618.27	106178.13	131409.68
As	96.00	50.04	73.92	188.33	95.08	150.54
B	1832.27	304.16	127.22	181.94	165.14	218.48
Ba	1926.68	1249.51	1590.69	1922.56	1490.73	2104.15
Be	1.29	1.68	0.60	2.75	0.98	0.97
Ca	389749.00	69707.26	37188.24	59670.74	46281.43	63775.27
Cd	2.90	3.19	14.34	12.32	11.94	16.89
Co	237.36	100.25	67.04	86.42	83.09	123.33
Cr	125.60	117.10	105.86	140.77	161.19	147.73
Cu	194.71	159.94	187.93	418.86	263.51	2119.16
Fe	172097.31	202264.83	169768.10	241932.89	214286.43	240667.70
K	55573.42	44509.33	22421.01	31750.85	29941.35	42908.15
Li	239.92	200.99	101.90	138.01	131.68	151.77
Mg	120449.07	64018.40	33548.94	42905.93	39474.76	51767.86
Mn	4159.15	4063.93	2808.75	5597.01	3491.51	3713.31
Mo	-5.30	-10.50	-6.14	-3.54	-6.01	26.57

Analyte	FNSG002	FNSG003	FNSG004	FNSG005	FNSG006	FNSG007
Na	31973.58	5218.60	3784.65	4670.46	4848.14	5754.70
Ni	113.86	109.50	107.46	151.63	148.43	149.36
Pb	62.35	-4.91	2483.55	1189.56	6048.41	4380.99
S	19651.05	4119.52	2767.65	3417.32	3429.97	7036.85
Sb	-46.25	-50.52	-28.16	-31.42	-43.03	-15.80
Se	239.08	234.84	193.63	287.06	254.66	256.89
Si	1529.11	1339.53	1345.20	1309.24	1471.05	1513.83
Sn	80.13	62.84	54.40	102.74	63.31	110.91
Sr	2476.89	672.40	389.72	493.54	431.18	647.73
Ti	6482.67	7488.77	5861.33	6689.07	7020.94	7250.36
Tl	5.17	2.43	3.80	-2.01	1.06	3.30
V	467.26	502.80	384.23	473.50	484.20	498.41
W	1276.36	682.05	83.66	109.62	82.15	387.62
Zn	1090.35	610.54	3053.49	1519.34	1594.23	1863.59
Analyte	**Joyce**	**LA 001**	**LA010**	**LA011**	**MS001**	**MS002**
Ag	-6.29	-4.97	-7.02	-7.54	-5.74	0.02
Al	366397.52	172164.26	331961.23	260572.98	211577.90	239091.58
As	29.54	33.02	23.05	16.01	9.31	-1.86
B	146.40	88.77	142.81	116.06	82.21	83.46
Ba	1381.20	488.76	1252.82	973.81	897.99	953.16
Be	17.15	5.73	12.84	9.43	12.05	14.77
Ca	43090.54	6354.15	12593.90	9334.29	22402.68	26649.89
Cd	9.40	3.58	5.52	4.31	4.29	3.99
Co	109.40	52.24	102.47	80.53	85.42	89.15
Cr	175.35	127.03	209.77	176.10	155.31	122.74
Cu	425.47	196.99	191.26	122.49	205.37	177.99
Fe	247998.58	179952.59	253290.05	195402.17	193766.29	191005.25
K	78570.97	30595.74	59282.35	45297.62	52580.71	57705.79
Li	326.40	124.49	286.38	215.57	228.69	267.44

Analyte	Joyce	LA 001	LA010	LA011	MS001	MS002
Mg	44415.39	15142.19	27289.48	21412.87	34294.78	40440.63
Mn	6253.70	2106.56	5113.95	3713.56	6390.24	6564.99
Mo	-3.30	-6.96	-13.76	-11.53	-7.78	-7.94
Na	2037.70	1570.31	2300.86	5001.42	2575.92	2298.16
Ni	149.30	85.01	153.38	126.46	121.81	113.88
Pb	264.45	113.85	100.66	62.85	120.32	106.21
S	4765.54	1172.70	1556.94	1612.73	1571.25	1374.20
Sb	-66.27	-41.63	-67.28	-50.01	-48.95	-51.82
Se	235.48	195.42	242.23	202.89	197.50	180.94
Si	2339.49	2771.33	1973.37	1070.88	1830.48	1906.51
Sn	65.60	31.59	49.27	44.43	51.52	56.93
Sr	297.48	74.71	175.68	132.70	152.38	171.27
Ti	10747.82	5772.88	9572.16	7032.01	7068.93	7352.54
Tl	0.76	4.80	1.59	0.73	-2.27	-0.30
V	408.55	296.95	462.88	352.50	264.11	259.99
W	4.93	27.24	10.07	30.20	524.84	1819.67
Zn	992.29	366.37	477.52	364.10	593.66	607.03

Analyte	PK001	PK010	PK012	PK020	PK030	Pool3B
Ag	-4.11	-2.71	-7.59	-5.06	-3.57	-3.92
Al	246283.32	242082.36	351585.52	251882.53	230717.39	463925.08
As	16.46	27.21	14.61	18.21	31.36	3.73
B	105.20	119.60	151.55	118.53	95.68	504.65
Ba	914.18	902.86	1247.37	890.27	800.07	2431.55
Be	11.06	9.80	16.93	11.21	9.17	11.69
Ca	17881.66	159578.81	51916.61	39253.32	64692.06	137490.78
Cd	4.60	5.26	5.35	4.15	4.78	10.84
Co	65.53	65.19	95.90	65.98	60.36	110.77
Cr	132.98	153.41	166.91	132.17	137.37	367.60
Cu	186.59	223.78	221.98	143.93	213.82	195.34

Analyte	PK001	PK010	PK012	PK020	PK030	Pool3B
Fe	160628.97	189568.99	229061.17	198163.53	182883.66	283054.20
K	53170.06	54848.46	66122.84	49829.27	45051.37	127578.51
Li	214.48	222.32	325.13	233.03	220.33	298.69
Mg	28904.59	34194.33	45809.29	31664.53	30154.55	100922.40
Mn	4113.84	3772.52	5607.11	3569.73	2964.28	4784.70
Mo	-6.08	-6.75	-11.53	-10.33	-5.82	-17.30
Na	2199.58	1935.18	5929.07	1718.86	1732.38	82949.88
Ni	102.77	115.96	150.16	104.39	111.53	255.75
Pb	92.47	201.30	139.41	76.43	139.80	110.95
S	1991.03	6257.82	1741.66	1379.22	2817.61	34340.47
Sb	-37.85	-47.89	-64.55	-51.77	-46.51	-78.37
Se	151.81	216.83	236.43	214.73	211.45	287.01
Si	1928.40	2876.07	1545.10	1350.78	1984.20	3085.61
Sn	49.65	35.79	57.93	41.56	38.80	95.41
Sr	133.69	339.10	217.19	158.54	135.49	1057.56
Ti	6553.69	6509.91	8131.87	6256.61	6484.56	9807.74
Tl	1.89	4.31	3.21	2.92	6.15	8.56
V	267.02	320.92	373.94	323.42	321.32	837.23
W	13.08	-0.41	20.82	34.92	23.47	-5.98
Zn	565.95	687.58	631.14	482.50	518.82	991.54

Analyte	ROCarrizo	TF001	TF010	TF020	TF021
Ag	0.38	-6.50	-4.65	-6.92	-5.91
Al	116873.55	172911.03	183859.62	266124.95	243952.78
As	46.89	23.97	11.78	19.74	11.72
B	129.33	90.88	82.79	95.15	98.17
Ba	239.05	457.06	647.94	954.72	847.91
Be	0.90	5.74	7.53	11.23	10.44
Ca	3161.28	6550.82	6272.09	11937.74	10875.88
Cd	2.34	2.81	3.79	4.32	3.57

Analyte	ROCarrizo	TF001	TF010	TF020	TF021
Co	9.13	54.73	61.92	71.58	73.30
Cr	59.74	129.17	126.39	174.13	170.11
Cu	14.93	183.66	92.77	114.66	101.71
Fe	42100.25	258560.69	219724.60	183255.44	219371.73
K	8528.56	31069.62	31339.71	45253.79	41723.57
Li	38.15	118.91	153.92	208.07	187.30
Mg	4049.57	15503.77	14715.19	21775.87	20755.09
Mn	150.59	1475.49	3385.49	3170.65	3091.83
Mo	0.89	-12.46	-13.09	-6.17	-10.45
Na	1179.95	1162.10	14537.34	5551.99	16621.02
Ni	31.25	83.68	88.60	138.86	123.48
Pb	-19.76	90.27	35.45	62.03	56.70
S	2441.95	1262.23	1783.68	1909.62	2613.82
Sb	8.62	-68.99	-58.61	-46.36	-56.98
Se	75.68	290.90	234.38	184.86	218.87
Si	2460.94	2506.88	2287.66	1988.15	1969.79
Sn	9.54	29.69	31.51	40.46	34.64
Sr	58.26	79.44	81.70	149.48	137.01
Ti	1630.42	6288.38	6180.64	7143.86	6775.79
Tl	11.61	5.39	2.11	4.30	1.89
V	114.66	389.57	332.72	322.09	357.69
W	1.71	22.02	12.46	12.75	6.71
Zn	120.42	342.42	333.12	365.83	361.77

ICP-MS

This data set reflects the same extraction done as the previous tale, but analyzed by ICP-MS for a better degree of sensitivity solely for W concentrations, reported as mg/kg.

Table A.3 Data for total extraction performed at US Army Engineers Research and Development Center, Environmental Chemistry Laboratory in Vicksburg, MS. This data set provides W concentrations in mg/kg.

Sample	W (mg/Kg)	Sample	W (mg/Kg)
CBR1_1a	16.14	FNSG004	80.52
CBR1_1c	246.82	FNSG005	104.14
CBR2_3a	16.56	FNSG006	80.92
CBR4_3a	27.02	FNSG007	378.15
Fallon1	7069.66	Joyce	21.86
Fallon2	333.57	LA001	33.11
Fallon3	25907.45	LA010	22.86
FNAS001	296.76	LA011	40.85
FNAS002	124.71	MS001	460.51
FNAS003	737.04	MS002	1515.95
FNAS004	92.63	PK001	25.23
FNAS005	59.45	PK010	19.84
FNAS006	76.32	PK012	31.24
FNAS007	61.52	PK020	41.26
FNPS001	37.37	PK030	37.35
FNPS002	37.60	Pool3B	28.02
FNPS003	107.37	TF001	26.61
FNSG001	179.74	TF010	20.04
FNSG002	1286.64	TF020	20.14
FNSG003	674.66	TF021	17.80

Correlation Plots

These are the correlation plots for W with select elements, separated by sampling location. The concentrations are in mg/kg with W on the X-axis and the other element on the Y-axis.

Fallon

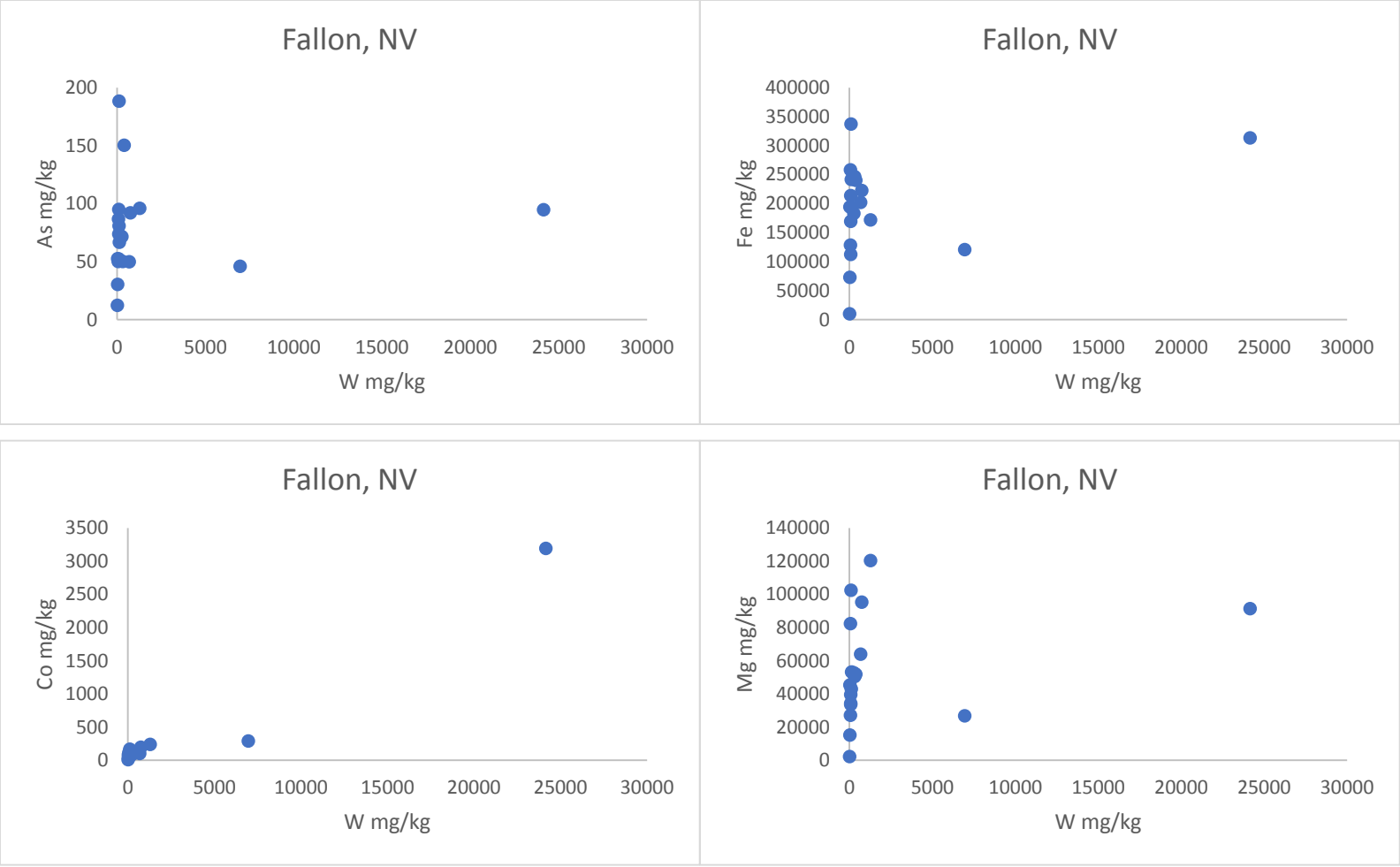
Fallon, NV
As mg/kg
W mg/kg
Fallon, NV
Fe mg/kg
W mg/kg
Fallon, NV
Co mg/kg
W mg/kg
Fallon, NV
Mg mg/kg
W mg/kg

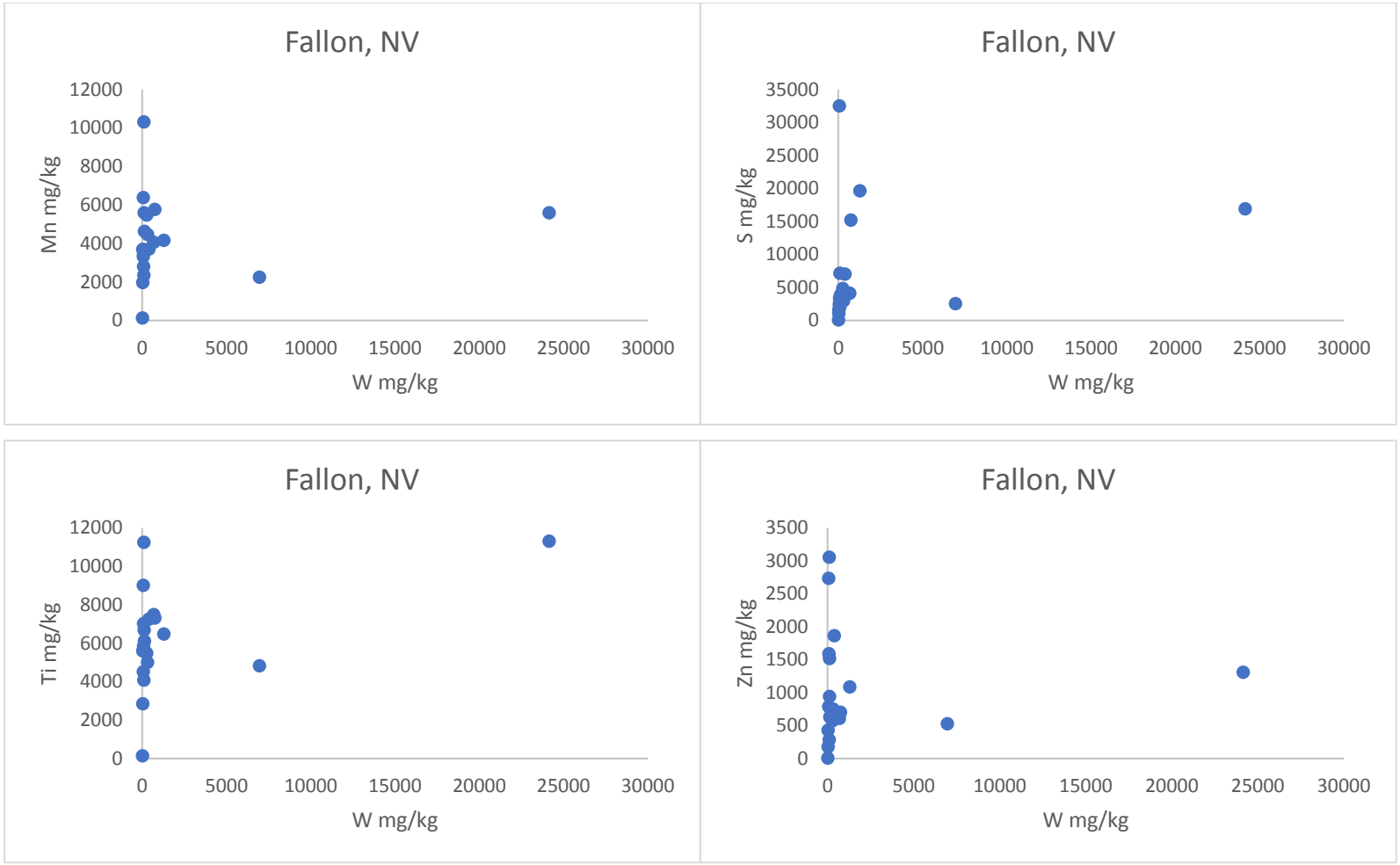
Fallon, NV
Mn mg/kg
W mg/kg
0
2000
4000
6000
8000
10000
12000
0
5000
10000
15000
20000
25000
30000
Fallon, NV
S mg/kg
W mg/kg
0
5000
10000
15000
20000
25000
30000
35000
0
5000
10000
15000
20000
25000
30000
Fallon, NV
Ti mg/kg
W mg/kg
0
2000
4000
6000
8000
10000
12000
0
5000
10000
15000
20000
25000
30000
Fallon, NV
Zn mg/kg
W mg/kg
0
500
1000
1500
2000
2500
3000
3500
0
5000
10000
15000
20000
25000
30000

Sierra Vista

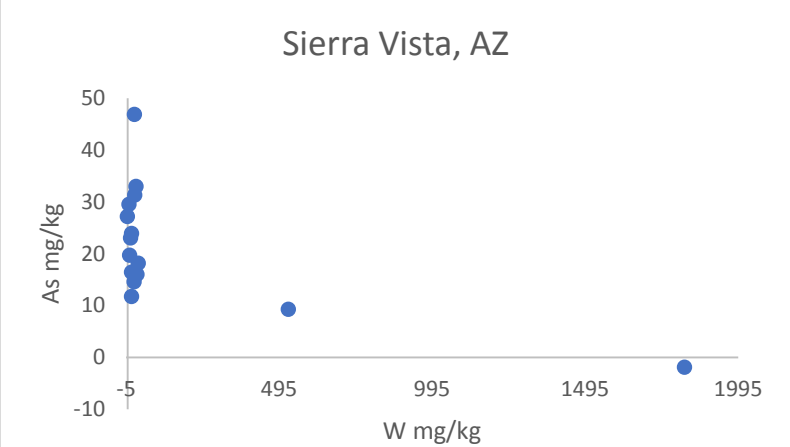

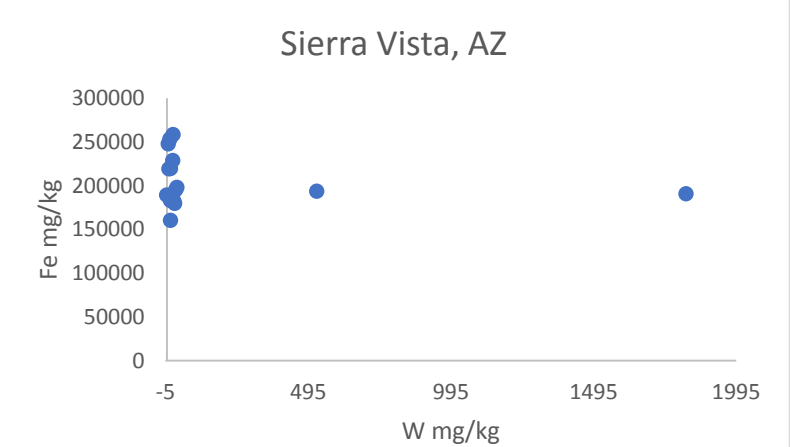

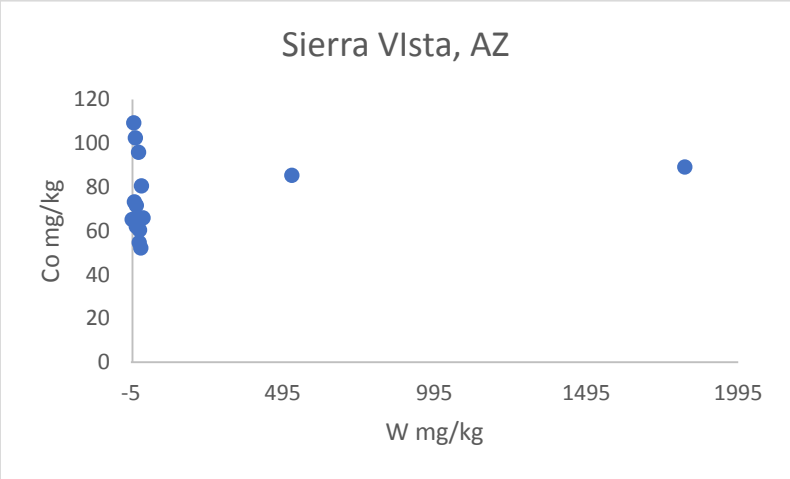

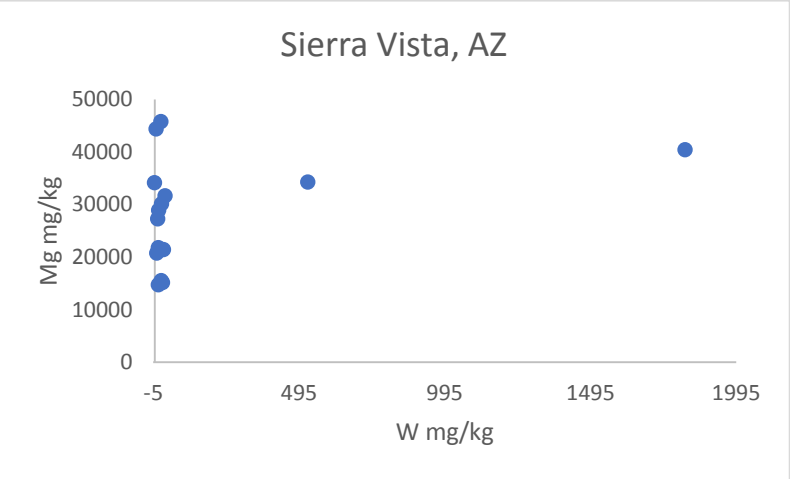

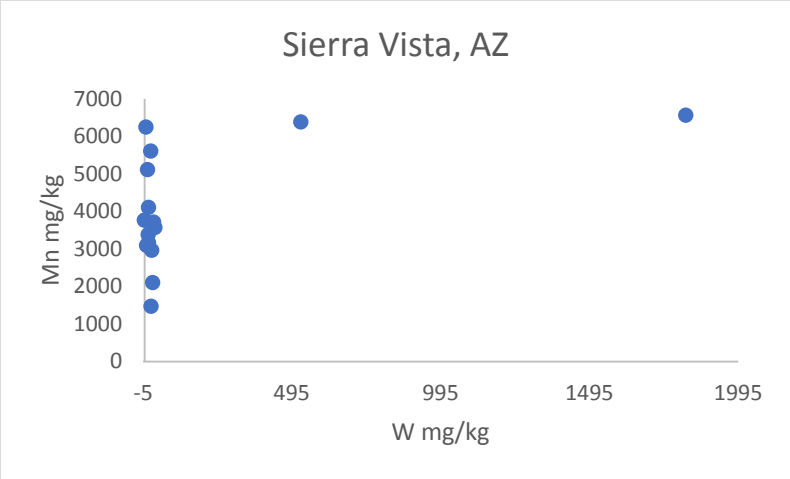
Sierra Vista, AZ
Mn mg/kg
7000
6000
5000
4000
3000
2000
1000
0
-5
495
995
1495
1995
W mg/kg

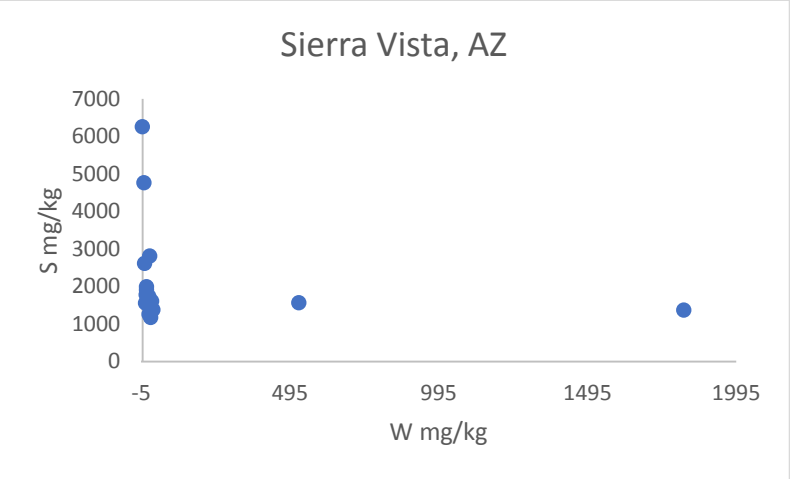
Sierra Vista, AZ
S mg/kg
7000
6000
5000
4000
3000
2000
1000
0
-5
495
995
1495
1995
W mg/kg

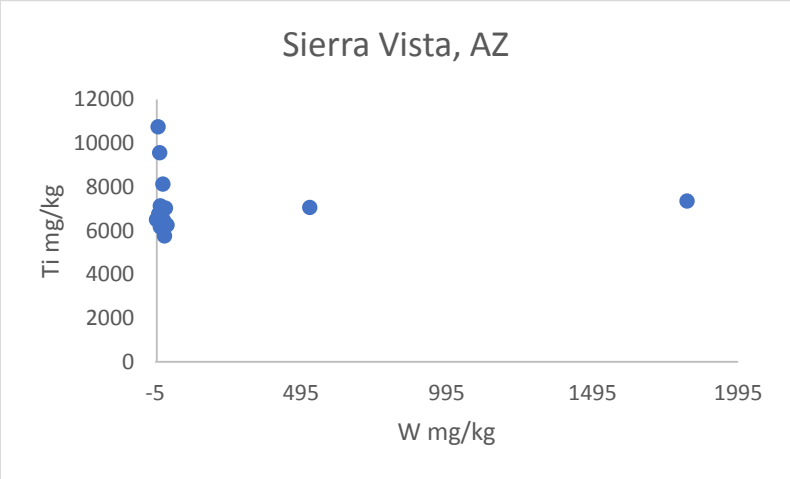
Sierra Vista, AZ
Ti mg/kg
12000
10000
8000
6000
4000
2000
0
-5
495
995
1495
1995
W mg/kg

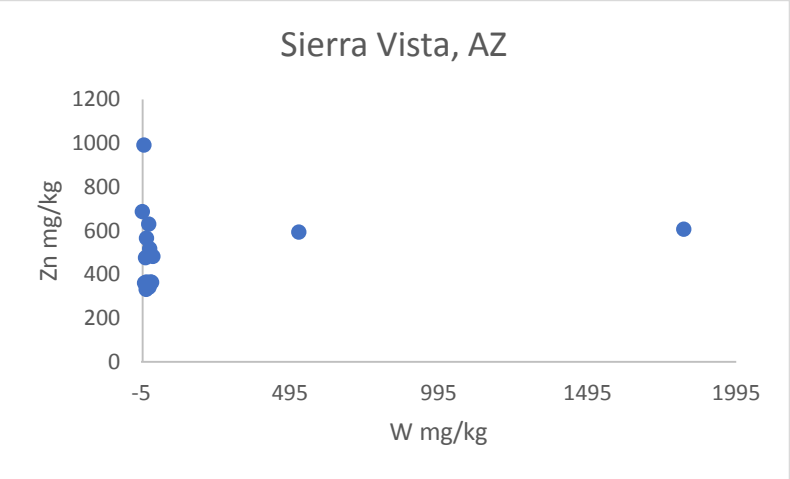
Sierra Vista, AZ
Zn mg/kg
1200
1000
800
600
400
200
0
-5
495
995
1495
1995
W mg/kg

Cheyenne Bottoms Refuge

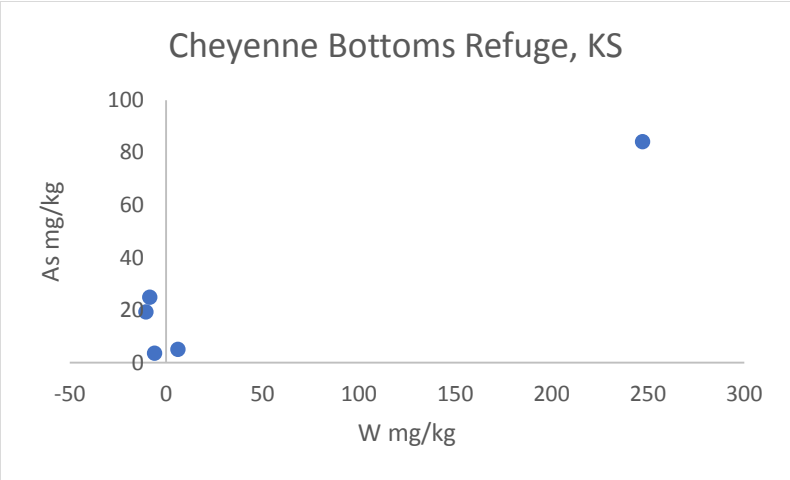

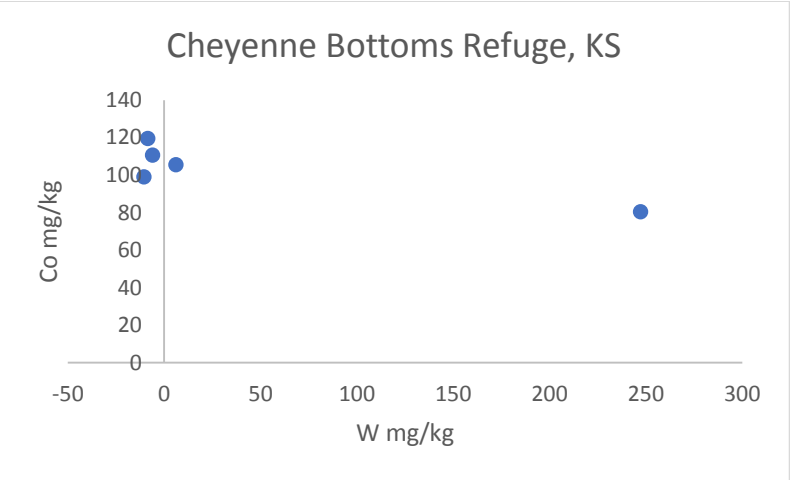

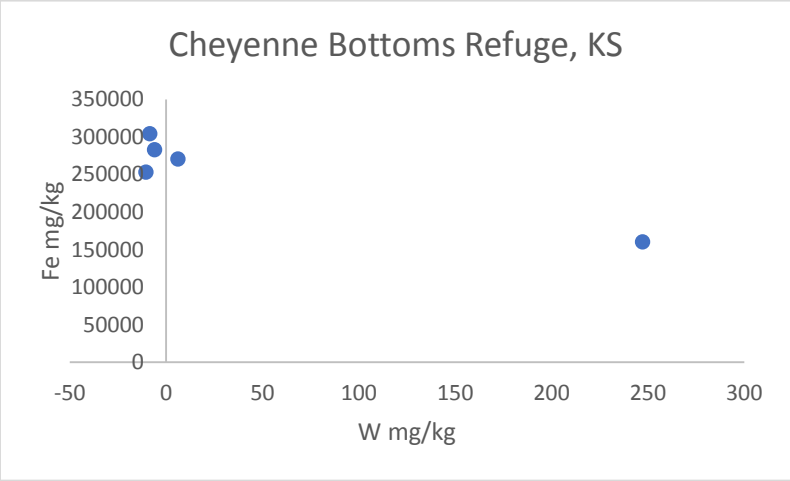

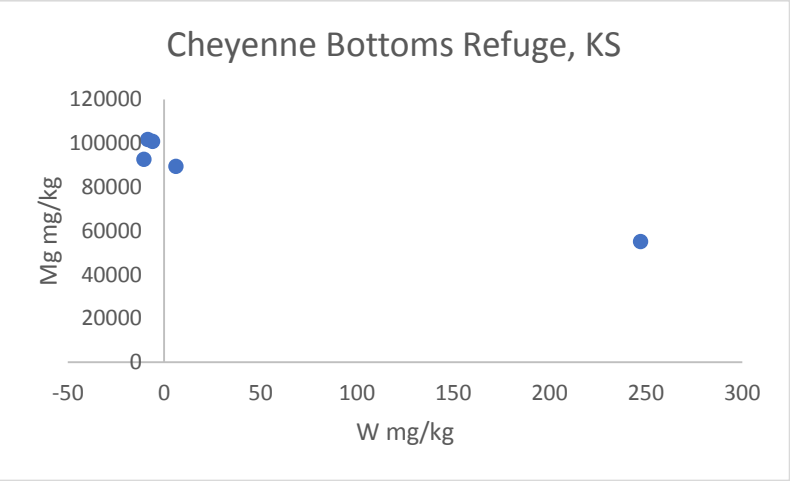

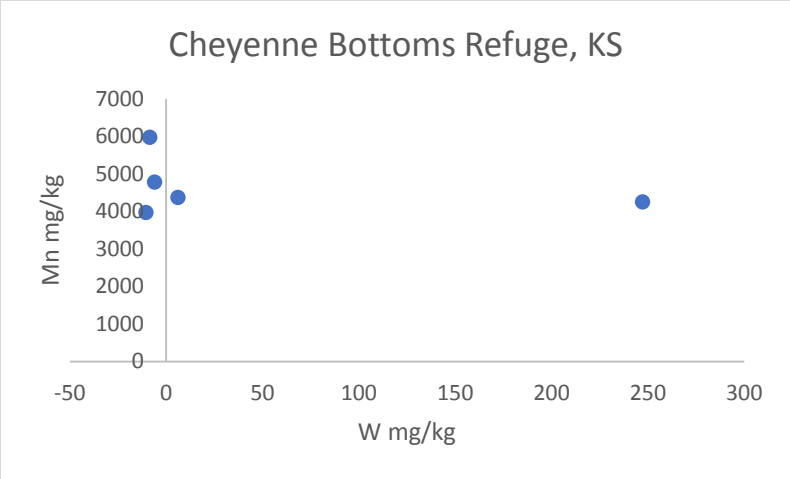
Cheyenne Bottoms Refuge, KS
Mn mg/kg
7000
6000
5000
4000
3000
2000
1000
0
-50
0
50
100
150
200
250
300
W mg/kg

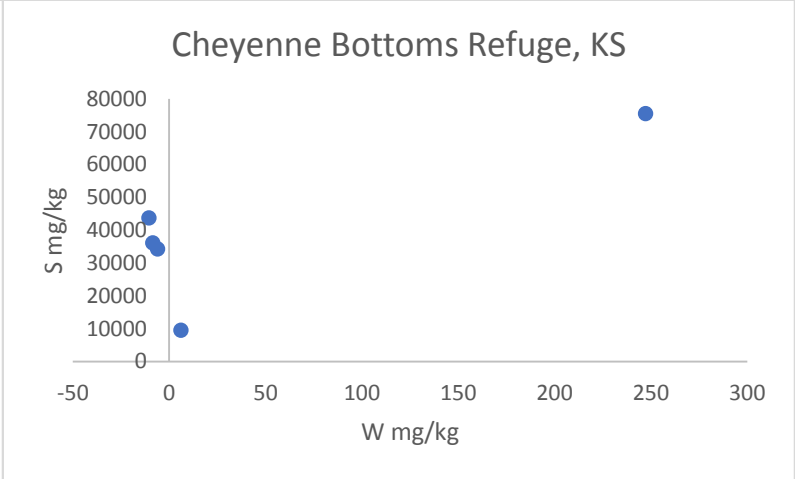
Cheyenne Bottoms Refuge, KS
S mg/kg
80000
70000
60000
50000
40000
30000
20000
10000
0
-50
0
50
100
150
200
250
300
W mg/kg

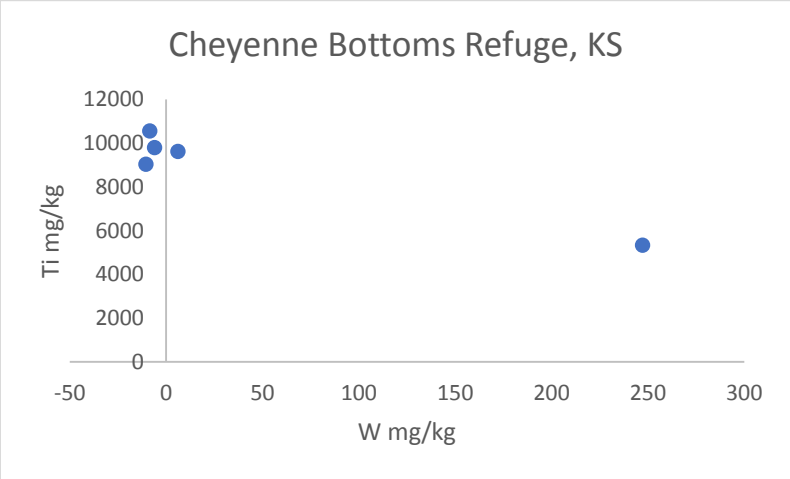
Cheyenne Bottoms Refuge, KS
Ti mg/kg
12000
10000
8000
6000
4000
2000
0
-50
0
50
100
150
200
250
300
W mg/kg

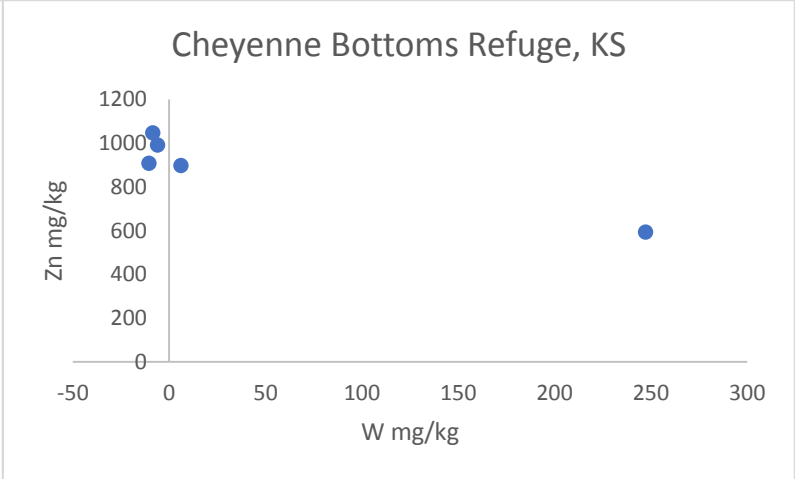
Cheyenne Bottoms Refuge, KS
Zn mg/kg
1200
1000
800
600
400
200
0
-50
0
50
100
150
200
250
300
W mg/kg

Correlation Plots with Removed Outliers

Each field site has outliers, or samples with significantly higher W than the others. For better comparison, these have been removed for each field site. In Fallon, samples Fallon 1 and Fallon 2 were removed. In Sierra Vista, samples MS001 and MS002 were removed. In Cheyenne Bottoms, sample CBR 1_1c was removed.

Fallon

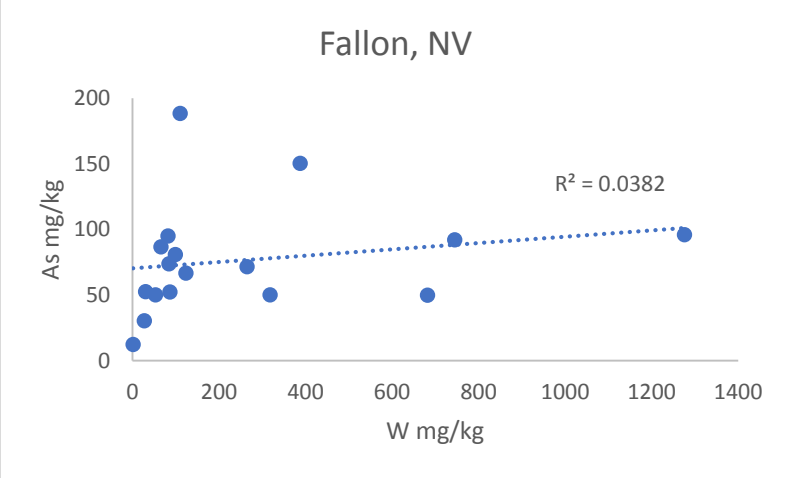
Fallon, NV
As mg/kg
W mg/kg
R² = 0.0382
0
50
100
150
200
0
200
400
600
800
1000
1200
1400

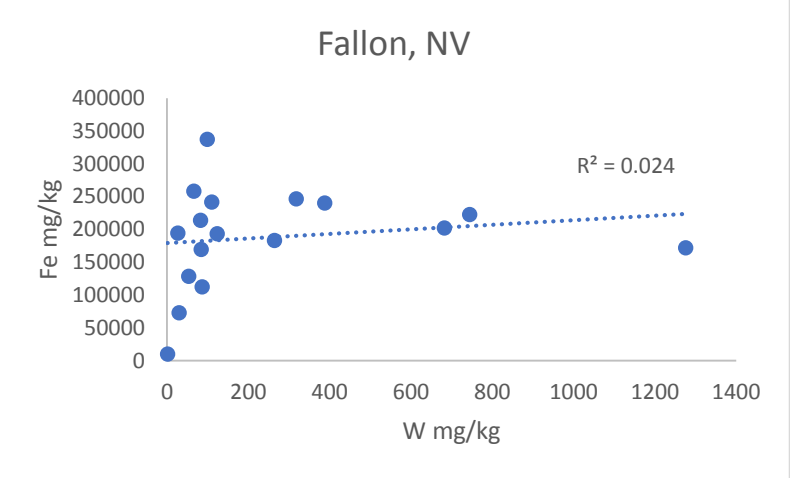
Fallon, NV
Fe mg/kg
W mg/kg
R² = 0.024
0
50000
100000
150000
200000
250000
300000
350000
400000
0
200
400
600
800
1000
1200
1400

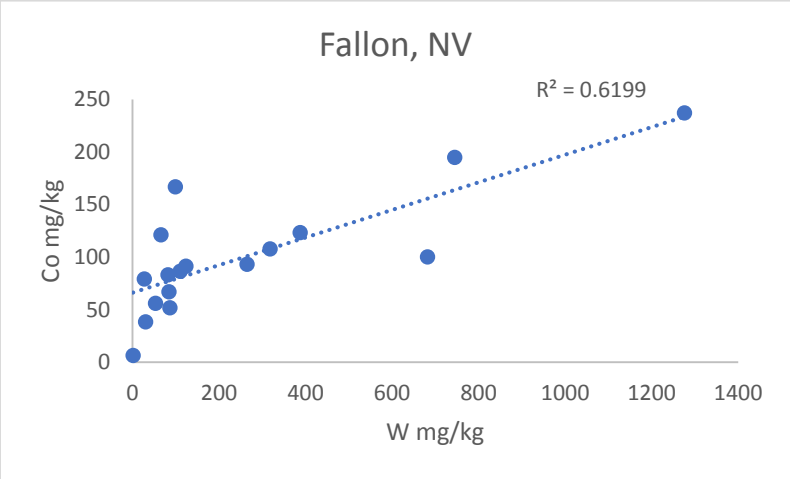
Fallon, NV
Co mg/kg
W mg/kg
R² = 0.6199
0
50
100
150
200
250
0
200
400
600
800
1000
1200
1400

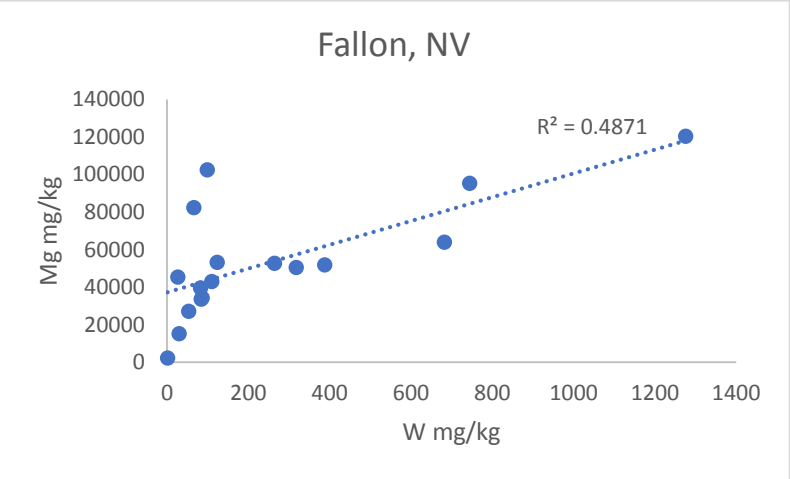
Fallon, NV
Mg mg/kg
W mg/kg
R² = 0.4871
0
20000
40000
60000
80000
100000
120000
140000
0
200
400
600
800
1000
1200
1400

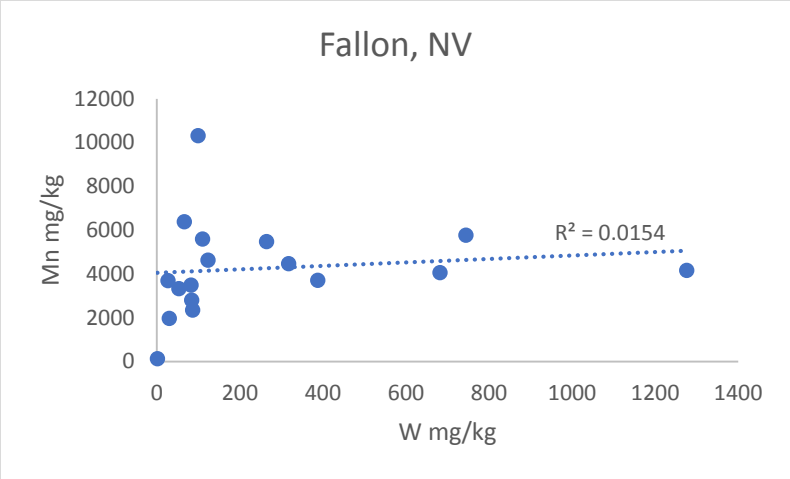
Fallon, NV
Mn mg/kg
W mg/kg
R² = 0.0154
0
2000
4000
6000
8000
10000
12000
0
200
400
600
800
1000
1200
1400

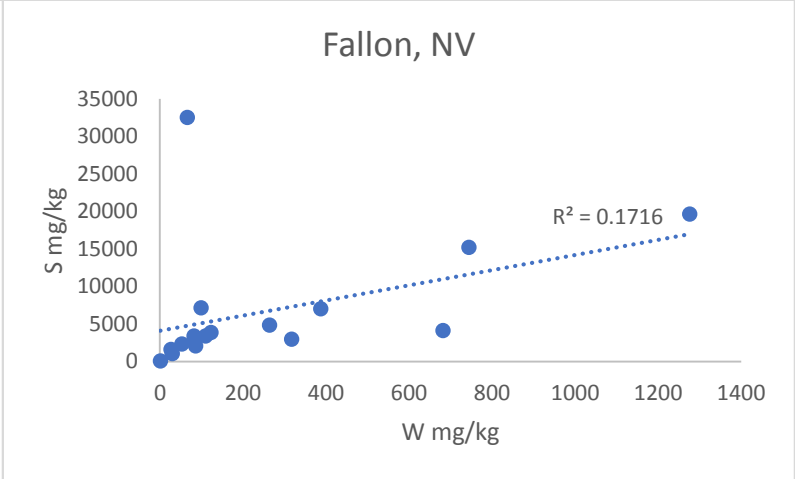
Fallon, NV
S mg/kg
W mg/kg
R² = 0.1716
0
5000
10000
15000
20000
25000
30000
35000
0
200
400
600
800
1000
1200
1400

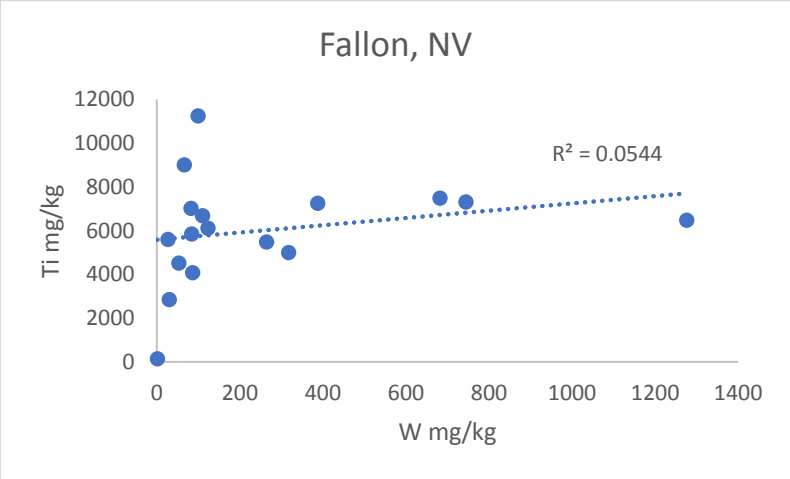
Fallon, NV
Ti mg/kg
W mg/kg
R² = 0.0544
0
2000
4000
6000
8000
10000
12000
0
200
400
600
800
1000
1200
1400

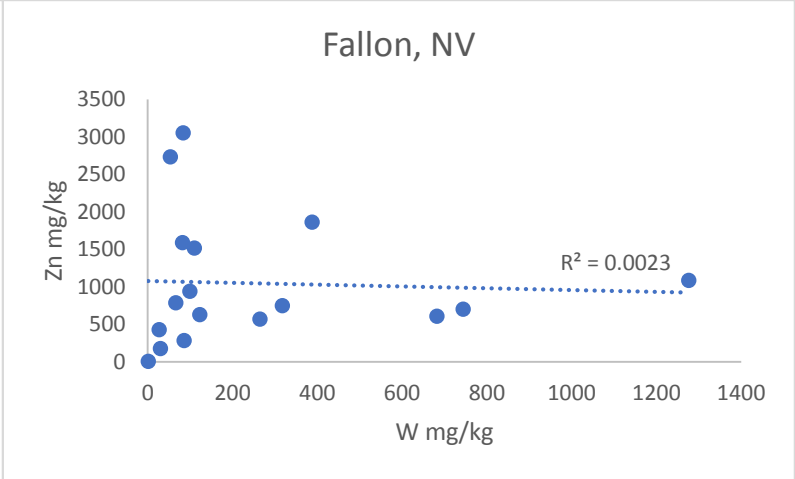
Fallon, NV
Zn mg/kg
W mg/kg
R² = 0.0023
0
500
1000
1500
2000
2500
3000
3500
0
200
400
600
800
1000
1200
1400

Sierra Vista

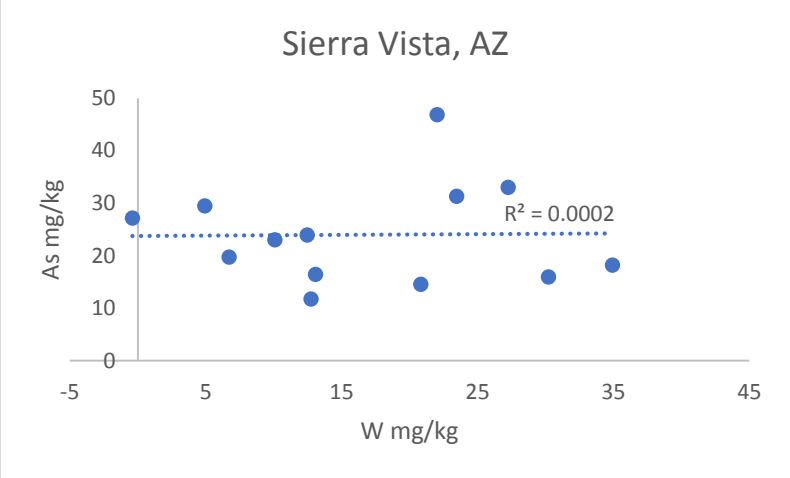

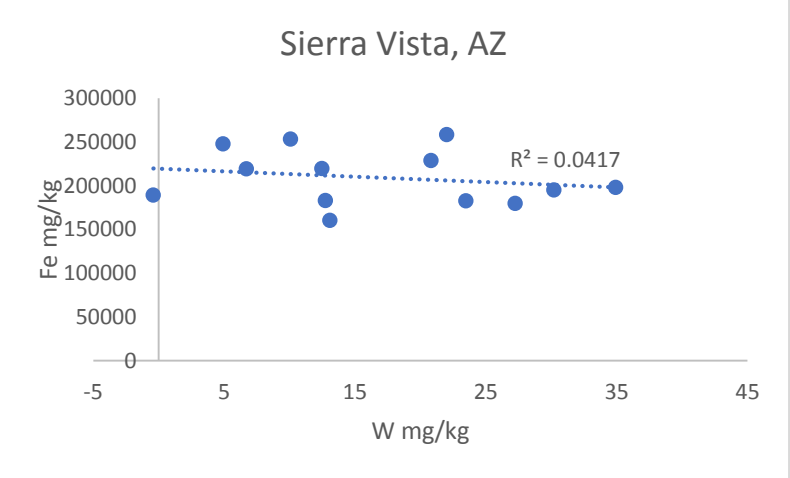

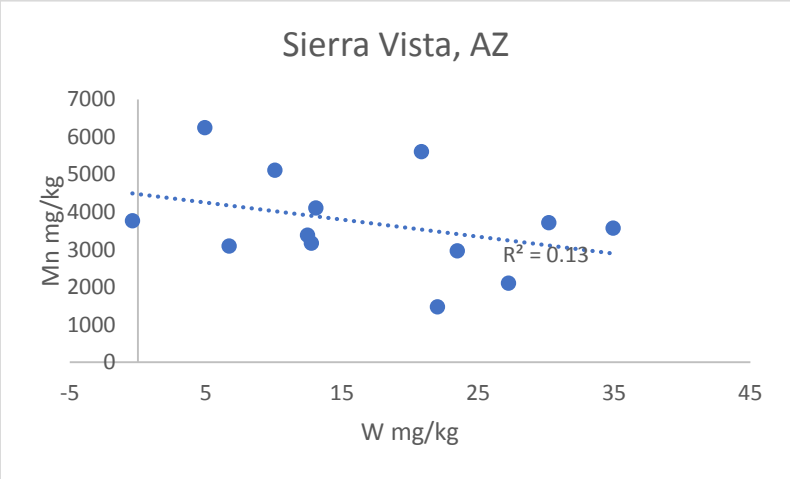

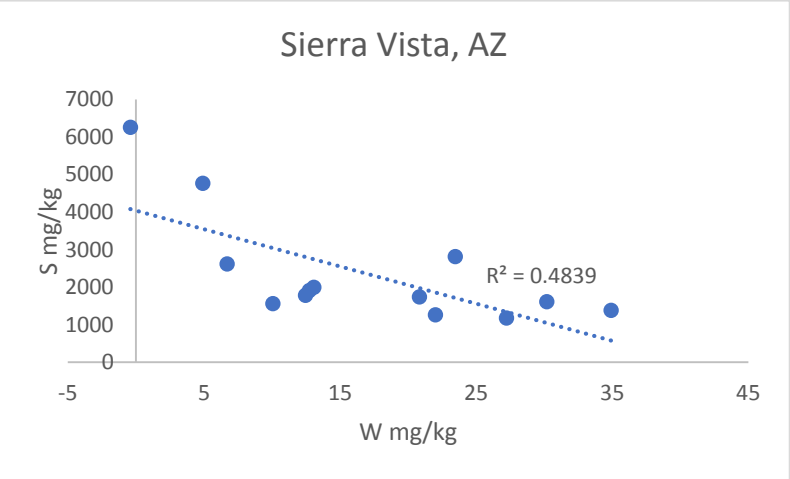

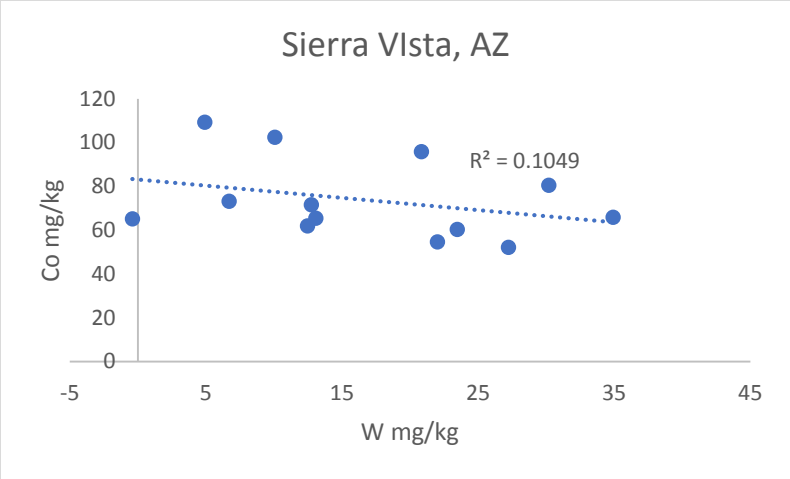
Sierra VIsta, AZ
Co mg/kg
W mg/kg
R² = 0.1049
120
100
80
60
40
20
0
-5
5
15
25
35
45

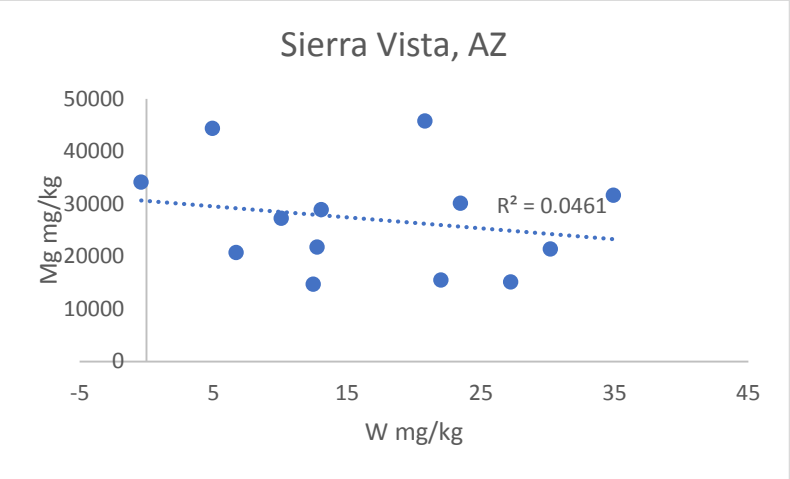
Sierra Vista, AZ
Mg mg/kg
W mg/kg
R² = 0.0461
50000
40000
30000
20000
10000
0
-5
5
15
25
35
45

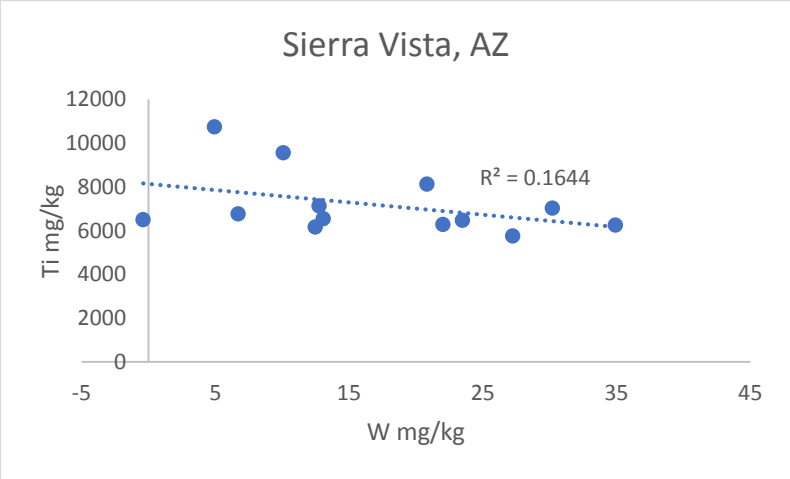
Sierra Vista, AZ
Ti mg/kg
W mg/kg
R² = 0.1644
12000
10000
8000
6000
4000
2000
0
-5
5
15
25
35
45

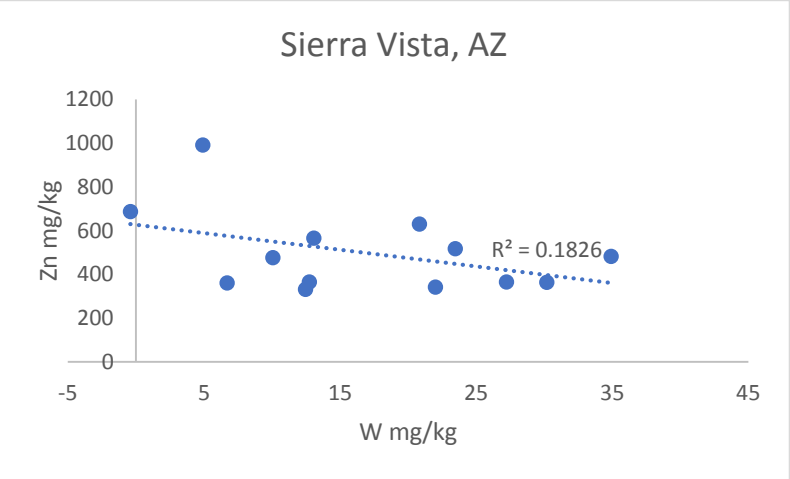
Sierra Vista, AZ
Zn mg/kg
W mg/kg
R² = 0.1826
1200
1000
800
600
400
200
0
-5
5
15
25
35
45

Cheyenne Bottoms Refuge

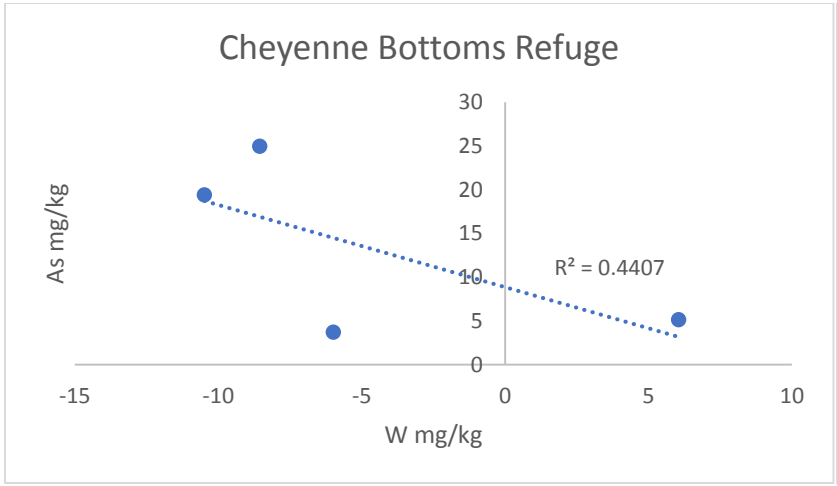

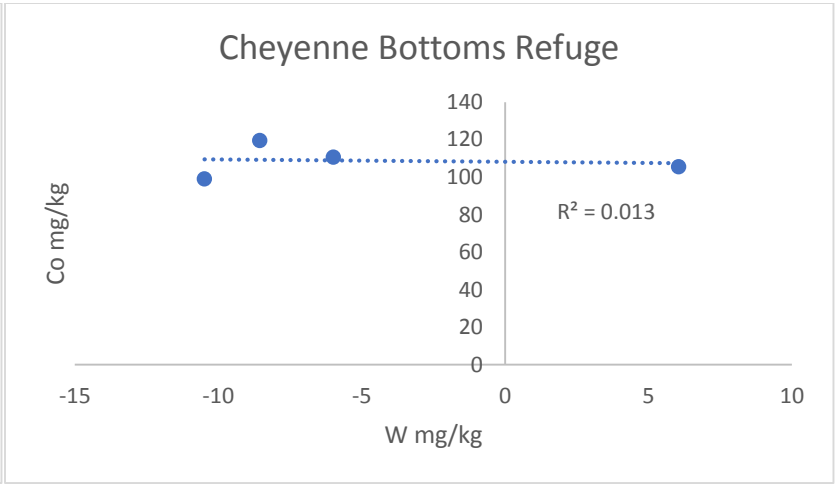

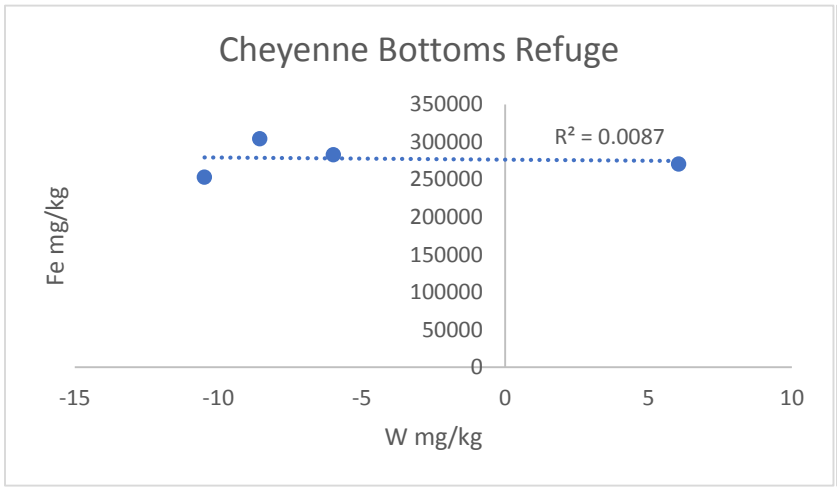

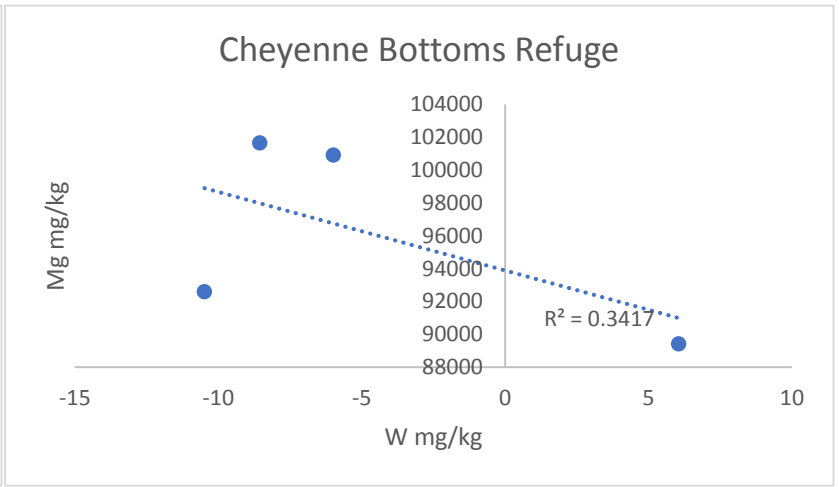

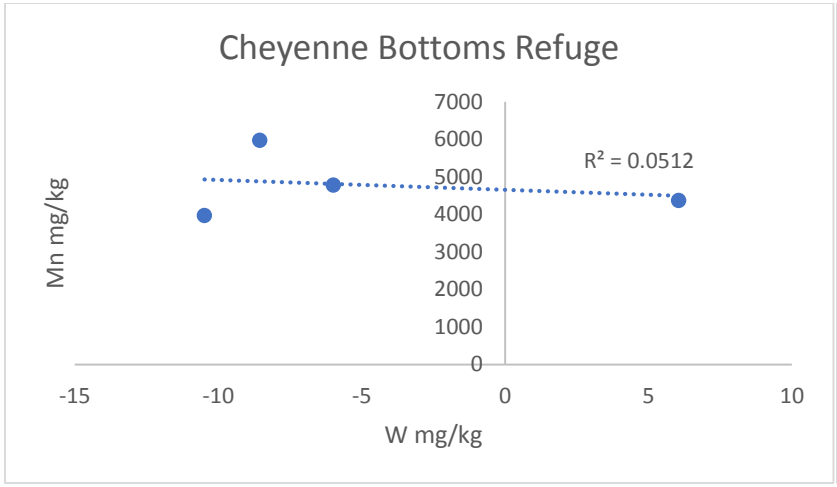
Cheyenne Bottoms Refuge
Mn mg/kg
W mg/kg
R² = 0.0512
7000
6000
5000
4000
3000
2000
1000
0
-15
-10
-5
0
5
10

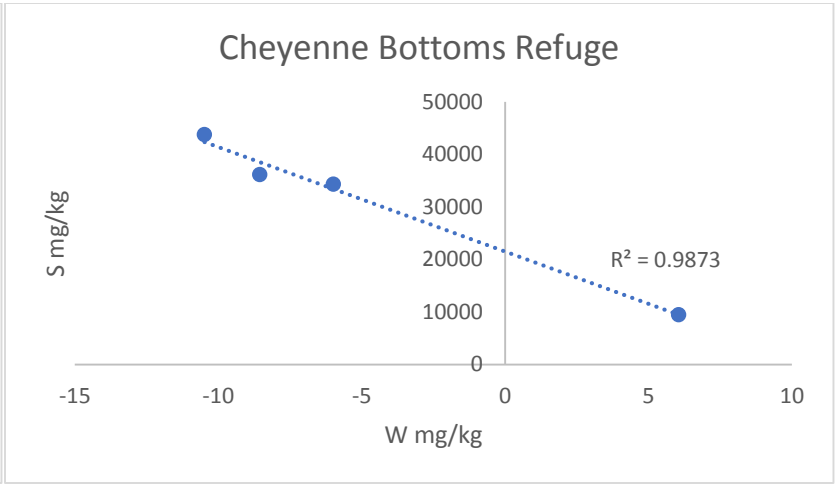
Cheyenne Bottoms Refuge
S mg/kg
W mg/kg
R² = 0.9873
50000
40000
30000
20000
10000
0
-15
-10
-5
0
5
10

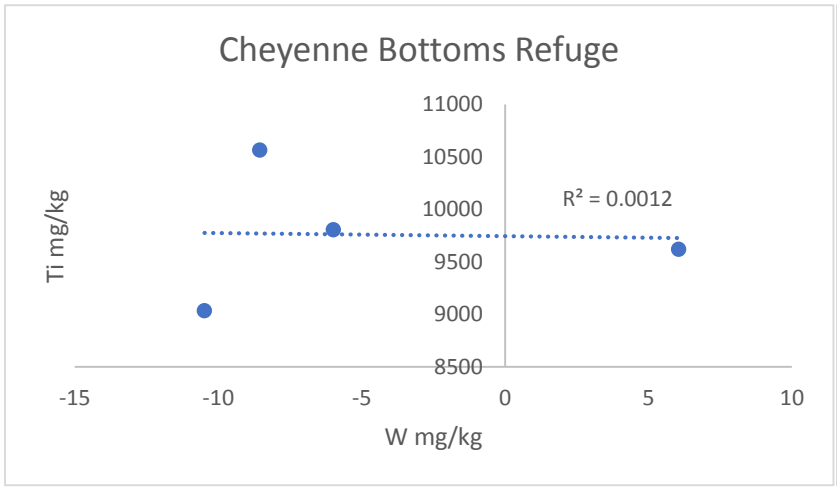
Cheyenne Bottoms Refuge
Ti mg/kg
W mg/kg
R² = 0.0012
11000
10500
10000
9500
9000
8500
-15
-10
-5
0
5
10

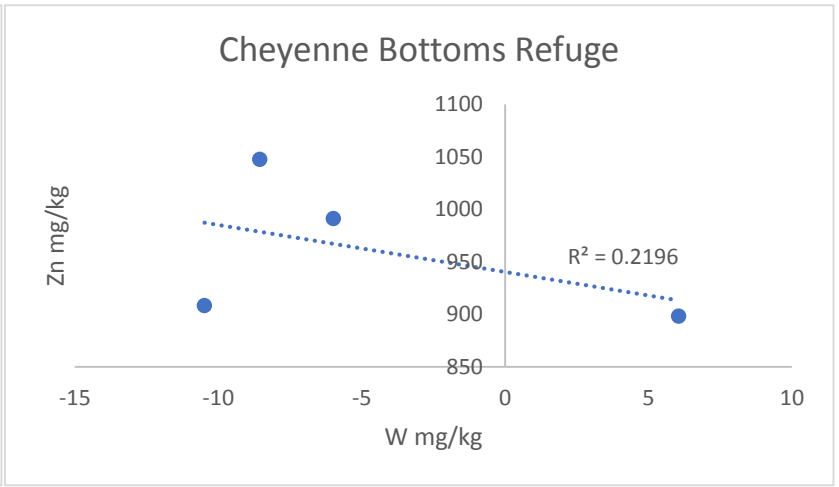
Cheyenne Bottoms Refuge
Zn mg/kg
W mg/kg
R² = 0.2196
1100
1050
1000
950
900
850
-15
-10
-5
0
5
10

A.4 Sequential Extractions

Listed here is the data for the sequential extractions performed at Kansas State University and analyzed at the US Army Engineer Research and Development Center, Environmental Chemistry Lab. The extractions were analyzed by both ICP-AES for multi-element and ICP-MS for just W.

ICP-AES

ICP-AES analysis of the sequential extractions, showing concentrations in mg/kg. Negative values indicate that the analyte measured was below detection limits.

Table A.4 Data for multi-element concentration in mg/kg for each phase of sequential extraction, analyzed by ICP-AES.

Analyte	Carrizo	CBR1_1a	CBR2_3a	CBR4_3a	fallon1	fallon2	fallon3	FNAS002
Ag								
Exchangeable	-0.68	0.40	0.16	-0.08	-0.10	0.01	0.08	-0.15
Carbonate	-0.66	0.21	-0.57	-0.50	-0.31	-0.36	0.06	-0.25
Mg Oxide	-0.19	-0.31	-0.56	-0.16	-0.19	-0.23	-0.13	-0.41
Fe Oxide	-1.30	-0.41	-1.04	-0.82	-0.77	-0.26	-0.68	-0.60
Organic Matter	-0.65	-1.26	-0.80	-0.71	-1.14	-0.41	-0.87	-0.85
Sulfide/Residual	-0.40	-0.71	-0.58	-0.78	-0.88	-0.47	-1.39	-1.23
Al								
Exchangeable	131.80	9.54	23.44	4.53	11.10	9.50	12.71	17.83
Carbonate	209.48	79.03	52.78	72.86	106.58	77.40	141.66	61.58
Mg Oxide	121.21	183.98	180.61	183.56	296.39	286.62	352.08	342.02
Fe Oxide	2461.50	3186.45	5869.75	4937.65	4487.81	5031.45	4740.32	5888.24
Organic Matter	2500.58	46908.84	6120.54	5750.48	1478.05	2675.12	1719.80	2806.43
Sulfide/Residual	2791.60	9358.21	8072.69	8279.51	15447.27	19833.33	17465.52	23058.54
As								
Exchangeable	0.25	3.12	4.41	2.48	2.42	7.28	3.07	4.45
Carbonate	5.35	12.11	9.83	7.91	6.25	7.85	9.06	9.03
Mg Oxide	-0.42	1.06	-0.01	0.49	0.79	1.21	0.48	1.06
Fe Oxide	12.61	8.40	13.69	11.79	18.68	20.20	22.00	23.60
Organic Matter	2.35	1.32	0.84	1.11	-7.14	3.24	-0.06	3.44
Sulfide/Residual	0.64	-1.16	-1.69	-1.55	-6.56	0.34	-2.84	-0.06
B								
Exchangeable	5.57	21.61	14.01	11.62	57.01	334.36	69.06	20.93
Carbonate	3.27	22.11	16.53	14.64	10.22	25.31	15.14	11.46
Mg Oxide	5.38	10.50	8.29	8.76	6.52	10.97	7.94	7.82
Fe Oxide	6.02	21.19	25.86	21.15	18.52	37.27	29.70	30.22
Organic Matter	4.42	6.61	5.44	5.04	4.53	6.35	4.72	5.32
Sulfide/Residual	6.07	10.86	10.62	9.93	16.21	20.18	20.78	23.06

Analyte	Carrizo	CBR1_1a	CBR2_3a	CBR4_3a	fallon1	fallon2	fallon3	FNAS002
Ba								
Exchangeable	105.72	334.46	434.67	362.88	166.51	175.77	100.60	312.07
Carbonate	4.24	325.88	167.48	288.38	76.29	110.80	164.08	114.15
Mg Oxide	0.50	35.20	21.60	32.90	19.82	21.67	23.77	21.49
Fe Oxide	5.14	25.72	24.58	25.88	40.96	44.21	79.42	41.54
Organic Matter	1.43	75.66	10.29	14.04	0.98	7.04	4.11	7.22
Sulfide/Residual	13.46	90.97	68.56	82.51	155.91	167.49	275.57	177.92
Be								
Exchangeable	-0.06	-0.09	-0.08	-0.06	-0.02	-0.02	-0.05	-0.06
Carbonate	-0.04	0.04	0.07	0.04	0.02	0.04	-0.02	0.00
Mg Oxide	0.00	0.30	0.29	0.31	0.07	0.13	0.07	0.11
Fe Oxide	-0.03	1.15	1.57	1.40	0.34	0.65	0.38	0.70
Organic Matter	-0.06	0.32	0.06	0.02	-0.08	-0.06	-0.07	-0.07
Sulfide/Residual	-0.02	0.02	0.04	0.02	-0.53	-0.66	-0.59	-0.87
Ca								
Exchangeable	4226.20	79608.32	71135.36	56406.80	19898.34	30850.81	37186.65	49783.44
Carbonate	302.65	63312.48	10780.87	14195.49	1908.74	3858.42	36337.19	8726.82
Mg Oxide	25.90	2853.24	934.08	1180.70	1081.70	1408.66	1710.78	1509.91
Fe Oxide	86.88	1261.98	885.37	996.70	3274.38	3371.59	3967.36	4514.97
Organic Matter	13.68	148.66	68.60	72.05	56.38	102.86	54.79	123.49
Sulfide/Residual	158.92	618.32	496.93	617.84	5912.40	5885.68	7599.41	7608.46
Cd								
Exchangeable	0.35	0.86	0.61	0.43	1.00	0.96	1.34	0.57
Carbonate	-0.12	0.90	0.61	0.46	0.06	0.22	0.29	0.04
Mg Oxide	0.04	0.27	0.28	0.28	0.09	0.11	0.08	0.08
Fe Oxide	-0.24	0.17	0.17	0.13	0.00	0.01	0.01	0.02
Organic Matter	0.03	0.22	0.21	0.14	-0.38	0.12	-0.08	0.16
Sulfide/Residual	0.13	0.22	0.22	0.19	-0.24	0.21	-0.23	0.08

Analyte	Carrizo	CBR1_1a	CBR2_3a	CBR4_3a	fallon1	fallon2	fallon3	FNAS002
Co								
Exchangeable	0.48	0.00	-0.05	-0.04	4.55	0.44	45.37	0.27
Carbonate	0.03	0.37	0.13	0.01	31.19	0.55	465.56	0.81
Mg Oxide	0.21	3.68	3.70	3.56	45.35	4.14	200.12	6.32
Fe Oxide	0.77	4.96	7.88	7.18	48.33	10.05	777.17	10.73
Organic Matter	0.07	1.07	0.83	0.69	0.66	0.44	7.78	0.53
Sulfide/Residual	0.95	5.06	4.58	4.26	23.60	15.29	307.57	19.11
Cr								
Exchangeable	0.16	0.23	0.20	0.19	0.39	0.27	1.19	0.20
Carbonate	0.33	-0.03	-0.15	-0.14	0.34	0.28	7.40	0.11
Mg Oxide	0.00	0.01	-0.03	0.01	0.05	-0.01	0.29	-0.04
Fe Oxide	2.31	2.39	5.76	5.28	3.99	3.30	33.37	2.75
Organic Matter	0.63	5.71	3.86	3.45	2.41	0.90	5.58	1.15
Sulfide/Residual	4.10	12.21	10.14	11.12	27.09	25.22	108.36	33.91
Cu								
Exchangeable	1.40	1.39	-0.46	0.89	1.78	3.77	5.08	2.06
Carbonate	0.37	0.27	-0.15	-0.03	0.89	1.01	2.27	0.97
Mg Oxide	-0.29	-0.06	-0.10	-0.12	0.14	0.18	2.68	0.14
Fe Oxide	-0.35	0.98	0.82	2.44	5.15	8.42	8.31	8.75
Organic Matter	1.64	22.77	19.65	18.10	8.57	19.29	14.93	19.27
Sulfide/Residual	3.53	10.58	7.89	6.75	15.04	18.59	19.74	20.86
Fe								
Exchangeable	21.60	1.83	8.12	1.91	3.56	4.09	11.53	8.62
Carbonate	31.66	33.00	12.14	20.55	15.55	12.03	21.25	8.03
Mg Oxide	54.97	347.95	238.03	142.80	221.80	231.89	230.10	237.69
Fe Oxide	7610.14	5935.13	8348.93	8606.94	8525.73	11502.81	9298.67	11791.32
Organic Matter	197.25	26223.63	2109.32	2029.22	117.55	728.42	276.81	702.33
Sulfide/Residual	5171.12	11026.74	10616.73	8928.85	36608.62	38384.69	44340.55	48020.11

Analyte	Carrizo	CBR1_1a	CBR2_3a	CBR4_3a	fallon1	fallon2	fallon3	FNAS002
K								
Exchangeable	1172.28	13105.50	9588.51	7684.84	7686.43	10522.09	8794.40	8179.68
Carbonate	-175.74	10.91	-7.60	-59.36	-11.07	27.45	48.02	-62.74
Mg Oxide	-420.78	-381.18	-397.01	-390.08	-231.55	-165.66	-245.06	-336.87
Fe Oxide	-408.33	1180.95	1826.95	1592.90	583.91	1014.15	778.89	909.33
Organic Matter	645.81	10208.83	1566.23	1468.29	579.07	883.84	712.94	997.04
Sulfide/Residual	96.56	2974.99	2643.69	2734.78	2254.03	3035.10	2517.55	3774.47
Li								
Exchangeable	3.46	13.70	10.58	8.36	9.05	11.24	7.97	7.29
Carbonate	-0.53	0.61	-0.06	0.76	0.08	0.36	0.10	-0.01
Mg Oxide	-1.05	-0.25	-0.29	0.29	-0.18	-0.08	0.22	0.05
Fe Oxide	0.49	12.67	18.76	17.31	12.86	20.26	18.37	23.34
Organic Matter	4.71	17.99	5.54	5.97	4.40	5.93	5.49	6.26
Sulfide/Residual	2.73	9.75	9.23	9.51	15.65	22.61	19.48	25.87
Mg								
Exchangeable	641.56	14425.03	8086.76	7702.41	2462.29	4835.40	4331.57	3897.42
Carbonate	1568.55	2604.04	2091.91	2123.47	1618.20	2148.88	2770.32	2011.43
Mg Oxide	9.10	183.65	176.95	165.57	103.92	249.00	249.89	204.44
Fe Oxide	107.76	3237.41	5061.85	4376.24	3875.48	6512.67	6694.60	7143.32
Organic Matter	30.16	4320.35	394.77	361.84	2.41	185.34	70.61	243.38
Sulfide/Residual	199.86	3083.15	2660.17	2831.78	5211.86	7126.11	6036.96	7955.02
Mn								
Exchangeable	37.83	29.71	0.61	1.44	117.50	38.51	93.30	193.40
Carbonate	3.35	365.65	325.88	178.52	202.18	164.99	367.65	475.84
Mg Oxide	0.90	460.23	661.92	655.89	318.05	333.89	87.66	455.84
Fe Oxide	10.80	179.55	345.43	252.16	225.84	341.68	288.15	326.60
Organic Matter	0.75	81.05	19.85	11.69	2.51	6.64	3.51	6.90
Sulfide/Residual	16.91	93.39	92.13	80.26	307.66	353.95	417.07	417.33

Analyte	Carrizo	CBR1_1a	CBR2_3a	CBR4_3a	fallon1	fallon2	fallon3	FNAS002
Mo								
Exchangeable	0.13	3.63	1.23	0.79	0.57	2.81	2.19	0.88
Carbonate	-0.05	0.26	0.13	0.06	-0.01	0.06	3.54	0.04
Mg Oxide	0.01	0.15	0.08	0.07	0.13	0.12	0.29	0.01
Fe Oxide	-0.88	0.05	-0.43	-1.01	-0.73	-0.48	2.99	-0.95
Organic Matter	0.23	0.37	0.08	0.08	-2.19	3.20	0.87	0.27
Sulfide/Residual	0.35	-0.40	-0.44	-0.43	-3.74	-2.00	0.74	-2.54
Na								
Exchangeable	-113.69	24242.88	17834.88	21083.90	2872.21	17812.35	6572.71	1684.73
Carbonate	-2436.71	-2175.40	-2364.96	-2365.66	-2037.75	-2025.01	-2028.68	-2228.36
Mg Oxide	-2791.67	-2748.82	-2780.56	-2772.29	-2638.02	-2643.85	-2654.35	-2720.79
Fe Oxide	-3083.46	-2722.09	-2778.71	-2815.72	-2305.06	-2282.41	-2277.54	-2184.77
Organic Matter	365233.56	347247.72	351438.31	360050.71	371076.87	359134.71	365264.43	358687.94
Sulfide/Residual	-754.18	2478.98	1460.95	938.59	3682.46	4635.40	4044.91	5104.79
Ni								
Exchangeable	2.39	1.10	0.67	0.63	1.15	1.00	4.35	0.90
Carbonate	0.45	3.84	2.58	2.01	3.69	1.33	13.93	2.21
Mg Oxide	0.06	3.50	4.24	5.70	1.88	1.32	4.96	2.64
Fe Oxide	1.50	15.45	23.31	22.10	13.06	13.07	71.91	17.26
Organic Matter	1.45	5.48	4.48	3.85	-0.30	1.99	1.88	2.30
Sulfide/Residual	2.40	11.47	8.59	7.87	10.83	12.69	31.63	15.99
P								
Exchangeable	11.94	78.25	176.53	79.82	462.66	890.71	1249.32	177.18
Carbonate	93.72	1136.61	1130.99	1215.31	448.55	525.97	758.93	517.18
Mg Oxide	5.62	443.66	263.69	371.38	497.29	649.84	582.18	615.37
Fe Oxide	356.01	417.90	636.41	502.59	1046.32	1065.08	1145.67	1383.98
Organic Matter	64.49	244.73	161.57	110.56	225.79	223.17	318.52	277.03
Sulfide/Residual	77.99	125.59	94.70	91.90	560.72	498.89	668.32	677.24

Analyte	Carrizo	CBR1_1a	CBR2_3a	CBR4_3a	fallon1	fallon2	fallon3	FNAS002
Pb								
Exchangeable	2.93	-5.29	-4.95	-4.74	-1.25	-2.42	-2.68	-3.63
Carbonate	2.45	13.74	11.13	10.44	4.51	12.67	36.71	8.30
Mg Oxide	0.80	0.92	1.34	1.39	1.93	5.16	4.42	2.04
Fe Oxide	5.97	9.77	15.45	13.46	12.63	27.39	34.15	19.98
Organic Matter	0.44	6.18	4.73	3.66	-1.53	1.96	-0.42	0.86
Sulfide/Residual	5.58	9.98	7.24	7.76	6.25	17.29	12.50	9.96
S								
Exchangeable	456.44	19733.55	11147.87	5495.95	1100.97	10355.23	2288.95	719.86
Carbonate	-104.96	350.16	68.03	56.39	-67.81	-44.20	49.27	-61.50
Mg Oxide	-13.78	28.33	31.32	-0.89	-5.96	2.53	1.67	-2.82
Fe Oxide	-182.35	521.35	418.32	18.10	-33.09	-67.03	32.08	214.98
Organic Matter	-29.78	1270.90	1245.59	166.43	71.58	48.10	92.73	143.15
Sulfide/Residual	148.17	3341.37	3925.01	445.70	439.79	590.42	684.11	474.49
Sb								
Exchangeable	1.25	1.17	0.33	0.46	3.80	3.57	0.50	1.78
Carbonate	-2.06	-2.83	-2.43	-2.61	-1.65	-1.90	-2.67	-2.31
Mg Oxide	0.24	-0.41	0.32	-0.28	0.53	0.32	0.47	0.15
Fe Oxide	-10.61	-6.32	-11.28	-10.11	-10.53	-10.24	-11.99	-12.48
Organic Matter	0.02	-0.20	-0.64	0.04	-9.91	1.03	-3.27	0.40
Sulfide/Residual	-0.55	-3.15	-2.21	-1.95	-19.12	-11.91	-22.57	-15.97
Se								
Exchangeable	2.20	15.70	13.29	14.24	7.12	11.62	9.48	11.94
Carbonate	46.63	58.34	56.24	55.88	48.40	51.81	58.90	49.47
Mg Oxide	-0.79	1.16	1.46	1.45	1.38	2.67	3.04	3.23
Fe Oxide	137.80	80.35	143.55	127.66	135.15	131.66	146.22	152.07
Organic Matter	-0.07	3.36	0.59	3.31	-13.41	-2.26	-6.52	-1.02
Sulfide/Residual	7.33	10.45	10.20	11.27	30.91	43.83	39.72	50.11

Analyte	Carrizo	CBR1_1a	CBR2_3a	CBR4_3a	fallon1	fallon2	fallon3	FNAS002
Si								
Exchangeable	176.48	1237.44	1465.67	1265.33	663.32	930.16	752.41	1034.69
Carbonate	197.62	1570.42	1470.49	1698.15	373.10	686.93	709.31	768.97
Mg Oxide	190.77	676.01	561.18	666.19	286.44	331.15	411.53	439.71
Fe Oxide	3246.38	15193.90	21536.72	19561.76	10123.65	13324.15	11511.73	14548.65
Organic Matter	3551.69	16622.32	14653.46	9970.73	8070.10	10806.76	9660.76	15819.36
Sulfide/Residual	2301.88	2274.61	2457.46	2909.22	1643.24	1850.70	2114.92	2536.13
Sn								
Exchangeable	0.78	8.97	4.29	3.95	2.04	3.56	2.60	0.62
Carbonate	7.34	2.45	6.39	5.91	7.08	7.22	4.03	5.92
Mg Oxide	-0.04	-0.52	0.05	-0.26	-0.07	0.11	-0.14	-0.15
Fe Oxide	24.77	16.35	34.96	29.46	29.15	30.74	35.36	36.59
Organic Matter	0.77	1.74	1.14	1.21	3.48	1.20	2.12	1.12
Sulfide/Residual	20.41	26.61	23.13	25.44	29.84	29.68	30.34	33.03
Sr								
Exchangeable	14.99	591.40	453.14	367.40	192.95	350.92	376.36	466.07
Carbonate	1.17	171.11	50.97	58.22	16.87	40.67	175.70	54.98
Mg Oxide	0.24	9.85	4.62	5.40	3.72	5.70	7.62	5.67
Fe Oxide	0.83	9.96	11.01	12.11	31.85	34.39	36.97	42.27
Organic Matter	1.19	9.45	3.42	3.78	0.40	2.19	0.89	2.22
Sulfide/Residual	5.22	21.69	17.75	22.45	120.18	122.23	116.22	134.44
Ti								
Exchangeable	-0.13	-1.65	-0.90	-1.21	-0.43	-0.68	-0.59	-0.82
Carbonate	0.87	0.44	0.33	0.88	0.39	0.50	-0.22	0.10
Mg Oxide	0.76	1.01	0.38	0.51	0.26	0.61	1.14	1.45
Fe Oxide	2.57	3.08	2.98	3.27	7.33	7.28	9.00	8.34
Organic Matter	20.54	178.34	120.40	122.64	159.62	106.94	138.11	150.25
Sulfide/Residual	237.63	802.39	654.79	787.91	2206.11	2799.65	2553.22	3477.08

Analyte	Carrizo	CBR1_1a	CBR2_3a	CBR4_3a	fallon1	fallon2	fallon3	FNAS002
Tl								
Exchangeable	0.42	1.79	1.52	1.95	2.96	2.56	2.52	1.15
Carbonate	-2.46	-1.77	-2.38	-2.46	-2.17	-2.31	-0.36	-2.68
Mg Oxide	-0.85	-1.76	-2.03	-2.00	-0.97	-0.95	-0.27	-1.72
Fe Oxide	-5.20	-3.62	-5.68	-5.29	-5.05	-5.58	-3.43	-5.27
Organic Matter	-0.37	-0.49	-0.24	0.20	2.43	-0.22	0.59	-0.01
Sulfide/Residual	0.51	1.28	0.69	1.00	1.45	-0.52	1.70	-0.78
V								
Exchangeable	0.24	1.41	1.46	1.10	0.81	1.19	1.87	0.55
Carbonate	0.10	2.04	1.25	1.25	0.83	0.60	1.33	0.45
Mg Oxide	0.15	5.15	3.38	2.72	2.63	4.01	2.56	2.68
Fe Oxide	15.36	22.47	31.43	25.11	19.21	30.03	19.62	28.85
Organic Matter	1.72	19.17	10.86	9.15	2.57	4.81	3.33	4.93
Sulfide/Residual	10.57	18.40	15.65	17.56	106.58	111.83	128.39	143.61
W								
Exchangeable	-0.26	-2.34	-2.55	-2.29	397.56	4.06	920.41	-0.19
Carbonate	-9.02	-10.34	-10.91	-11.01	30.93	-8.77	83.73	-10.02
Mg Oxide	0.11	-0.16	-0.12	-0.19	7.07	0.33	15.46	0.40
Fe Oxide	-18.79	-12.97	-19.29	-17.72	212.40	-15.80	250.77	-20.04
Organic Matter	3.56	2.71	-0.03	25.35	4427.20	46.02	1722.65	6.78
Sulfide/Residual	5.13	8.36	1.74	37.95	3385.09	39.05	3580.19	20.37
Zn								
Exchangeable	7.75	3.60	1.59	3.35	8.66	5.34	7.36	4.78
Carbonate	5.35	5.43	3.38	2.18	43.46	19.50	61.51	11.99
Mg Oxide	0.80	5.30	4.70	2.49	25.53	21.39	26.14	12.48
Fe Oxide	9.43	41.36	67.81	49.87	111.92	113.48	127.16	94.87
Organic Matter	0.86	11.21	8.48	6.32	6.55	3.19	1.72	2.63
Sulfide/Residual	9.92	41.07	34.35	35.78	71.31	89.67	86.13	90.18

Analyte	FNPS003	FNSG001	FNSG002	FNSG003	LA001	LA010	LA011	MS001
Ag								
Exchangeable	-0.36	0.26	0.54	0.32	-0.64	-0.65	-0.41	-0.38
Carbonate	-0.76	-0.32	0.81	-0.38	-0.90	-1.17	-0.95	-1.08
Mg Oxide	-0.30	-0.16	-0.14	-0.23	-0.28	-0.53	-0.43	-0.31
Fe Oxide	-1.04	-1.00	-0.59	-0.94	-1.51	-1.83	-1.78	-1.43
Organic Matter	-0.93	-0.38	-0.80	-1.12	-0.72	-1.07	-1.08	-1.20
Sulfide/Residual	-1.69	-0.95	-0.95	-1.16	-1.50	-1.90	-1.40	-2.13
Al								
Exchangeable	9.77	11.27	17.53	11.14	176.95	14.58	15.10	11.39
Carbonate	130.59	50.18	46.48	146.62	230.45	166.00	137.37	126.46
Mg Oxide	404.40	317.45	284.92	367.72	244.72	207.28	155.71	208.09
Fe Oxide	7860.08	6259.26	5401.11	5947.33	5250.81	6500.89	4956.58	4835.16
Organic Matter	4412.69	2857.72	1490.65	2473.67	4775.23	7277.47	5140.44	3414.25
Sulfide/Residual	28716.61	19366.37	19088.73	20577.84	12766.90	18817.05	11014.96	24752.12
As								
Exchangeable	0.72	4.09	7.42	3.41	0.33	0.29	0.11	0.42
Carbonate	10.75	7.95	12.35	7.91	5.06	4.97	4.06	5.36
Mg Oxide	3.06	0.87	1.08	0.58	-0.74	-0.50	-0.31	-0.17
Fe Oxide	35.59	24.54	28.12	17.08	16.85	11.59	11.65	13.58
Organic Matter	7.99	3.34	3.93	2.92	5.37	2.31	2.04	1.70
Sulfide/Residual	2.12	-0.16	0.56	-0.28	-1.76	-1.15	-0.35	-3.66
B								
Exchangeable	98.23	24.97	1115.39	93.54	5.60	5.76	4.82	4.79
Carbonate	18.87	14.97	162.44	16.50	3.21	3.15	3.05	2.79
Mg Oxide	8.74	7.96	21.62	8.66	4.93	5.13	4.55	4.37
Fe Oxide	36.34	32.82	74.52	29.80	10.03	12.94	9.36	9.75
Organic Matter	5.27	5.22	6.41	5.05	4.24	4.02	3.56	3.21
Sulfide/Residual	22.14	19.43	20.35	19.98	20.76	19.48	13.28	16.06

Analyte	FNPS003	FNSG001	FNSG002	FNSG003	LA001	LA010	LA011	MS001
Ba								
Exchangeable	394.44	347.00	121.07	223.92	155.31	453.07	325.08	299.60
Carbonate	229.92	137.01	306.34	107.31	7.81	35.50	25.38	47.13
Mg Oxide	40.48	26.69	56.33	25.65	7.84	37.87	21.30	45.47
Fe Oxide	59.92	49.29	108.71	58.21	15.90	32.71	25.19	33.97
Organic Matter	8.46	7.82	2.14	1.29	2.26	5.15	4.07	2.88
Sulfide/Residual	165.81	157.18	208.39	190.45	42.15	54.26	39.58	63.98
Be								
Exchangeable	-0.06	-0.02	-0.05	-0.06	0.15	-0.03	-0.07	-0.08
Carbonate	0.05	0.01	-0.09	0.04	0.17	0.53	0.28	0.46
Mg Oxide	0.27	0.11	0.13	0.16	0.15	0.32	0.19	0.55
Fe Oxide	1.52	0.77	0.76	0.82	1.03	2.04	1.31	2.11
Organic Matter	-0.08	-0.06	-0.09	-0.09	0.03	0.07	0.01	0.00
Sulfide/Residual	-0.82	-0.72	-0.54	-0.64	0.15	0.32	0.18	0.83
Ca								
Exchangeable	23194.10	46666.13	60030.77	41689.05	4574.86	9950.20	6955.89	14236.52
Carbonate	2251.59	7002.57	127681.08	6540.58	210.89	476.62	305.73	1240.64
Mg Oxide	2114.66	1586.25	4701.77	1730.24	77.48	54.28	43.24	633.91
Fe Oxide	3360.64	4718.36	7639.13	3821.53	376.82	522.78	213.25	1390.85
Organic Matter	111.20	125.51	76.36	43.18	18.52	22.23	18.01	53.57
Sulfide/Residual	3526.46	6202.84	6157.59	5241.45	870.85	852.30	596.64	2159.31
Cd								
Exchangeable	0.38	0.62	0.51	0.76	1.34	0.80	0.56	1.37
Carbonate	0.06	0.13	0.35	0.18	-0.07	-0.06	-0.05	-0.01
Mg Oxide	0.14	0.11	0.10	0.09	0.06	0.25	0.15	0.15
Fe Oxide	0.04	0.02	0.01	0.07	0.02	-0.05	-0.11	-0.02
Organic Matter	0.16	0.19	0.15	0.13	0.11	0.16	0.10	0.11
Sulfide/Residual	0.19	0.11	0.15	0.13	0.15	0.21	0.18	0.32

Analyte	FNPS003	FNSG001	FNSG002	FNSG003	LA001	LA010	LA011	MS001
Co								
Exchangeable	0.00	0.40	4.49	0.53	3.83	-0.01	2.27	1.24
Carbonate	0.02	1.22	8.97	1.62	0.90	0.10	0.87	0.66
Mg Oxide	14.74	6.25	8.74	4.77	6.17	21.60	13.74	12.32
Fe Oxide	12.93	12.63	53.65	11.94	3.72	3.83	2.96	5.31
Organic Matter	0.75	0.62	1.59	0.40	0.27	0.20	0.16	0.19
Sulfide/Residual	19.86	15.34	21.08	15.95	14.81	11.10	7.44	15.78
Cr								
Exchangeable	0.24	0.24	0.31	0.21	0.12	0.22	0.18	0.15
Carbonate	0.26	-0.03	0.34	0.25	0.09	0.11	0.19	0.27
Mg Oxide	-0.05	0.09	0.05	0.06	-0.08	-0.10	0.04	-0.10
Fe Oxide	8.62	2.22	2.60	3.92	8.57	14.68	11.85	4.94
Organic Matter	1.07	1.54	1.24	0.79	1.34	1.86	1.30	1.88
Sulfide/Residual	24.11	24.51	23.06	22.82	27.53	42.47	34.98	77.96
Cu								
Exchangeable	1.26	2.89	5.88	3.31	9.38	1.31	1.09	1.32
Carbonate	1.99	0.33	0.83	0.48	14.43	5.64	1.95	0.96
Mg Oxide	2.19	-0.28	-0.09	-0.12	8.92	5.37	1.81	1.10
Fe Oxide	20.52	3.36	4.13	5.46	32.93	20.06	10.61	9.62
Organic Matter	23.31	19.35	19.61	19.36	19.62	12.75	5.93	26.56
Sulfide/Residual	26.00	17.36	22.01	18.10	18.65	20.07	14.02	33.82
Fe								
Exchangeable	1.96	4.89	28.58	7.10	7.52	9.73	17.02	5.84
Carbonate	27.29	7.84	27.68	22.16	16.65	12.43	23.72	23.88
Mg Oxide	434.51	234.27	187.50	227.90	178.50	289.09	182.02	407.90
Fe Oxide	22106.12	13232.35	12154.10	11592.90	15876.08	24084.87	17183.55	15582.23
Organic Matter	1097.73	744.53	126.96	90.63	267.15	449.24	382.45	325.60
Sulfide/Residual	45249.74	38753.30	34734.68	38886.45	65975.24	56829.81	35538.16	46714.87

Analyte	FNPS003	FNSG001	FNSG002	FNSG003	LA001	LA010	LA011	MS001
K								
Exchangeable	1621.46	8639.71	23372.87	10351.51	2657.14	2646.17	1609.42	2742.29
Carbonate	-131.15	-6.88	380.06	54.26	-233.51	-223.20	-232.65	-198.24
Mg Oxide	-428.51	-300.59	-186.82	-208.31	-400.16	-448.37	-446.08	-394.52
Fe Oxide	35.70	1035.93	1269.33	1217.32	71.56	152.97	104.84	555.23
Organic Matter	695.27	953.86	775.42	769.44	866.95	940.07	816.97	891.58
Sulfide/Residual	3365.93	3258.86	3380.51	3689.12	2324.23	3594.67	2689.37	7696.68
Li								
Exchangeable	10.57	8.06	21.81	8.79	5.21	4.51	3.73	3.87
Carbonate	0.48	-0.02	6.09	0.03	-0.01	-0.29	-0.35	-0.60
Mg Oxide	0.39	-0.20	0.66	0.27	-0.55	-0.47	-0.19	-0.48
Fe Oxide	31.58	24.36	31.73	24.67	8.48	21.61	12.93	14.39
Organic Matter	5.17	5.80	5.67	5.58	5.32	6.42	5.68	4.55
Sulfide/Residual	38.30	21.91	24.51	25.11	12.15	19.32	14.01	41.98
Mg								
Exchangeable	9912.79	4487.49	15257.56	6755.81	968.31	2462.88	1897.91	1747.84
Carbonate	1837.07	2128.95	12964.25	2094.06	1357.80	1510.07	1285.80	1477.29
Mg Oxide	111.22	231.58	1093.26	264.02	13.50	25.76	22.85	38.24
Fe Oxide	7358.86	7739.61	17759.42	8005.09	616.12	889.33	826.44	1714.41
Organic Matter	261.13	234.79	18.83	9.44	40.90	69.86	63.96	47.08
Sulfide/Residual	11725.67	6741.07	10120.53	7861.81	2648.40	3710.42	2713.63	9007.41
Mn								
Exchangeable	1.01	304.13	76.17	177.70	510.14	145.17	558.63	1317.71
Carbonate	60.13	804.73	606.51	433.31	60.63	107.48	146.69	277.96
Mg Oxide	1296.74	536.63	203.26	360.96	316.45	1314.65	617.47	1188.24
Fe Oxide	769.01	395.31	470.79	319.11	130.92	246.07	155.18	355.35
Organic Matter	15.06	7.80	4.73	2.22	1.68	2.87	2.18	3.15
Sulfide/Residual	485.98	349.56	332.15	364.59	320.85	335.32	213.44	475.27

Analyte	FNPS003	FNSG001	FNSG002	FNSG003	LA001	LA010	LA011	MS001
Mo								
Exchangeable	0.54	1.07	2.27	1.29	0.22	0.08	0.24	0.26
Carbonate	0.10	0.06	0.22	0.07	0.04	-0.01	-0.08	-0.04
Mg Oxide	0.14	0.16	0.09	0.06	0.10	0.04	-0.09	-0.01
Fe Oxide	1.24	-1.12	-0.88	-1.04	-1.46	-2.29	-1.74	-1.09
Organic Matter	1.17	0.35	0.28	0.20	0.40	0.22	0.06	0.35
Sulfide/Residual	-1.90	-2.18	-1.61	-2.13	-3.49	-3.08	-1.62	-2.26
Na								
Exchangeable	40360.77	2254.99	27336.45	1771.78	-399.78	-333.41	3311.15	540.93
Carbonate	-2156.82	-2222.61	-1713.83	-2132.29	-2506.93	-2506.84	-2498.10	-2517.92
Mg Oxide	-2716.66	-2692.86	-2695.20	-2683.25	-2814.58	-2843.55	-2815.15	-2824.31
Fe Oxide	-1835.39	-2171.01	-2285.35	-2255.90	-2984.75	-2861.67	-2994.54	-2878.26
Organic Matter	348125.84	357534.37	367961.21	355894.69	360959.41	363969.15	359586.91	352647.92
Sulfide/Residual	8808.34	5171.28	5938.23	4454.35	882.54	32.47	-469.32	1173.93
Ni								
Exchangeable	0.52	0.79	1.60	0.99	3.49	4.32	4.50	1.99
Carbonate	1.34	1.39	1.20	1.62	0.54	2.36	2.38	2.32
Mg Oxide	8.00	1.73	0.82	1.96	0.24	4.66	2.76	3.26
Fe Oxide	15.45	17.84	18.88	16.02	6.37	9.29	7.70	9.60
Organic Matter	1.98	2.44	1.26	0.71	2.36	2.77	2.73	2.03
Sulfide/Residual	17.66	12.70	15.71	13.13	12.91	19.74	16.04	44.28
P								
Exchangeable	2.87	245.21	2996.99	425.61	15.82	7.36	6.18	22.76
Carbonate	402.49	514.20	1674.22	676.53	127.22	77.21	71.81	136.87
Mg Oxide	1094.33	633.67	688.40	757.16	37.41	4.34	2.84	246.18
Fe Oxide	650.02	1520.62	1318.38	1038.65	720.66	420.19	379.10	1137.43
Organic Matter	155.57	335.45	461.39	370.92	256.28	180.94	111.52	298.46
Sulfide/Residual	169.31	547.19	576.42	445.97	221.99	221.61	159.29	514.82

Analyte	FNPS003	FNSG001	FNSG002	FNSG003	LA001	LA010	LA011	MS001
Pb								
Exchangeable	-3.25	-3.11	-4.35	-3.71	19.30	-0.80	-0.40	-0.88
Carbonate	0.91	9.40	9.31	3.86	14.83	4.80	3.85	5.25
Mg Oxide	0.74	2.27	0.88	1.34	15.12	9.33	5.84	6.63
Fe Oxide	15.22	23.81	28.52	12.44	36.72	32.64	23.37	41.42
Organic Matter	0.59	0.99	0.50	-0.55	1.73	2.85	1.39	4.13
Sulfide/Residual	13.23	9.77	12.31	8.14	15.68	16.46	10.31	21.30
S								
Exchangeable	5538.13	793.48	14016.71	1206.86	320.84	401.92	654.12	569.98
Carbonate	-8.59	-54.50	317.78	-38.73	-106.13	-95.59	-93.13	-108.03
Mg Oxide	0.36	0.89	24.09	-3.66	-14.65	-10.94	-15.87	-12.63
Fe Oxide	-105.82	337.56	299.92	-28.02	-77.53	154.99	-149.14	51.69
Organic Matter	-0.92	227.12	227.33	130.55	6.52	40.42	-15.70	-9.11
Sulfide/Residual	318.24	530.90	641.40	408.39	159.84	139.36	176.22	135.58
Sb								
Exchangeable	1.77	1.98	1.64	1.33	1.65	1.23	0.94	1.06
Carbonate	-2.31	-2.22	-2.89	-2.16	-2.26	-2.22	-1.78	-1.95
Mg Oxide	-0.01	0.37	0.10	-0.32	0.32	0.14	-0.07	-0.32
Fe Oxide	-15.03	-13.65	-12.69	-11.63	-13.13	-17.13	-14.00	-13.92
Organic Matter	0.42	0.82	0.96	0.79	0.57	0.22	-0.12	0.00
Sulfide/Residual	-14.89	-13.26	-11.61	-13.16	-19.76	-18.40	-10.35	-14.99
Se								
Exchangeable	8.68	8.96	11.18	11.92	3.53	0.80	3.11	2.93
Carbonate	49.56	51.23	61.93	47.60	47.50	48.51	46.05	46.60
Mg Oxide	3.00	2.68	3.50	1.78	0.00	1.06	-0.14	1.94
Fe Oxide	151.12	159.02	150.45	138.92	147.22	163.81	146.40	152.28
Organic Matter	-0.66	-1.57	-0.16	3.99	0.17	-0.13	3.06	-0.15
Sulfide/Residual	47.17	42.30	38.93	42.30	66.59	60.76	36.30	47.28

Analyte	FNPS003	FNSG001	FNSG002	FNSG003	LA001	LA010	LA011	MS001
Si								
Exchangeable	1099.61	1303.78	3328.49	1064.59	434.72	374.00	330.77	378.36
Carbonate	1083.78	870.35	5918.67	886.86	175.49	353.86	311.27	305.69
Mg Oxide	557.08	425.49	602.56	448.07	193.32	200.90	224.36	194.85
Fe Oxide	19520.19	14989.45	15253.66	16435.75	6466.94	9231.64	7252.17	8253.66
Organic Matter	15895.10	17244.67	14992.55	12600.64	7201.65	8748.89	6600.23	9118.13
Sulfide/Residual	2482.03	1879.53	2758.86	1932.50	1860.94	2643.72	2805.52	2452.32
Sn								
Exchangeable	8.55	1.74	10.50	3.93	1.05	1.79	1.70	-0.02
Carbonate	7.58	6.18	12.21	6.02	6.96	7.43	6.24	7.04
Mg Oxide	-0.45	-0.09	0.26	-0.11	0.06	-0.10	0.08	-0.25
Fe Oxide	33.58	38.51	45.14	34.96	26.39	28.10	26.78	28.80
Organic Matter	1.21	1.15	1.16	0.96	0.52	0.79	0.65	0.72
Sulfide/Residual	35.81	29.01	33.34	31.31	23.96	26.31	28.34	33.57
Sr								
Exchangeable	456.42	491.03	638.07	386.70	26.82	78.15	57.60	82.02
Carbonate	42.03	51.88	606.46	44.52	1.17	3.33	1.97	6.47
Mg Oxide	8.11	6.31	24.20	6.78	0.37	0.46	0.27	1.54
Fe Oxide	53.50	43.96	64.29	41.42	3.55	5.90	2.50	6.35
Organic Matter	3.14	2.31	0.62	0.53	0.54	1.15	0.94	0.60
Sulfide/Residual	89.82	113.07	101.16	108.07	13.59	15.29	9.68	18.30
Ti								
Exchangeable	-0.58	-1.01	-0.71	-0.80	-0.13	-0.26	-0.16	-0.35
Carbonate	1.12	0.15	-1.54	0.57	0.28	0.72	1.02	0.81
Mg Oxide	1.06	0.71	1.19	1.19	0.40	0.81	0.79	0.24
Fe Oxide	9.21	7.14	5.65	6.58	14.06	14.66	13.95	6.60
Organic Matter	138.14	161.42	100.08	70.27	75.69	100.68	88.32	75.27
Sulfide/Residual	3762.33	2840.07	2517.58	2888.27	1738.03	1981.94	1287.11	2202.16

Analyte	FNPS003	FNSG001	FNSG002	FNSG003	LA001	LA010	LA011	MS001
Tl								
Exchangeable	1.14	1.09	1.49	1.11	-0.85	0.52	-0.65	-2.03
Carbonate	-2.23	-3.47	-1.66	-2.43	-2.28	-2.58	-2.64	-2.65
Mg Oxide	-3.04	-1.33	-0.56	-1.31	-1.23	-3.24	-2.10	-2.81
Fe Oxide	-6.58	-6.55	-5.72	-5.56	-5.26	-5.86	-5.62	-5.74
Organic Matter	-0.21	-0.22	-0.23	-0.21	-0.15	0.12	-0.18	-0.32
Sulfide/Residual	-0.70	-1.61	0.11	-1.80	-1.07	0.41	-0.32	-0.25
V								
Exchangeable	0.44	0.40	1.33	1.09	0.13	0.37	0.18	0.13
Carbonate	1.53	0.32	0.87	1.06	0.30	0.21	0.21	0.18
Mg Oxide	16.74	2.53	2.09	4.08	1.30	2.86	2.17	2.03
Fe Oxide	85.51	29.70	34.17	29.50	33.33	53.10	37.85	23.24
Organic Matter	9.54	5.59	6.08	5.27	3.23	5.31	2.86	3.38
Sulfide/Residual	113.33	112.02	94.17	102.48	94.65	82.67	51.72	55.65
W								
Exchangeable	-1.56	1.58	22.65	2.92	-0.40	-0.82	-0.49	-1.35
Carbonate	-9.94	-8.78	-9.69	-9.26	-9.20	-8.88	-8.69	-9.35
Mg Oxide	-0.35	-0.19	0.26	0.70	0.07	-0.27	-0.44	-0.37
Fe Oxide	-16.53	-19.68	-15.30	-16.72	-18.84	-19.60	-19.42	-18.88
Organic Matter	46.66	17.16	21.91	78.57	8.21	6.48	0.30	25.38
Sulfide/Residual	33.57	41.45	310.38	33.48	52.48	5.43	3.36	6.63
Zn								
Exchangeable	4.38	4.68	5.23	4.83	34.41	8.04	5.76	10.53
Carbonate	2.31	15.02	27.49	11.92	6.89	5.96	7.37	9.79
Mg Oxide	3.98	14.89	26.49	12.79	2.53	2.17	1.57	6.87
Fe Oxide	105.44	112.75	146.76	98.94	53.36	33.77	23.39	71.70
Organic Matter	3.35	2.82	0.08	0.23	2.39	2.24	2.10	2.63
Sulfide/Residual	122.52	78.16	83.30	88.21	60.03	70.10	48.41	131.92

Analyte	PK012	PK020	TF001	FNAS004	MS002
Ag					
Exchangeable	-0.01	-0.28	-0.52	-0.15	-0.62
Carbonate	-0.92	-0.98	-0.98	-0.50	-0.88
Mg Oxide	-0.60	-0.34	-0.49	-0.07	-0.55
Fe Oxide	-1.52	-1.37	-1.49	-0.99	-1.55
Organic Matter	-1.28	-0.99	-0.91	-1.00	-1.42
Sulfide/Residual	-1.46	-1.61	-1.43	-1.32	-0.88
Al					
Exchangeable	9.80	13.22	241.28	10.24	12.93
Carbonate	226.49	201.96	282.07	116.31	73.36
Mg Oxide	346.82	352.39	202.69	352.71	175.84
Fe Oxide	5252.89	6017.56	5010.50	6610.59	5079.85
Organic Matter	3628.60	132354.44	3599.58	3044.60	4644.48
Sulfide/Residual	17810.24	13644.32	11348.12	21727.17	12378.18
As					
Exchangeable	1.22	1.35	0.02	7.28	0.29
Carbonate	5.32	5.37	4.48	11.31	5.29
Mg Oxide	-0.08	-0.59	-0.14	2.41	-0.24
Fe Oxide	14.17	13.78	16.27	19.97	11.49
Organic Matter	2.81	1.76	3.59	3.40	-0.30
Sulfide/Residual	-1.96	-2.54	-2.77	0.26	-2.62
B					
Exchangeable	6.47	7.25	4.33	49.88	4.64
Carbonate	4.59	3.96	2.30	10.57	2.76
Mg Oxide	4.12	3.97	3.34	7.97	3.89
Fe Oxide	12.44	12.24	7.51	28.70	9.57
Organic Matter	3.18	3.27	2.84	5.02	3.11
Sulfide/Residual	13.54	15.43	17.44	20.60	8.55

Analyte	PK012	PK020	TF001	FNAS004	MS002
Ba					
Exchangeable	348.70	279.72	91.32	286.19	284.69
Carbonate	109.91	41.84	8.22	77.28	51.21
Mg Oxide	52.43	52.95	2.20	20.90	47.25
Fe Oxide	30.15	30.16	14.39	56.26	39.10
Organic Matter	2.05	78.78	2.26	6.47	5.52
Sulfide/Residual	46.18	41.59	32.31	191.35	31.52
Be					
Exchangeable	-0.08	-0.10	0.12	-0.09	-0.09
Carbonate	0.46	0.30	0.08	0.00	0.32
Mg Oxide	0.28	0.29	0.03	0.15	0.57
Fe Oxide	2.29	1.94	0.69	0.96	2.58
Organic Matter	-0.03	1.03	-0.03	-0.09	0.04
Sulfide/Residual	0.69	0.31	0.17	-0.67	0.40
Ca					
Exchangeable	44714.74	36943.95	2913.25	47702.36	17722.50
Carbonate	4389.78	2296.91	182.48	4045.56	1832.87
Mg Oxide	842.23	851.18	66.08	1659.28	557.89
Fe Oxide	1655.23	847.62	387.63	3914.10	1329.43
Organic Matter	65.00	104.60	26.38	102.80	70.01
Sulfide/Residual	1640.60	1259.73	1005.83	5199.74	917.24
Cd					
Exchangeable	0.47	0.49	0.66	0.43	0.40
Carbonate	-0.02	0.01	-0.10	0.04	0.00
Mg Oxide	0.16	0.17	0.06	0.11	0.21
Fe Oxide	-0.07	-0.01	-0.06	0.06	-0.06
Organic Matter	0.06	0.13	0.06	0.13	0.05
Sulfide/Residual	0.21	0.21	0.14	0.10	0.18

Analyte	PK012	PK020	TF001	FNAS004	MS002
Co					
Exchangeable	0.50	0.05	1.62	0.04	-0.05
Carbonate	0.54	0.25	0.86	0.06	0.07
Mg Oxide	16.56	16.66	1.04	6.64	12.76
Fe Oxide	4.67	4.06	2.76	9.99	5.83
Organic Matter	0.39	0.51	0.17	0.49	0.21
Sulfide/Residual	11.39	10.41	10.79	15.97	7.33
Cr					
Exchangeable	0.25	0.21	0.14	0.26	0.23
Carbonate	0.39	0.09	0.16	0.04	0.06
Mg Oxide	0.04	0.07	-0.05	-0.04	0.00
Fe Oxide	11.79	10.31	6.45	5.20	4.61
Organic Matter	1.23	2.19	0.91	0.69	2.13
Sulfide/Residual	27.27	18.14	23.06	23.40	17.93
Cu					
Exchangeable	2.74	1.47	4.10	4.77	0.85
Carbonate	2.06	1.33	6.88	0.91	-0.03
Mg Oxide	2.51	2.39	3.48	0.80	-0.14
Fe Oxide	20.32	14.38	23.00	14.79	4.89
Organic Matter	7.36	8.60	12.39	14.75	18.92
Sulfide/Residual	22.35	15.30	15.83	18.88	16.43
Fe					
Exchangeable	6.45	1.56	5.95	4.17	9.15
Carbonate	16.73	7.31	25.26	31.03	16.32
Mg Oxide	181.75	184.07	67.98	203.66	347.30
Fe Oxide	18369.05	17703.21	12225.23	13067.34	17456.65
Organic Matter	1314.02	25770.69	282.00	755.16	646.51
Sulfide/Residual	41483.69	47358.90	65382.71	40298.29	21329.87

Analyte	PK012	PK020	TF001	FNAS004	MS002
K					
Exchangeable	4697.83	3210.74	2047.92	2967.43	2846.96
Carbonate	-179.41	-240.93	-228.21	-133.48	-192.31
Mg Oxide	-401.91	-410.18	-396.54	-397.20	-403.54
Fe Oxide	493.52	431.11	52.48	596.15	632.75
Organic Matter	871.94	10283.70	768.15	810.56	977.59
Sulfide/Residual	6046.88	3466.02	2106.91	3616.29	3691.81
Li					
Exchangeable	3.73	4.83	3.16	9.05	3.24
Carbonate	-0.49	-0.26	-0.71	0.43	-0.60
Mg Oxide	0.04	-0.48	-0.23	0.26	-0.03
Fe Oxide	13.95	15.64	6.77	28.50	16.21
Organic Matter	5.17	41.57	4.45	5.39	5.01
Sulfide/Residual	27.94	17.83	11.85	25.99	22.07
Mg					
Exchangeable	3206.79	2653.23	651.49	5830.62	2678.08
Carbonate	1739.16	1518.52	1444.25	1764.27	1566.35
Mg Oxide	93.16	97.63	7.86	178.54	54.74
Fe Oxide	1749.01	1799.47	669.28	8095.99	2205.67
Organic Matter	149.75	3793.14	42.82	222.79	116.23
Sulfide/Residual	6819.47	4043.03	2478.52	8203.68	4814.16
Mn					
Exchangeable	288.49	63.43	202.68	14.19	3.98
Carbonate	289.40	164.51	49.00	107.19	91.51
Mg Oxide	1275.65	1292.30	37.90	691.16	1693.74
Fe Oxide	264.16	200.60	76.39	334.02	412.16
Organic Matter	9.44	66.68	2.09	6.46	6.06
Sulfide/Residual	360.70	326.86	318.74	390.16	215.93

Analyte	PK012	PK020	TF001	FNAS004	MS002
Mo					
Exchangeable	1.04	0.22	0.14	2.68	0.26
Carbonate	0.08	-0.02	-0.02	0.06	-0.06
Mg Oxide	-0.08	-0.02	0.04	0.14	0.02
Fe Oxide	-1.55	-1.76	-1.16	-0.69	-1.42
Organic Matter	0.23	-0.06	0.32	0.51	0.17
Sulfide/Residual	-2.16	-2.58	-3.32	-2.16	-1.00
Na					
Exchangeable	4179.39	-698.59	-867.86	7196.93	307.57
Carbonate	-2519.16	-2634.54	-2631.93	-2253.17	-2518.90
Mg Oxide	-2820.10	-2868.79	-2877.03	-2693.65	-2805.05
Fe Oxide	-2903.59	-3059.37	-3017.86	-2098.05	-2970.07
Organic Matter	354149.30	358728.83	362133.48	351046.09	346142.00
Sulfide/Residual	-120.10	-427.30	-800.09	4425.41	-524.84
Ni					
Exchangeable	2.11	0.78	2.66	0.74	0.49
Carbonate	3.66	2.09	0.45	1.38	1.14
Mg Oxide	8.87	8.85	0.07	4.10	5.00
Fe Oxide	11.23	10.53	4.82	16.02	11.30
Organic Matter	1.20	5.44	2.16	1.60	2.98
Sulfide/Residual	17.22	10.85	11.12	13.81	12.52
P					
Exchangeable	12.81	33.75	13.73	57.07	13.37
Carbonate	925.49	399.29	110.45	582.29	257.76
Mg Oxide	336.96	338.23	23.75	820.53	194.49
Fe Oxide	972.30	799.54	646.95	937.80	1123.28
Organic Matter	235.33	164.25	157.54	195.49	287.73
Sulfide/Residual	307.55	259.91	191.32	478.16	197.73

Analyte	PK012	PK020	TF001	FNAS004	MS002
Pb					
Exchangeable	-3.81	-3.39	17.05	-3.88	-2.15
Carbonate	7.76	3.51	10.99	1.74	2.53
Mg Oxide	11.66	11.83	3.99	1.55	4.08
Fe Oxide	44.84	36.94	24.07	12.29	39.36
Organic Matter	0.69	7.30	1.24	-0.29	7.89
Sulfide/Residual	12.37	12.79	12.19	7.83	9.15
S					
Exchangeable	754.35	244.62	229.11	883.78	318.55
Carbonate	-84.71	-107.40	-110.09	-71.11	-115.02
Mg Oxide	-9.66	-10.98	-14.49	-4.43	-9.25
Fe Oxide	-61.49	-140.43	-61.17	39.38	-101.45
Organic Matter	-17.29	-13.97	0.10	3.60	-30.51
Sulfide/Residual	134.81	166.35	156.13	326.39	94.69
Sb					
Exchangeable	0.90	0.55	1.41	1.33	1.01
Carbonate	-2.73	-2.13	-2.23	-1.96	-2.33
Mg Oxide	0.02	-0.05	-0.34	0.36	0.03
Fe Oxide	-13.75	-14.64	-12.40	-12.59	-14.63
Organic Matter	0.06	-0.03	-0.10	0.72	-0.78
Sulfide/Residual	-13.20	-15.09	-20.22	-13.41	-7.10
Se					
Exchangeable	10.41	11.35	0.70	12.39	4.60
Carbonate	52.77	49.77	47.40	50.49	50.66
Mg Oxide	2.60	3.31	0.45	3.05	3.48
Fe Oxide	143.64	154.33	145.64	142.63	158.12
Organic Matter	0.48	-0.79	-1.72	1.39	0.71
Sulfide/Residual	40.57	46.99	68.28	41.69	19.47

Analyte	PK012	PK020	TF001	FNAS004	MS002
Si					
Exchangeable	652.19	684.27	307.71	960.23	706.15
Carbonate	781.10	722.59	172.71	784.84	322.55
Mg Oxide	420.06	348.42	165.69	506.84	271.76
Fe Oxide	9700.63	10872.61	5720.44	17482.56	9634.33
Organic Matter	5012.54	8277.42	5402.07	12841.27	7200.37
Sulfide/Residual	2008.78	3042.16	2071.46	2267.60	1751.05
Sn					
Exchangeable	-0.62	-1.05	0.93	2.73	0.76
Carbonate	7.12	6.50	7.43	6.73	7.21
Mg Oxide	0.05	-0.10	0.08	-0.13	-0.13
Fe Oxide	27.03	30.08	27.11	35.60	31.26
Organic Matter	1.30	0.96	0.61	0.89	0.82
Sulfide/Residual	30.63	27.89	25.72	32.01	18.74
Sr					
Exchangeable	146.67	91.40	19.20	481.04	96.94
Carbonate	10.51	5.27	1.37	34.97	7.56
Mg Oxide	1.42	1.42	0.29	6.43	1.87
Fe Oxide	5.24	4.20	3.70	46.64	5.26
Organic Matter	0.65	6.19	0.48	2.03	1.01
Sulfide/Residual	13.52	13.33	11.03	109.78	8.81
Ti					
Exchangeable	-1.01	-0.84	-0.08	-1.06	-0.43
Carbonate	0.48	0.15	0.84	1.48	0.85
Mg Oxide	0.78	0.87	0.24	0.94	0.36
Fe Oxide	8.36	9.21	15.92	8.77	6.07
Organic Matter	87.71	225.45	72.74	113.63	113.87
Sulfide/Residual	1808.11	1752.49	1627.12	3011.50	1003.87

Analyte	PK012	PK020	TF001	FNAS004	MS002
Tl					
Exchangeable	0.98	0.78	-0.07	0.93	0.66
Carbonate	-2.75	-2.50	-2.13	-2.14	-2.66
Mg Oxide	-3.23	-3.21	-0.57	-1.88	-3.62
Fe Oxide	-5.84	-5.91	-5.18	-5.81	-7.00
Organic Matter	-0.41	-0.40	-0.26	-0.34	0.10
Sulfide/Residual	0.71	0.10	0.36	-1.60	0.63
V					
Exchangeable	0.30	0.30	0.15	1.56	0.21
Carbonate	0.57	0.38	0.32	1.04	0.31
Mg Oxide	5.04	5.02	0.60	6.22	2.35
Fe Oxide	41.60	37.62	25.29	37.52	26.79
Organic Matter	4.31	3.25	2.03	5.30	3.75
Sulfide/Residual	53.01	64.29	91.92	104.90	23.85
W					
Exchangeable	-1.62	-1.87	-0.80	0.58	-1.49
Carbonate	-10.02	-9.78	-9.33	-9.24	-8.87
Mg Oxide	-0.08	-0.19	-0.08	0.46	0.54
Fe Oxide	-19.05	-19.95	-19.92	-16.67	-12.36
Organic Matter	10.74	1.23	11.47	20.34	247.36
Sulfide/Residual	4.17	4.86	7.52	75.24	135.64
Zn					
Exchangeable	5.65	4.21	14.23	4.32	5.08
Carbonate	11.83	8.67	5.80	2.45	4.60
Mg Oxide	9.57	9.63	1.48	4.67	5.83
Fe Oxide	44.80	55.29	39.57	85.87	57.31
Organic Matter	2.65	7.51	2.29	5.23	3.33
Sulfide/Residual	95.13	63.79	62.22	93.89	63.74

ICP-MS

Data from the ICP-MS analysis of the sequential extractions performed at KSU with concentration in mg/kg and percent of total.

Table A.5 Data for W concentration in mg/kg for every phase of sequential extraction (Phase 1-6), analyzed by ICP-MS. With each phases percent contribution to the total W from each sample.

Sample	Phase 1	%	Phase 2	%	Phase 3	%	Phase 4	%	Phase 5	%	Phase 6	%
Fallon 1	367404.55	4.19	38021.72	0.43	7367.04	0.08	207058.63	2.36	4791174.91	54.59	3365424.29	38.35
Fallon 2	4200.57	4.41	426.72	0.45	366.14	0.38	2214.88	2.33	48901.39	51.40	39033.90	41.03
Fallon 3	909103.47	13.77	90225.05	1.37	15455.99	0.23	238118.41	3.61	2014707.87	30.52	3332619.53	50.49
FNSG001	2311.82	4.06	680.53	1.19	113.13	0.20	1689.11	2.96	20508.50	35.98	31691.13	55.60
FNSG002	21515.55	6.21	1734.49	0.50	498.17	0.14	4963.43	1.43	24665.65	7.12	292897.16	84.59
FNSG003	4164.53	3.42	551.54	0.45	308.08	0.25	2495.71	2.05	83966.07	69.05	30117.64	24.77
FNAS002	1710.21	5.79	222.72	0.75	140.66	0.48	1170.05	3.96	7802.89	26.43	18476.51	62.58
FNAS004	2739.33	2.75	262.73	0.26	327.59	0.33	3079.65	3.09	23626.60	23.69	69680.35	69.88
FNPS003	553.92	0.48	198.63	0.17	178.06	0.16	2323.42	2.02	80387.92	70.01	31181.41	27.16
CBR1_1a	596.24	1.75	190.11	0.56	37.55	0.11	142.36	0.42	25271.36	74.35	7753.28	22.81
CBR4_3a	954.28	1.13	156.54	0.18	72.31	0.09	636.55	0.75	47741.01	56.40	35092.39	41.45
CBR2_3a	211.05	6.06	77.96	2.24	15.77	0.45	66.77	1.92	958.33	27.52	2152.92	61.82
La001	103.89	0.66	87.45	0.56	20.81	0.13	399.90	2.54	11385.29	72.30	3749.54	23.81
La010	116.32	0.41	104.76	0.37	13.97	0.05	262.39	0.92	24661.00	86.40	3384.91	11.86
LA011	123.04	2.79	73.05	1.65	12.40	0.28	100.15	2.27	1574.92	35.67	2532.30	57.35
MS001	106.02	0.31	121.58	0.36	74.16	0.22	820.16	2.42	27923.43	82.48	4810.75	14.21
MS002	180.55	0.03	458.16	0.08	484.56	0.09	6504.17	1.19	423228.90	77.33	116432.45	21.27
PK012	437.59	3.69	97.99	0.83	26.68	0.23	277.90	2.34	7958.60	67.13	3056.91	25.78
PK020	262.57	1.47	65.42	0.37	15.33	0.09	318.76	1.79	13361.12	75.01	3789.60	21.27
TF001	81.90	0.39	120.96	0.58	16.29	0.08	479.84	2.28	15302.61	72.86	5000.04	23.81

Appendix B - Water Chemistry

The only water samples that were able to be collected were surface water samples collected at Cheyenne Bottoms refuge.

B.1 Sample list

The samples with chemical parameters (recorded with Hach® Hydrolab).

Table B.1 Sample list of water collected at Cheyenne Bottoms Refuge, with coordinates in UTM, with water quality parameters.

3/9/2012										
Sample	**X (UTM)**	**Y (UTM)**	**pH**	**T**	**ORP**	**Sp. Con.**	**LDO**	**TDS**	**Res.**	**Salinity**
W1	531639	4258991	7.09	53.3	426	195119.8	18.5	12.49	0.051	11.58
W2	531649	4259583	7.22	57.5	436	5310.7	15.13	3.3996	0.188	2.92
W3	531651	4258991	7.39	56	428	5341.2	14.63	3.4205	0.187	2.94
W4	528299	4257492	7.18	56.1	466	3495	11.2	2.23	0.286	1.9
5/31/2012										
Sample	**X**	**Y**	**pH**	**T**	**ORP**	**Sp. Con.**	**LDO**	**TDS**	**Res.**	**Salinity**
WS1	531642	4258975	7.06	67	506	30856	9.34	19.697	0.031	19
WS2	531669	4258954	6.98	70	470	18594	1.7	11.92	0.05	11
WS3	532512	4257322	6.8	71	489	3370	9.03	2.15	0.29	
WS4	530051	4259793	7.39	74.4	474	4379.6	9.61	2.8	0.228	0.39

B.2 Chemistry

Water samples were (Act Labs Canada) analyzed for anions and multi-element concentrations.

Table B.2 Anion data for collected Cheyenne Bottoms water samples analyzed by Ion Chromatograph at ACTlabs in Canada.

Sample	Cl (mg/L)	NO_2 (mg/L)	Br (mg/L)	NO_3 (mg/L)	PO_4 (mg/L)	SO_4 (mg/L)
WS	9530	< 1	13.5	< 1	2.23	4710
WS2	5100	< 0.5	12.1	< 0.5	< 1	2960
WS3	588	< 0.1	1.01	0.44	0.39	684
WS4	866	< 0.3	< 0.7	0.64	< 0.5	895

Table B.3 ICP analysis of water samples from Cheyenne Bottoms, showing elements of interest in µg/L.

Sample	As (µg/L)	Ca (µg/L)	Co (µg/L)	Cu (µg/L)	Fe (µg/L)	Mg (µg/L)	Mn (µg/L)	Mo (µg/L)	W (µg/L)
WS1	30.91	1814315	1.223	1.16	234	533138.1	2109.04	8.920	0.376
WS2	37.83	858955	1.458	<0.05	30	382320.8	2224.40	18.059	0.261
WS3	28.47	150839	0.659	10.52	67	45499.0	53.74	7.617	0.513
WS4	14.28	279773	0.548	3.75	<1	67473.9	157.87	17.294	0.272

Appendix C - Spectroscopic Data

Various forms of spectroscopic analyses conducted during this work including, µXRF and µXANES from National Synchrotron Light Source, Brookhaven National Lab, and SEM/EDX from Kansas State University.

C.1 µXRF

This is the collection of all µXRF image maps for Fallon, Cheyenne Bottoms, and Sierra Vista. These images depict W intensity across an area of 1 x 1mm (unless otherwise specified) and numbered "hotspots" represent areas where a µXANES spectra was collected. The corresponding spectra is labeled the same as the map with the letter s (spot) and a number corresponding with the labeled point. Areas without spots, or maps without spots are because spectra were not collected there due to low concentrations.

Fallon

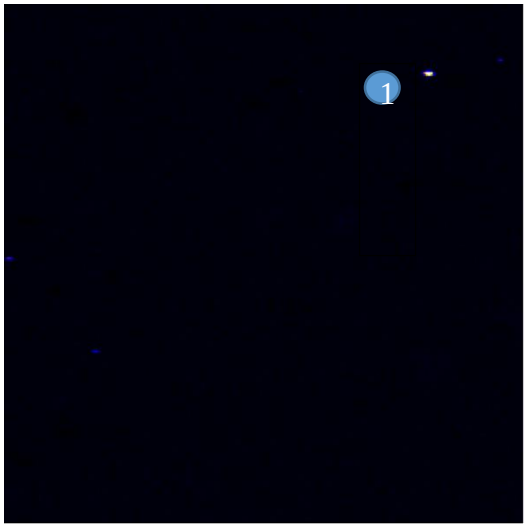

FNAS001 M4

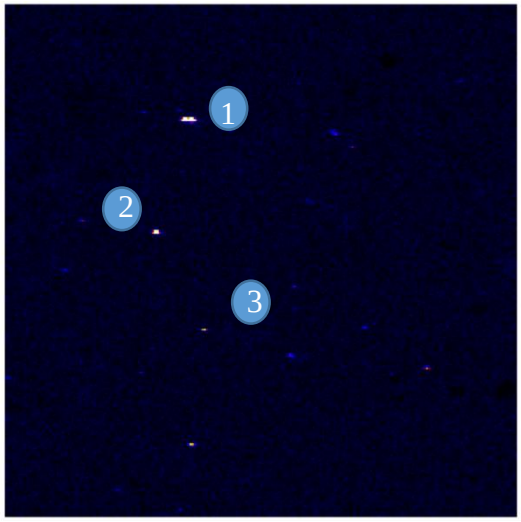

FNSG001 M1

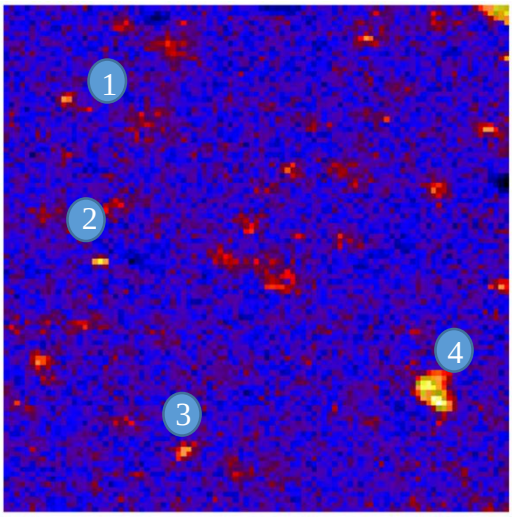

FNAS002 M2

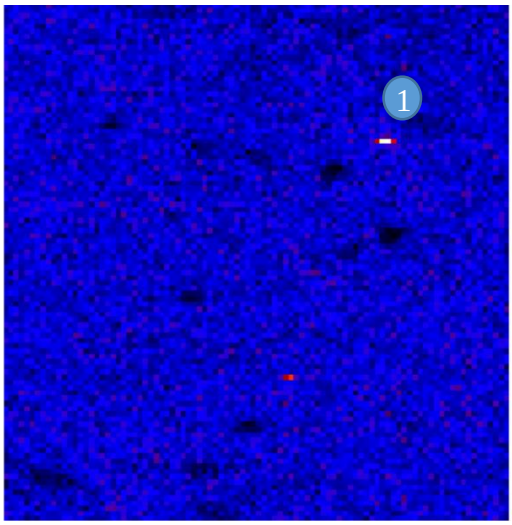

FNAS001 M3

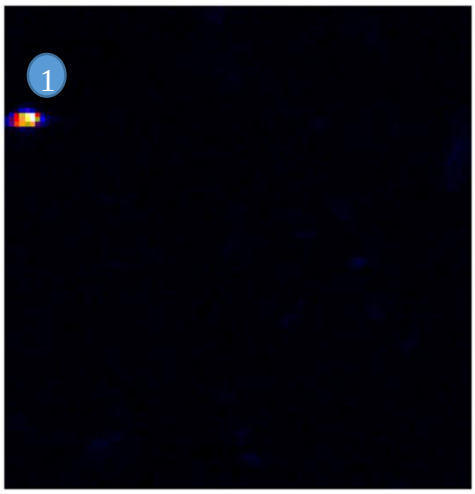

FNSG001 M2

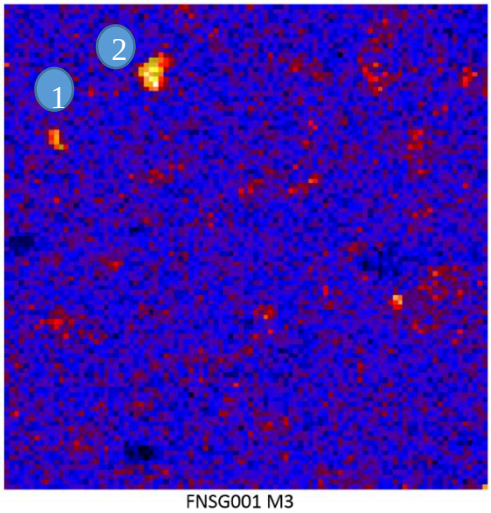

FNSG001 M3

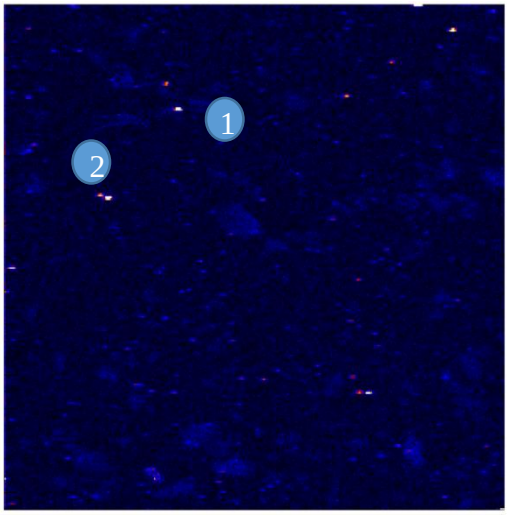

W Fallon1 m1 3x3

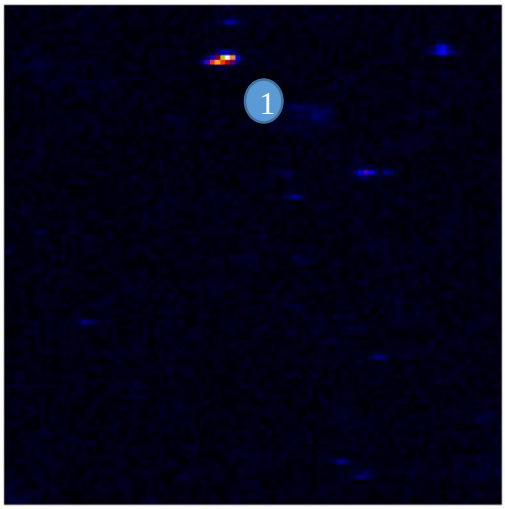

W Fallon1 m2

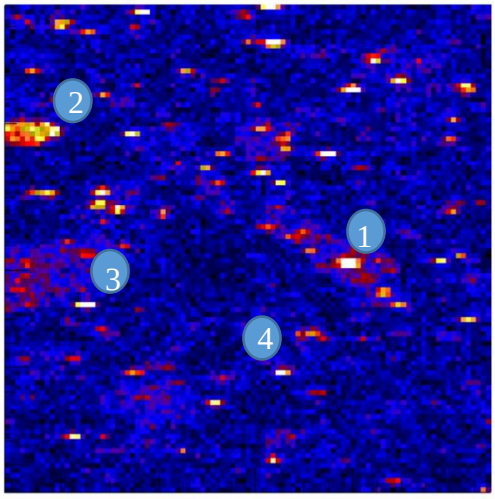

W_fallon3_m4_fly

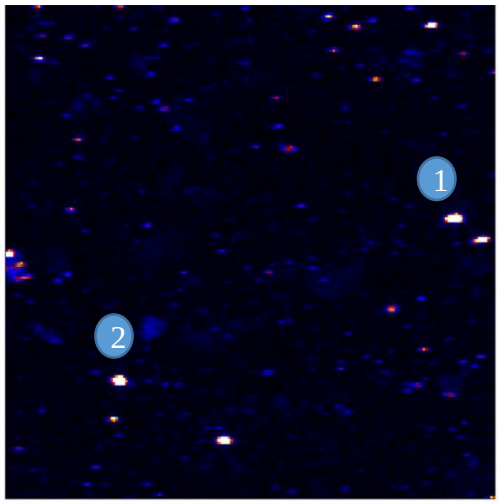

W_fallon3_m5_fly
2x2mm

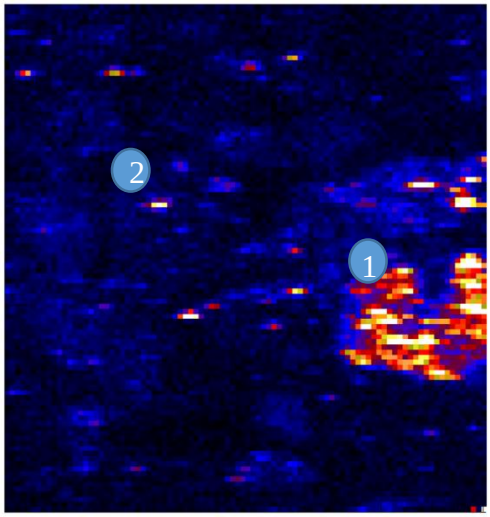

W Fallon 3 m2

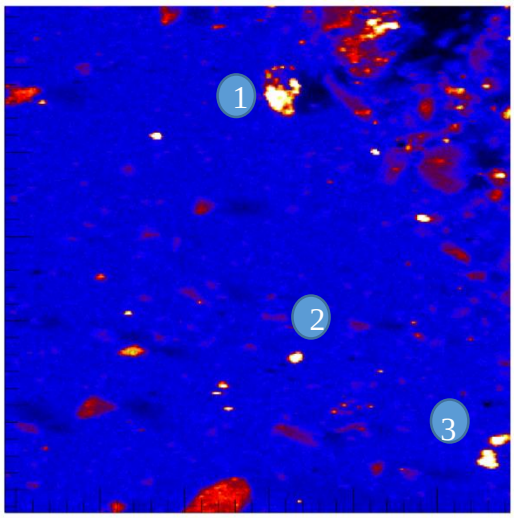

W Fallon 3 m3-3x3mm

Cheyenne Bottoms

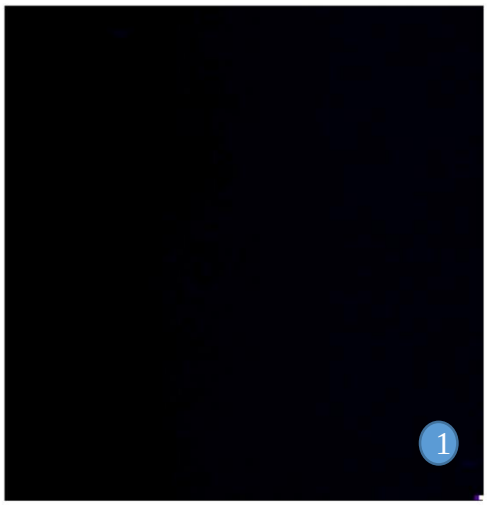

CB4_3a_m1

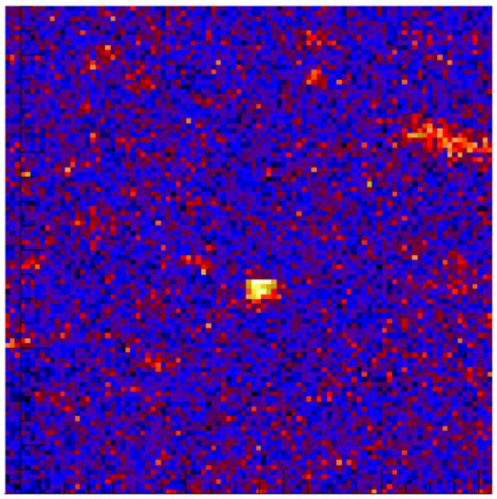

CB4_3a_m4

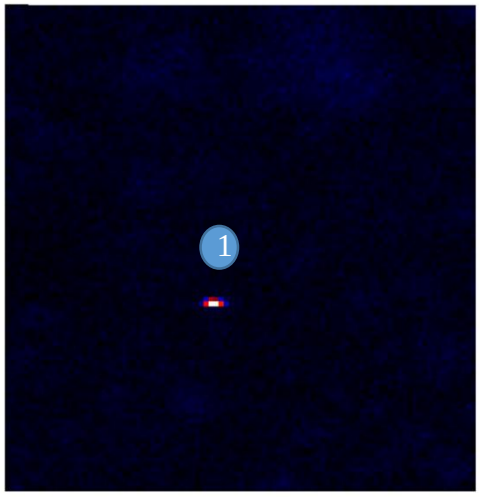

CB2_3a_m1

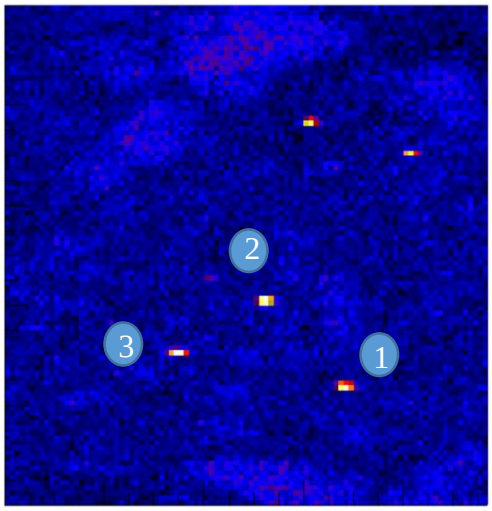

CB2_3a_m2

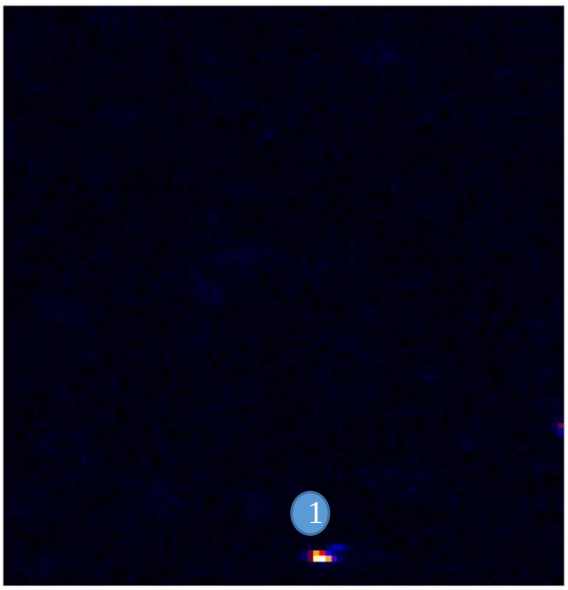

CB5_3a_m1

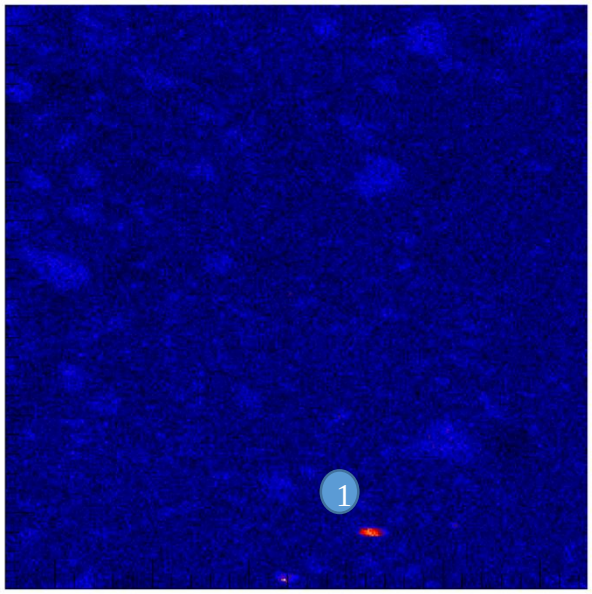

CB5_3a_m2 3x3

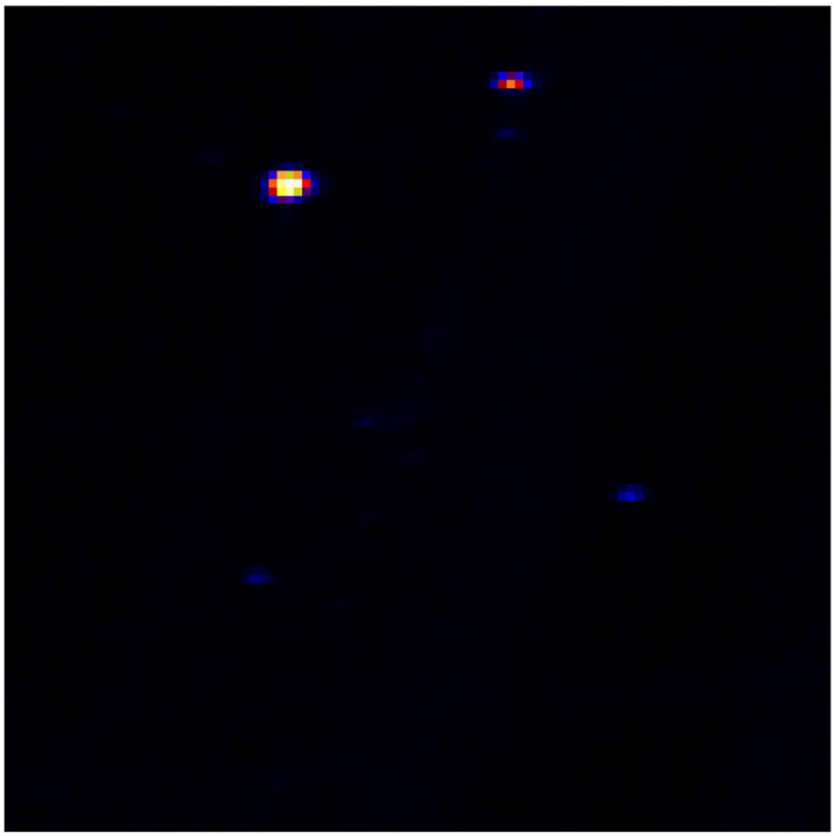

CBcat_m1

Sierra Vista

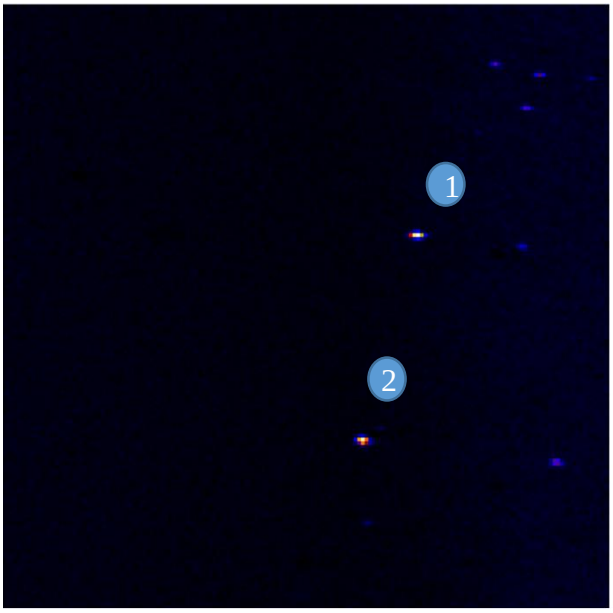

LA001 M1

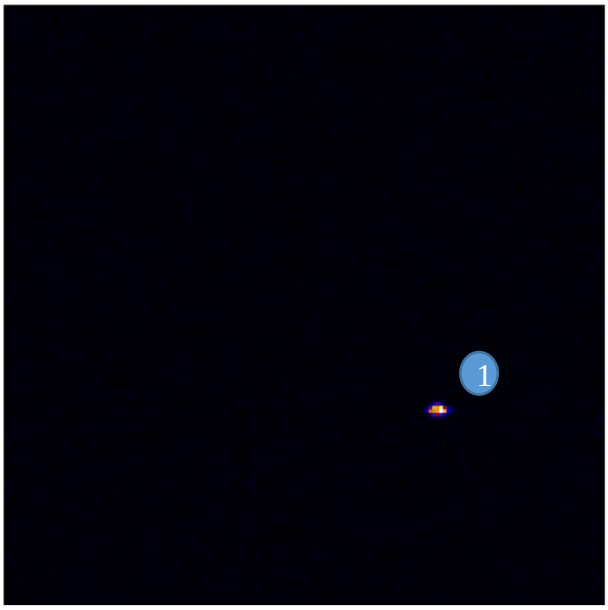

LA010 M1

C.2 μXANES

This section contains all of the W spectra collected for the scans run at National Synchrotron Light Source Brookhaven National Lab, organized by sampling site. The y-axis represents intensity while the x-axis represents the energy in electron volts (eV). The μXANES method scans across an energy range to identify an unknown, by established a “white line” or peak that identifies an element, when compared with known standard spectra.

Standards

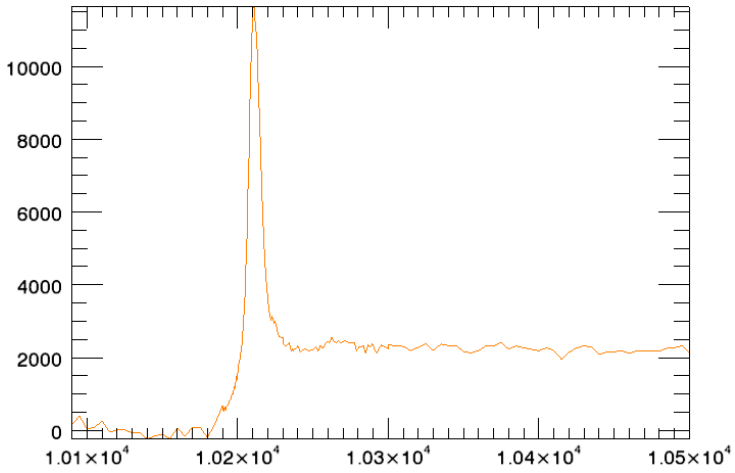

WCl

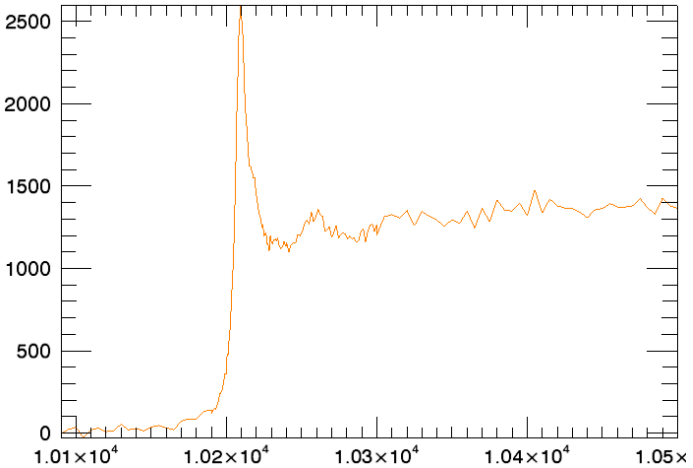

WS2

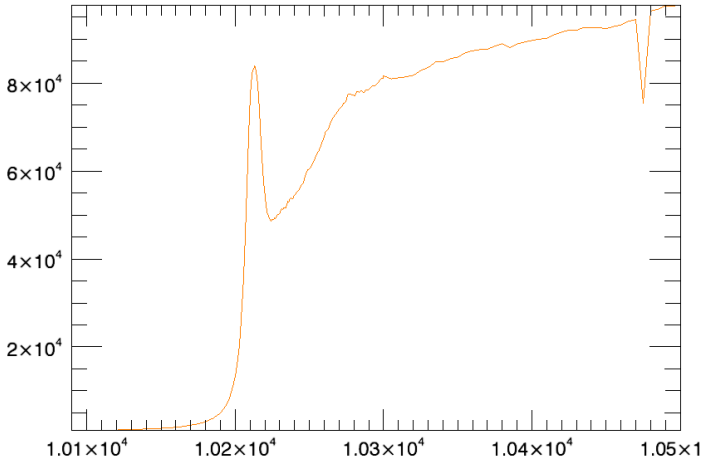

WO3

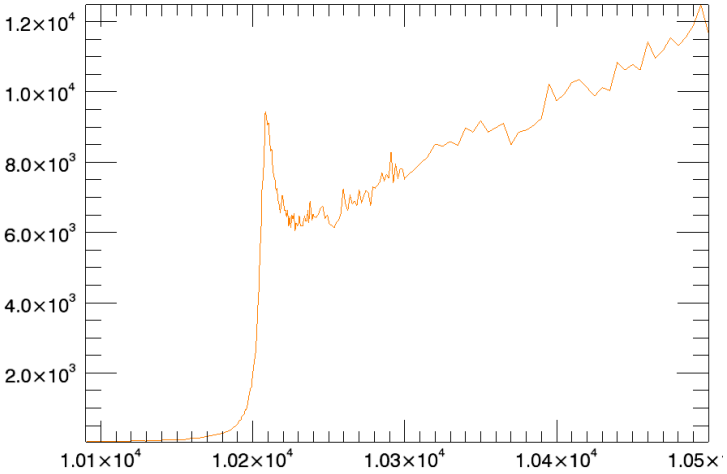

W metal powder

Fallon

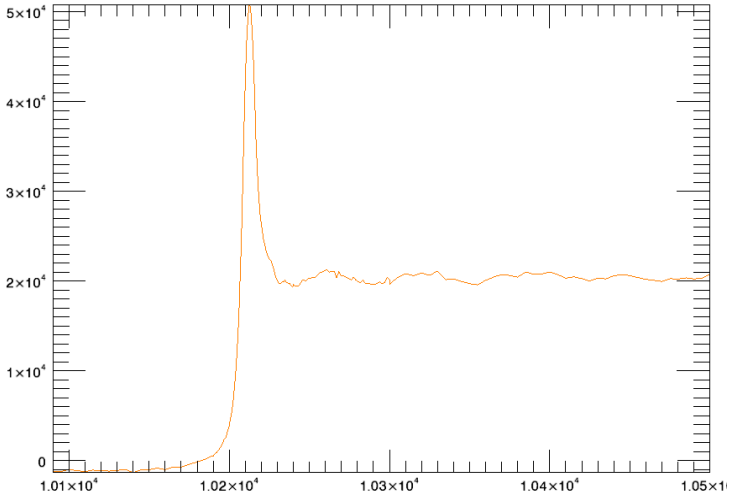

W Fallom3 m2s1

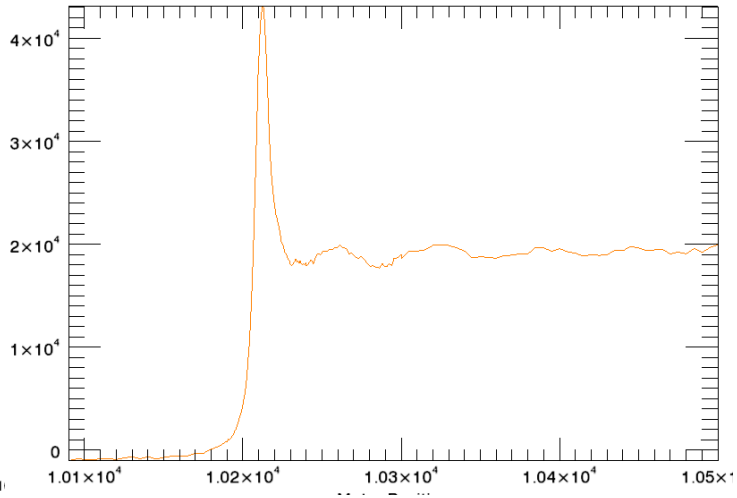

W Fallon3 m2s2

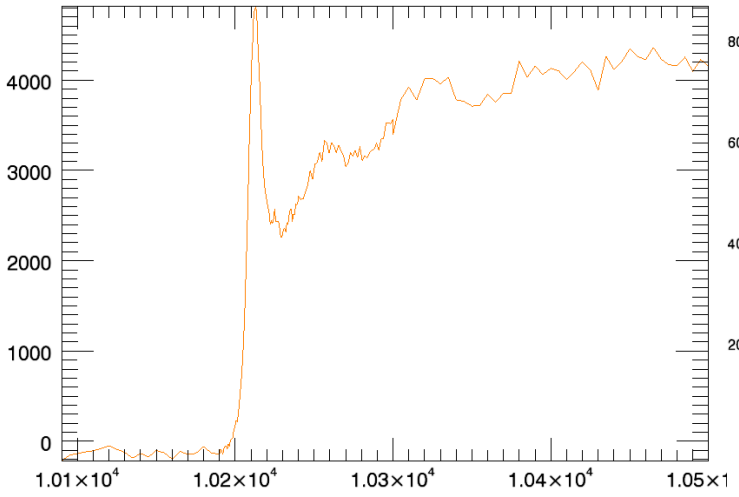

W Fallon3 m4s1

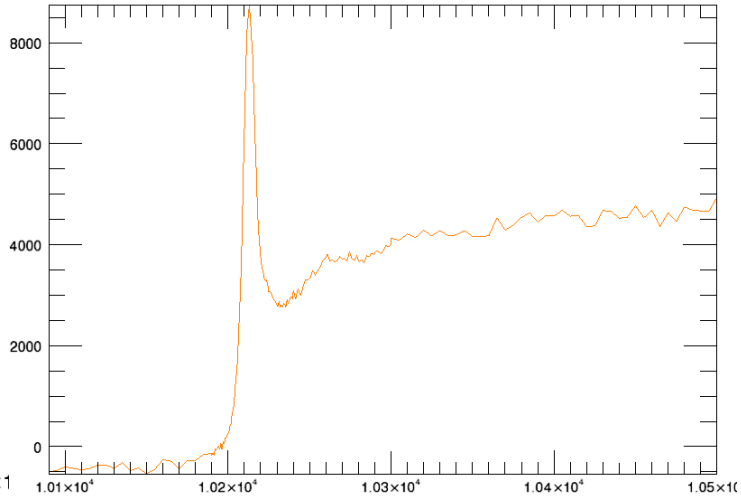

W fallon3 m4s2

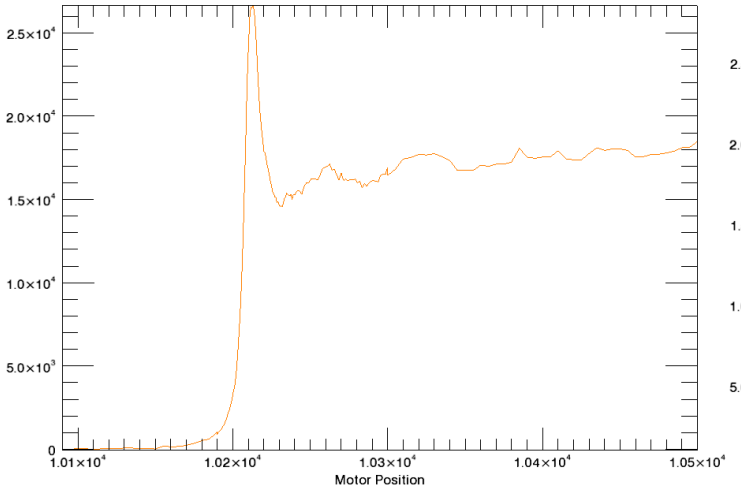

W Fallon3 m4s3

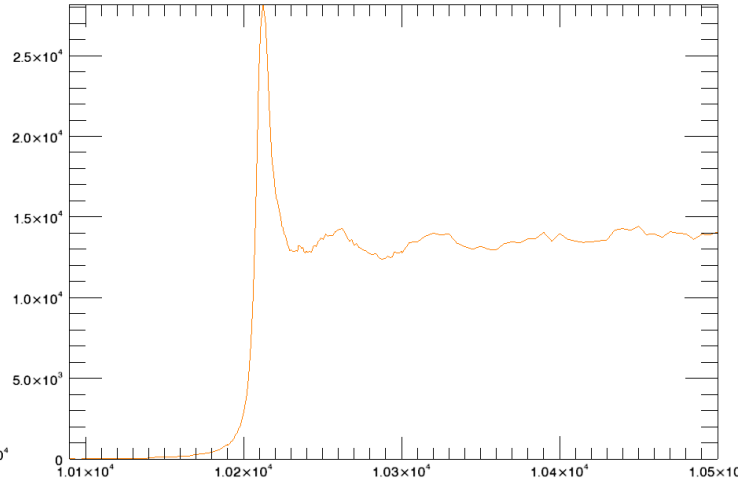

W Fallon3 m4s4

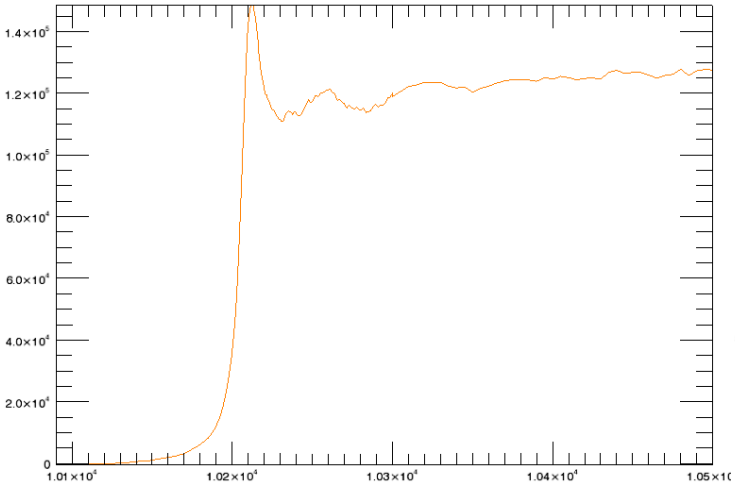

W Fallon3 m5s1

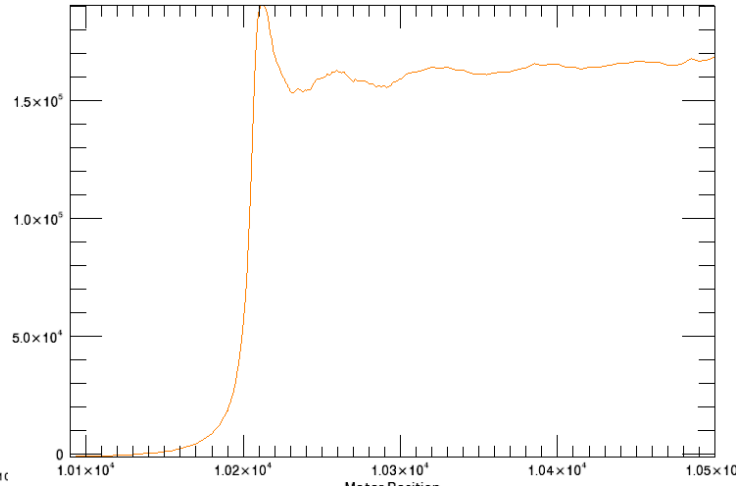

W Fallon3 m5s2

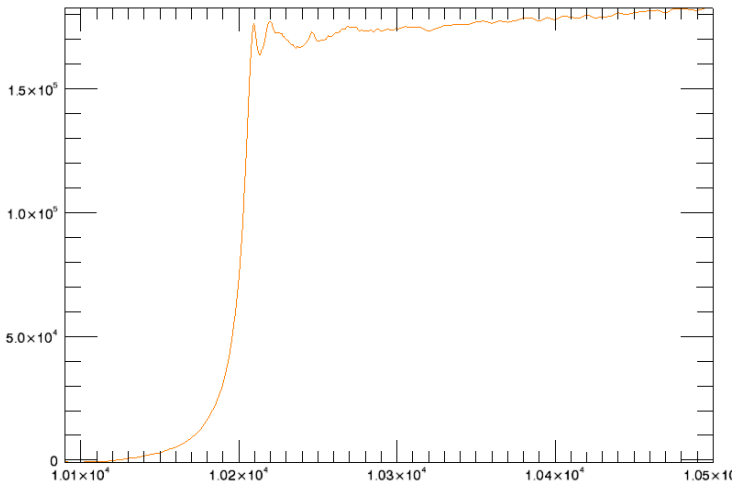

W Fallon3 m5s3

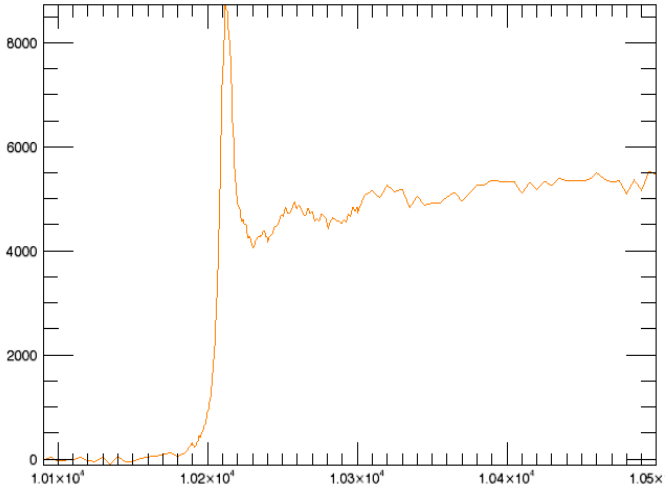

W Fallon1 m1s1

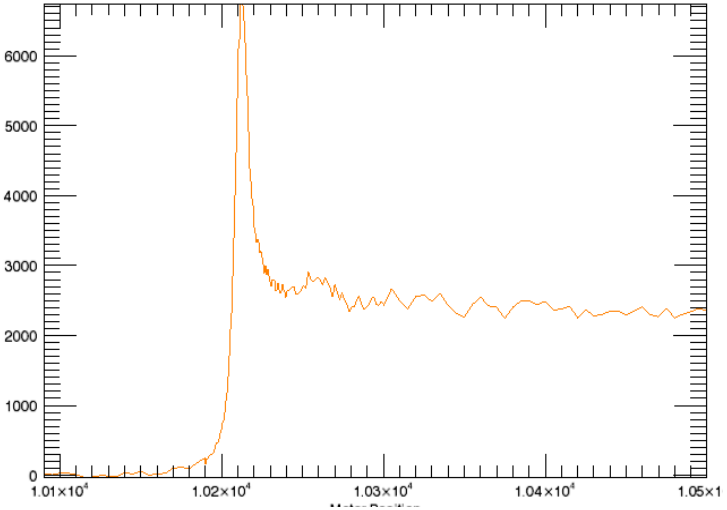

W Fallon1 m1s2

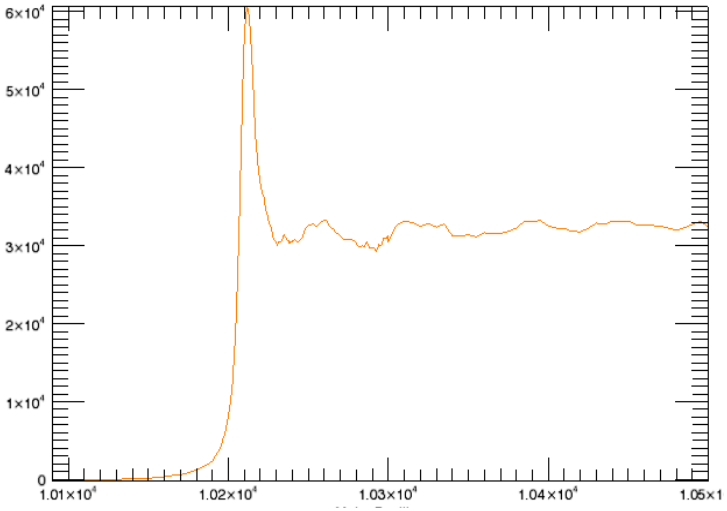

Fallon1 m1s3

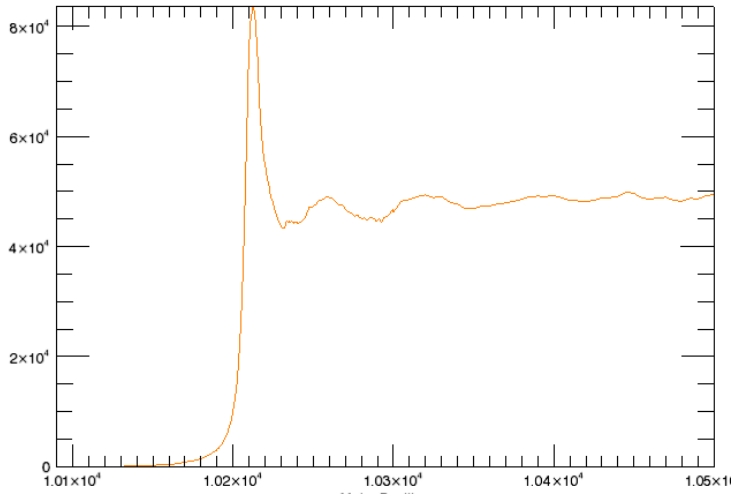

Fallon1 m2s1

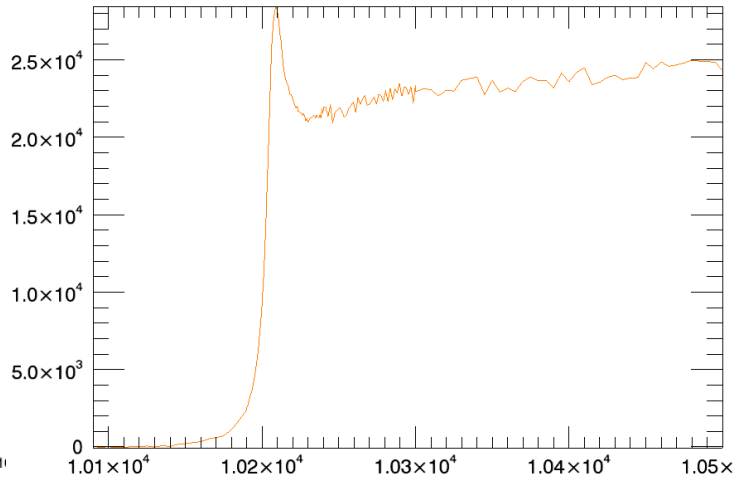

FNSG001 m2s1

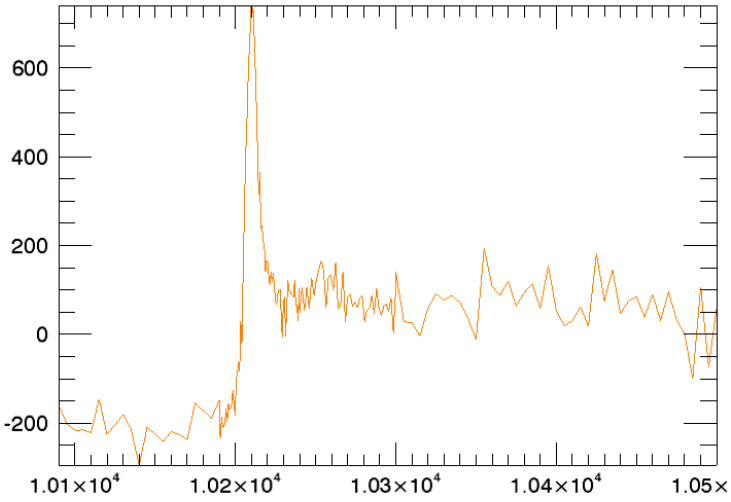

FNAS002 m2s2

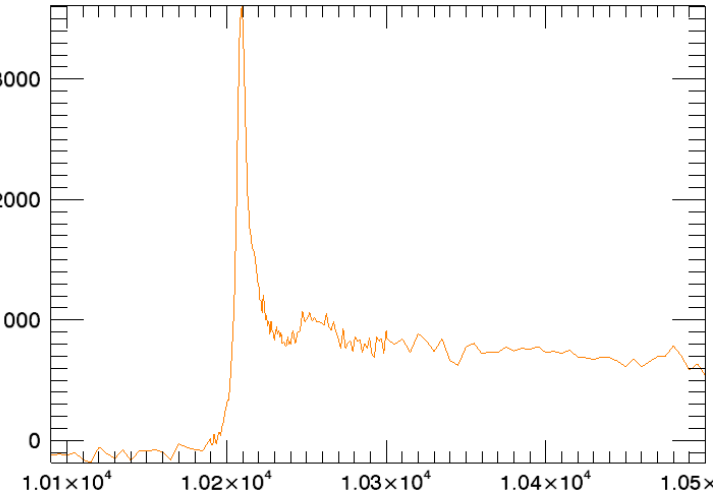

FNSG001 m3s1

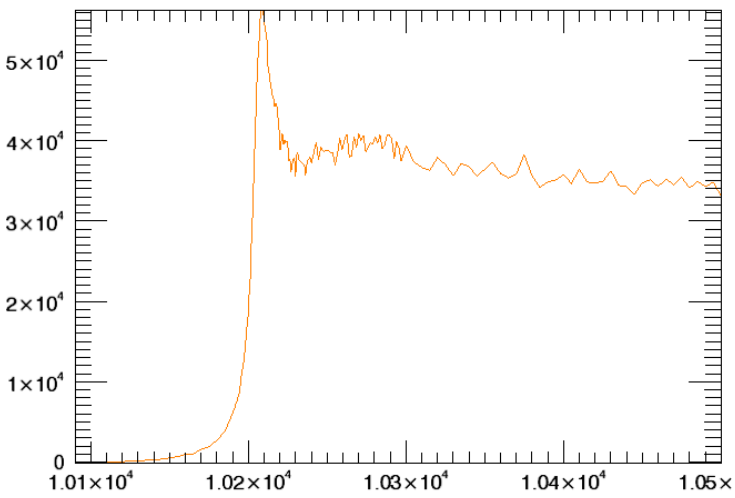

FNAS001 m4s1

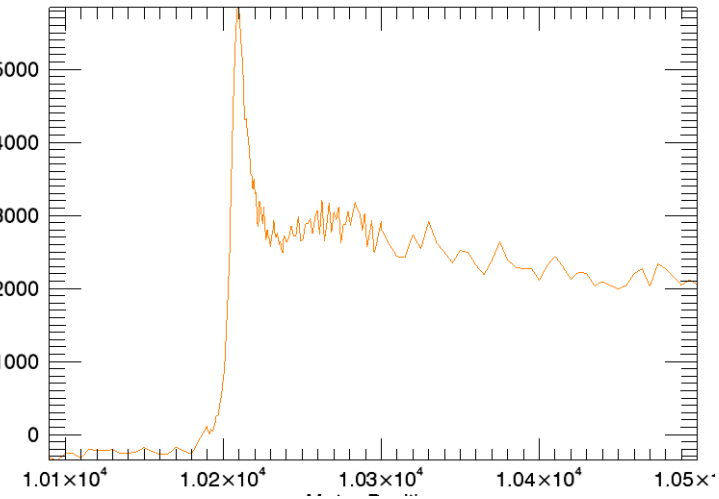

FNAS001 m4s2

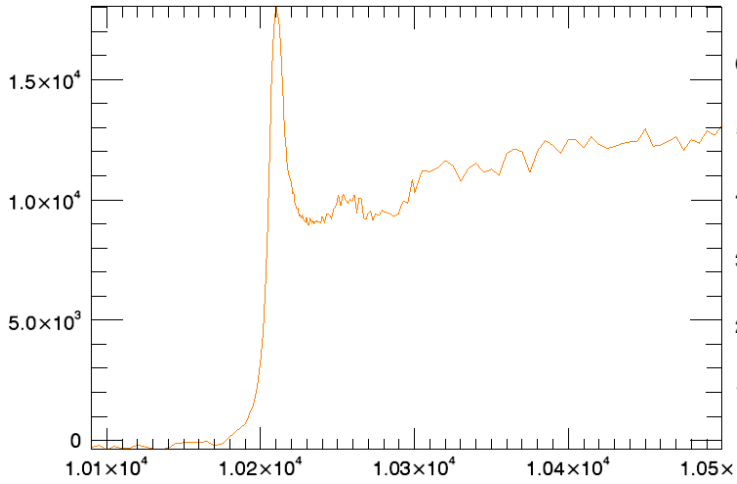

FNAS001 m4s3

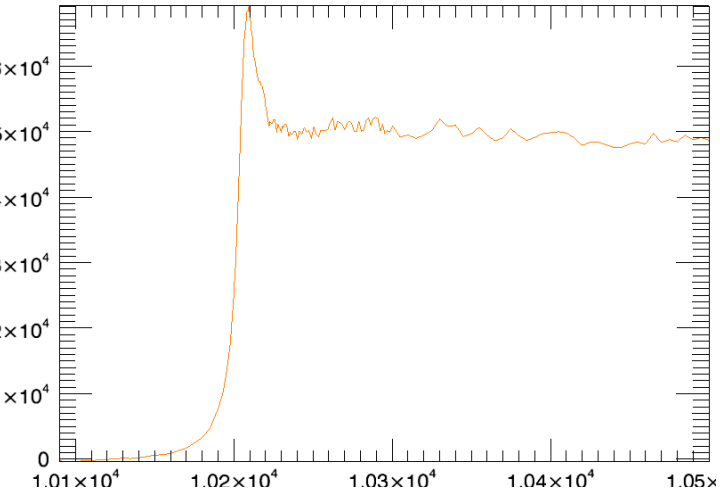

FNSG001 m1s1

Cheyenne Bottoms

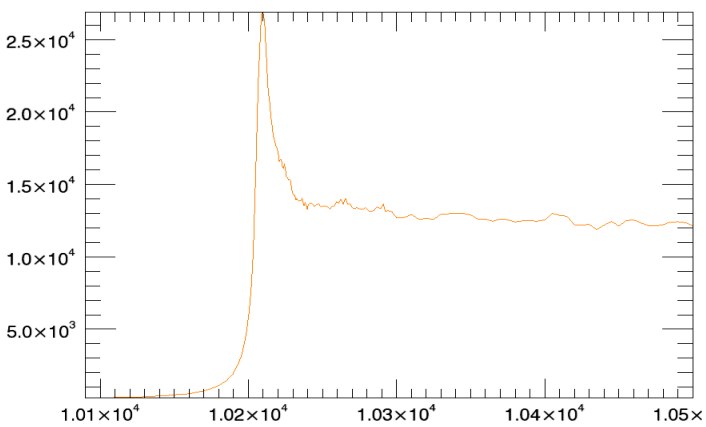

CB2_3a m1s1

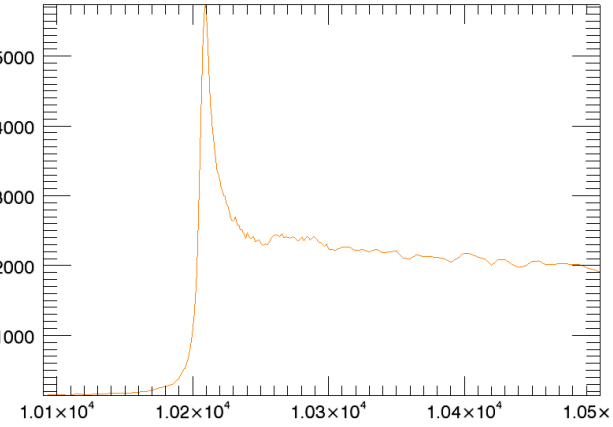

CB2_3a m2s1

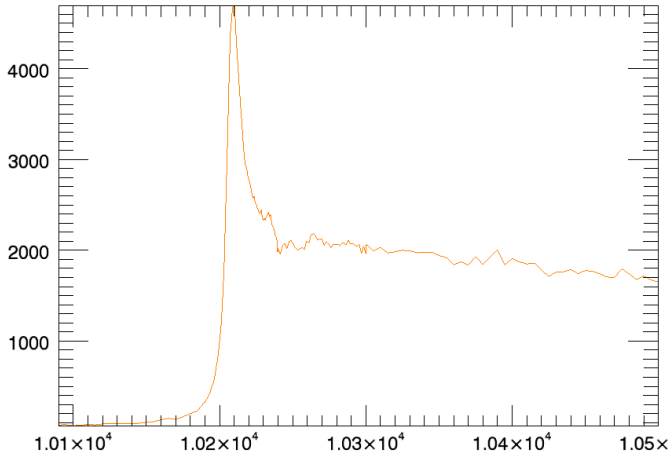

CB2_3a m2s3

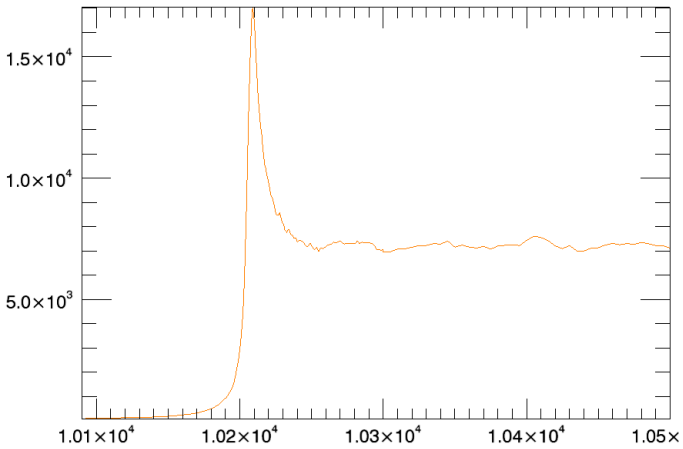

CB2_3a m2s4

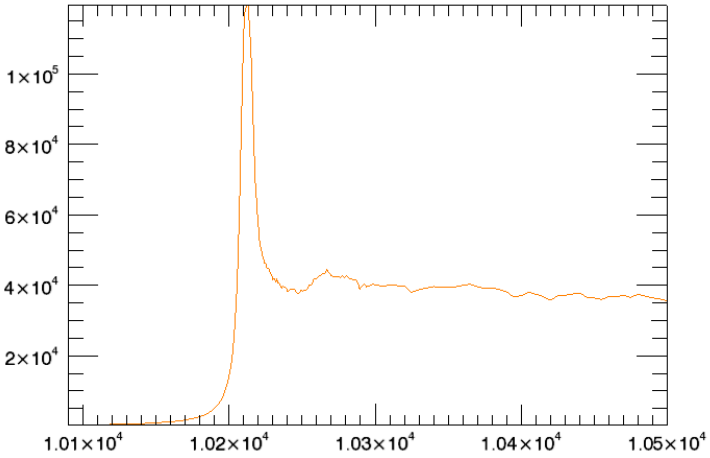

CB5_3a m1s1

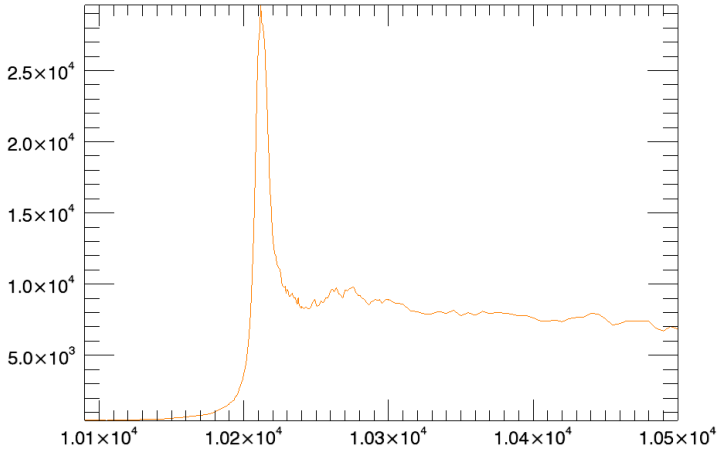

CB5_3a m1s2

Sierra Vista

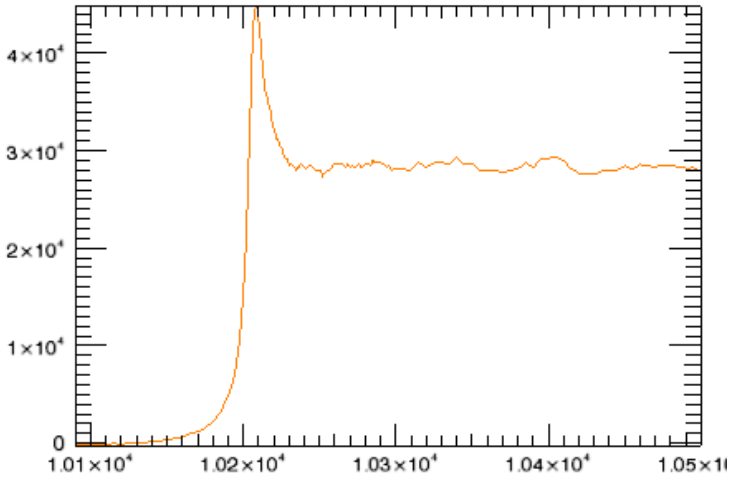

LA001 m1s1

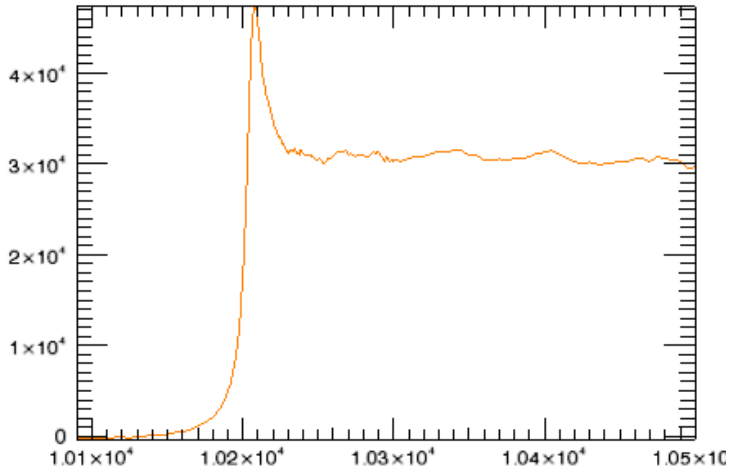

LA001 m1s2

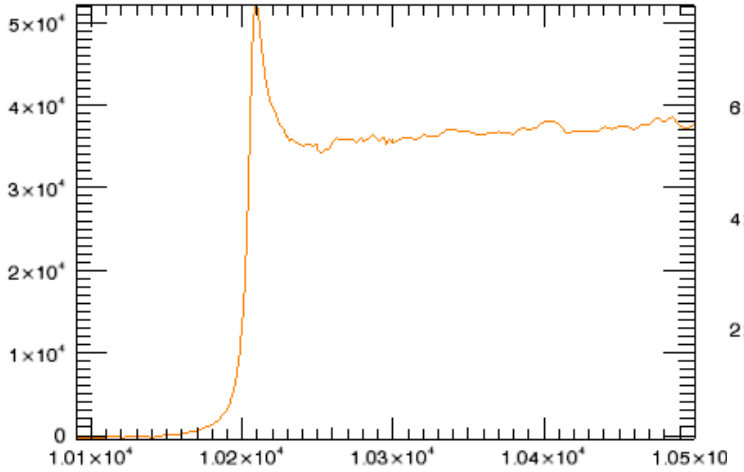

LA001 m1s3

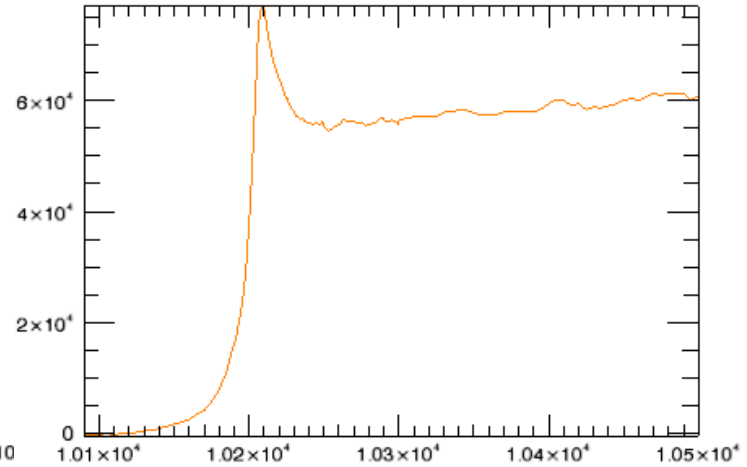

LA010 m1s1

C.3 SEM-EDX

Fallon 3

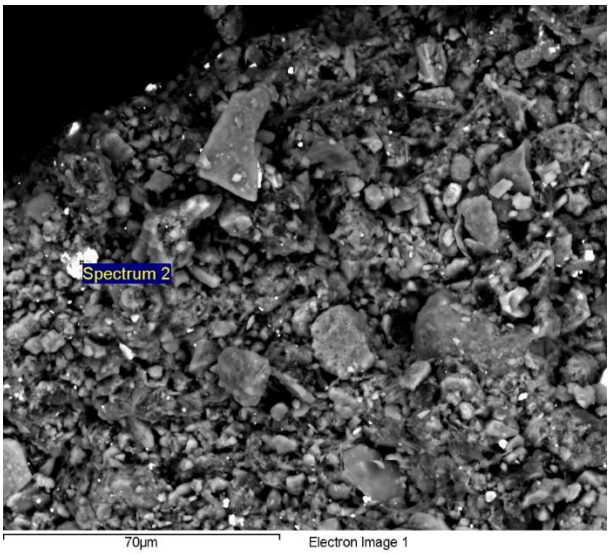

Element	Weight%	Atomic%
C K	-4.41	-9.78
O K	45.38	75.55
Na K	0.62	0.72
Mg K	1.15	1.26
Al K	3.54	3.50
Si K	11.61	11.01
S K	0.23	0.19
K K	1.69	1.15
Ca K	2.92	1.94
Ti K	17.21	9.57
Fe K	5.97	2.85
W M	14.09	2.04
Totals	100.00	

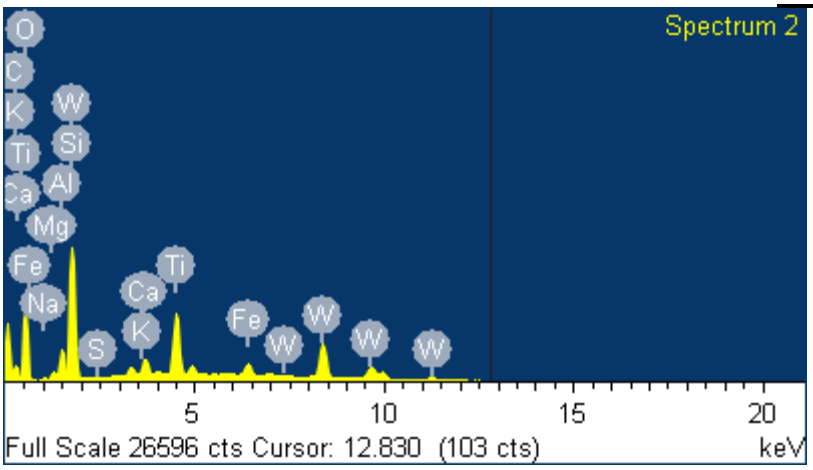


Electron Image 1
C Ka1_2
O Ka1
Na Ka1_2
Mg Ka1_2


Al Ka1
Si Ka1
S Ka1
K Ka1
Ca Ka1

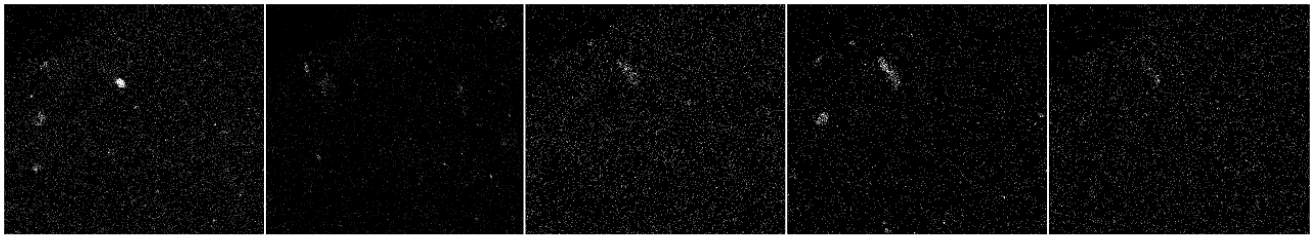
Ti Ka1
Fe Ka1
Co Ka1
W La1
Mn Ka1


Cu Ka1
Zn Ka1
P Ka1
As Ka1
Mo La1

Fallon 3

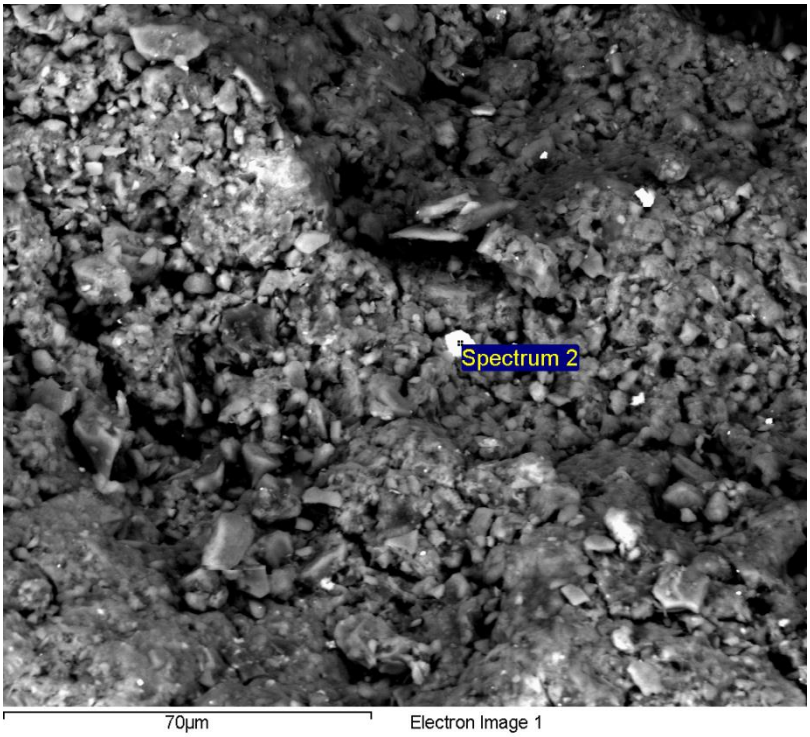

Element	Weight%	Atomic%
O K	27.17	75.88
Na K	0.28	0.54
Al K	1.97	3.26
K K	0.76	0.86
Ca K	1.38	1.54
Mn K	0.95	0.77
Fe K	1.27	1.02
Ta M	9.31	2.30
W M	56.91	13.83
Totals	100.00	

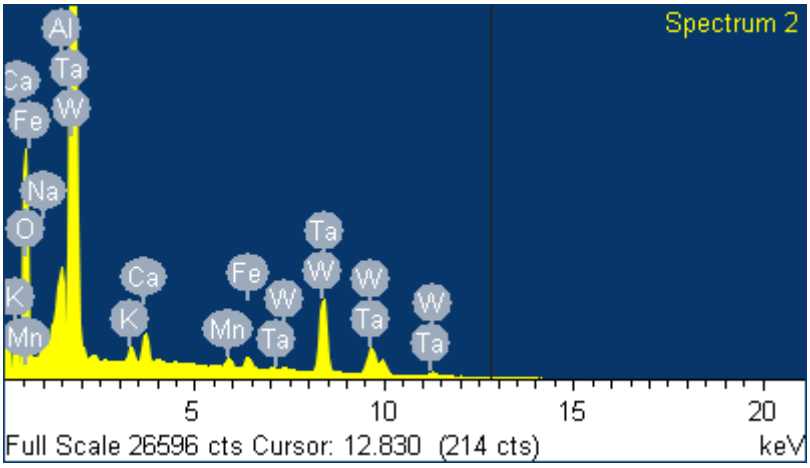

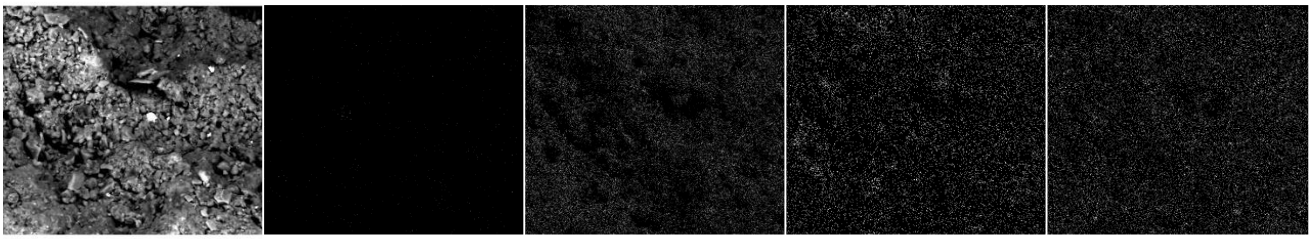
Electron Image 1
C Ka1_2
O Ka1
Na Ka1_2
Mg Ka1_2


Al Ka1
Si Ka1
S Ka1
Cl Ka1
K Ka1

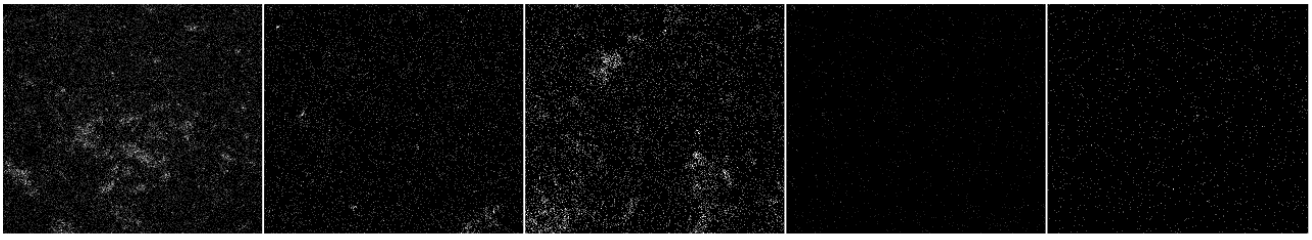
Ca Ka1
Ti Ka1
Mn Ka1
Fe Ka1
Zn Ka1

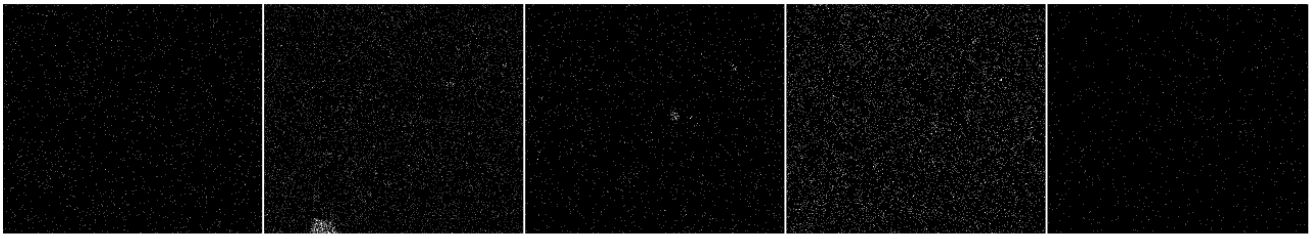
Cu Ka1
Mo La1
W La1
P Ka1
As Ka1

CBR 4_3a

Element	Weight%	Atomic%
C K	-33.20	-78.04
O K	73.05	128.90
Na K	0.89	1.09
Mg K	1.54	1.79
Al K	9.51	9.95
Si K	26.22	26.36
S K	2.55	2.24
K K	3.27	2.36
Ca K	0.83	0.58
Fe K	5.36	2.71
Ba L	10.00	2.06
Totals	100.00	

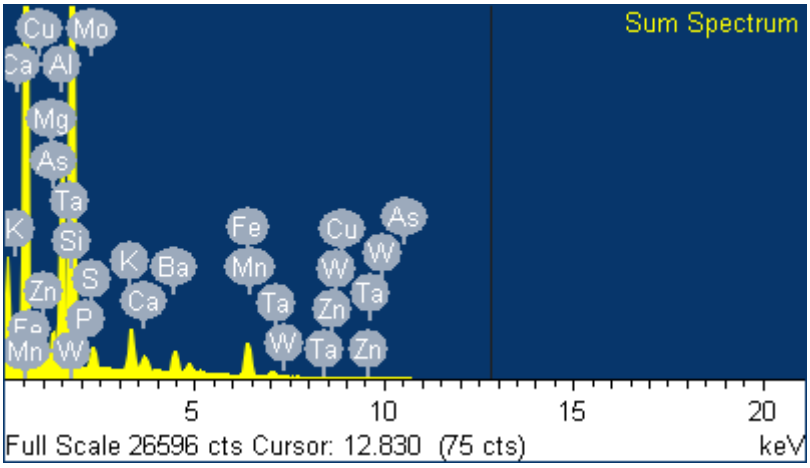

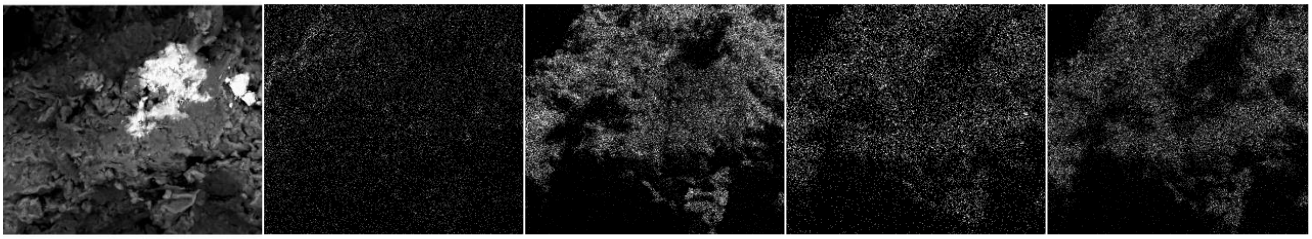
Electron Image 1
C Ka1_2
O Ka1
Mg Ka1_2
Al Ka1

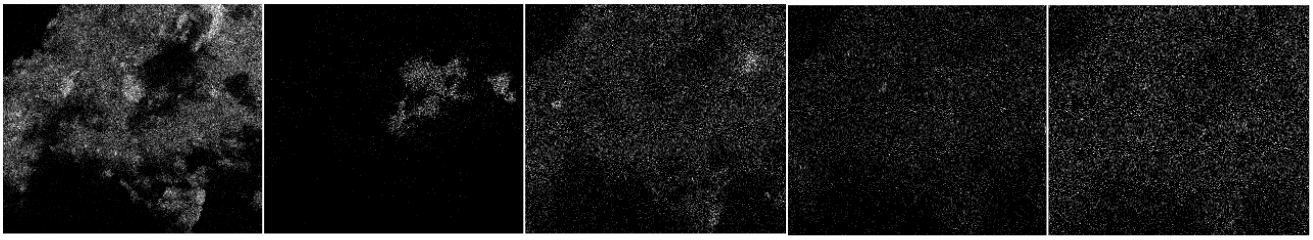
Si Ka1
S Ka1
K Ka1
Ca Ka1
Fe Ka1

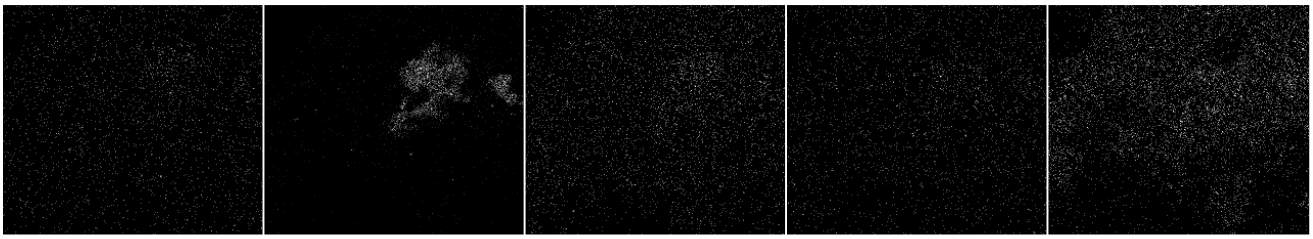
Zn Ka1
Ba La1
Mn Ka1
Cu Ka1
P Ka1

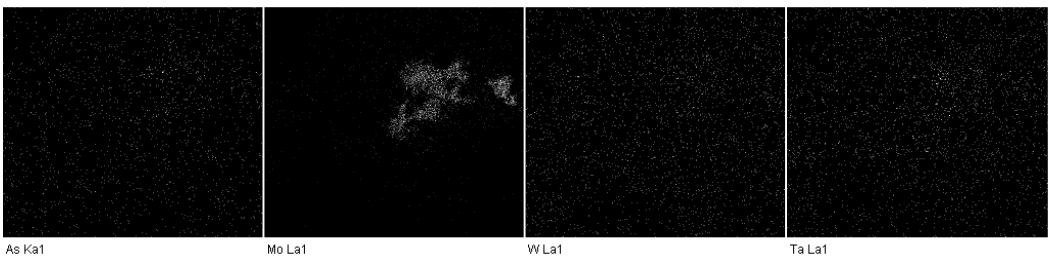
As Ka1
Mo La1
W La1
Ta La1

CBR 4_3a

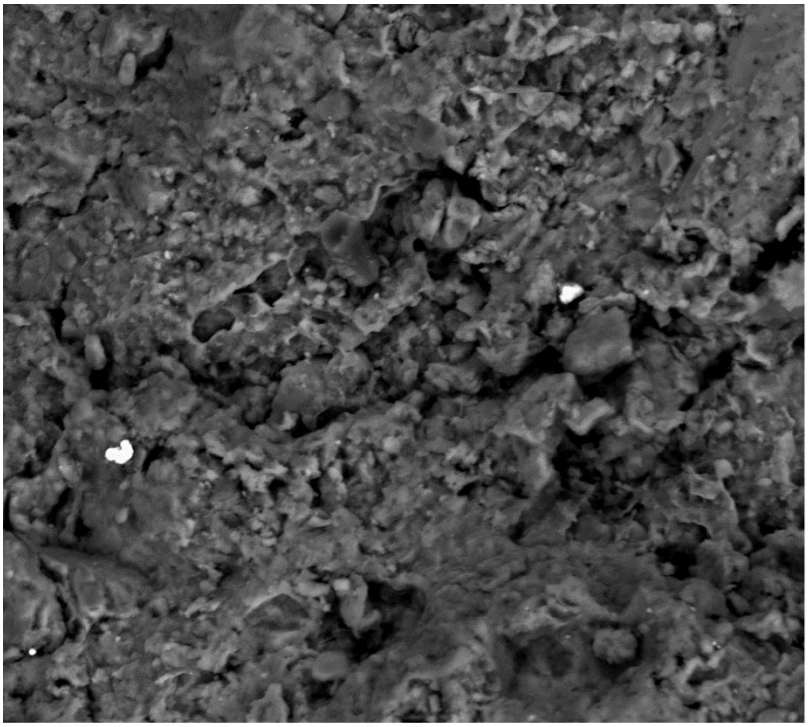

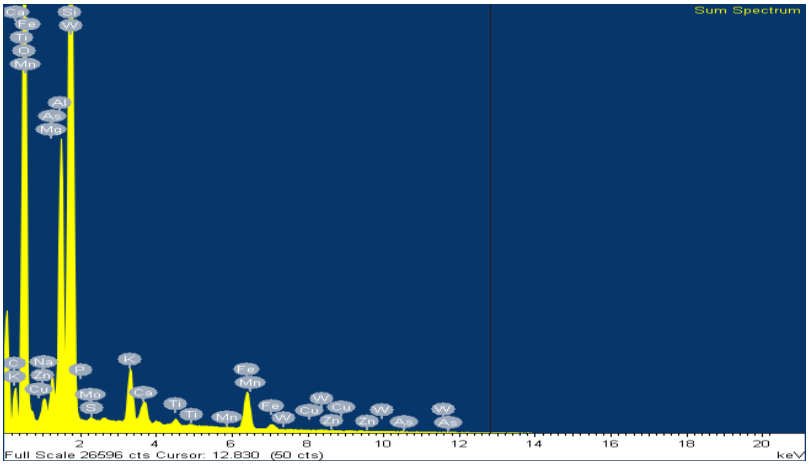

Element	Weight%	Atomic%
O K	38.61	60.92
Mg K	1.22	1.27
Al K	13.41	12.55
Si K	16.52	14.85
S K	5.00	3.94
K K	1.35	0.87
Ca K	0.96	0.60
Fe K	2.82	1.27
Zn K	0.15	0.06
Ba L	19.97	3.67
Totals	100.00	

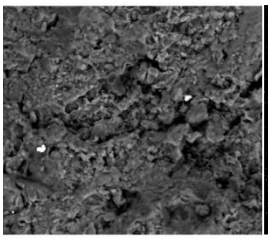
Electron Image 1

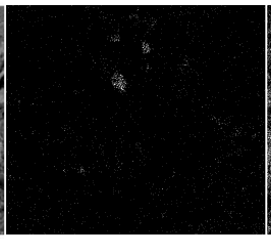
C Ka1_2


O Ka1

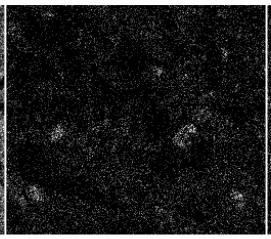
Na Ka1_2

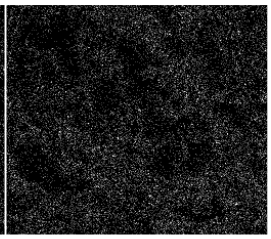
Mg Ka1_2

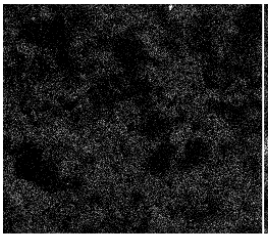
Al Ka1

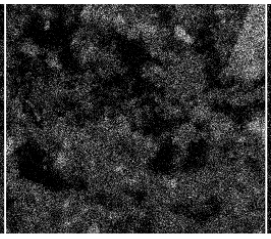
Si Ka1

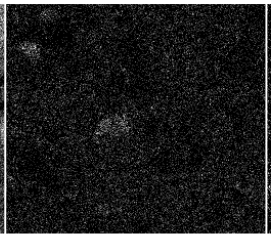
K Ka1

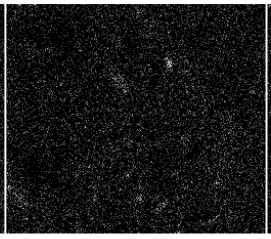
Ca Ka1

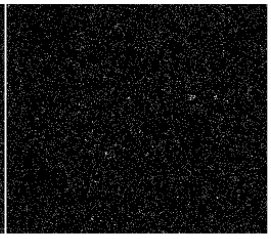
Ti Ka1

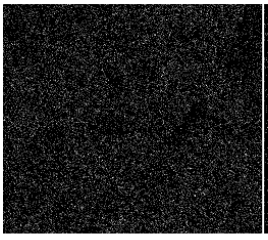
Fe Ka1

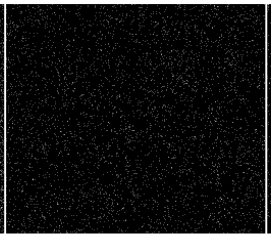
Mn Ka1

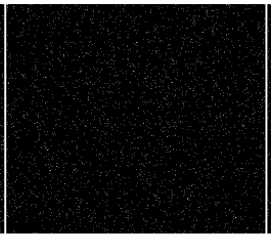
Cu Ka1

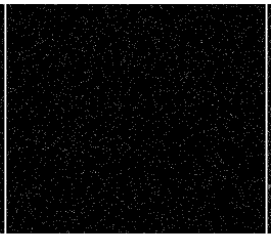
Zn Ka1


P Ka1

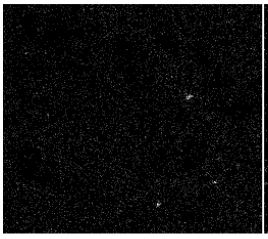
S Ka1

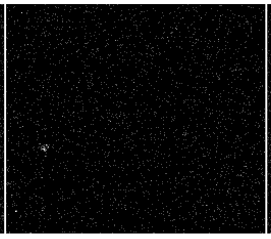
W La1

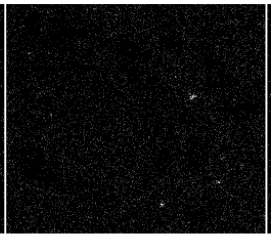
Mo La1

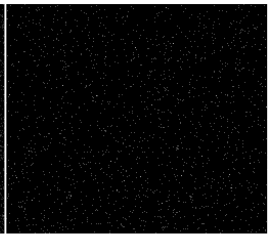
As Ka1